

Control of Heavy-Duty Trucks: Environmental and Fuel Economy Considerations

by

Jianlong Zhang

Petros Ioannou

Center for Advanced Transportation Technologies

University of Southern California

EE-Systems, EEB200, MC2562

Los Angeles, CA 90089

Abstract

In this project we investigate the effect of heavy-duty trucks, equipped with different Adaptive Cruise Control (ACC) systems, operating in mixed traffic with manually driven passenger vehicles, on the environment and traffic flow characteristics. The sluggish dynamics of trucks whether manual or ACC that is due to their limited acceleration capabilities filters speed disturbances caused by leading vehicles and lead to beneficial effects on the environment and traffic flow characteristics. This response however may lead to higher travel times in certain situations as well as invite cut-ins from neighboring lanes causing additional disturbances. A new ACC design that is developed and experimentally tested reduces some of the negative effects of trucks in mixed traffic.

Keywords: heavy-duty truck, vehicle following control, adaptive cruise control, fuel economy, emission, traffic flow characteristics

Executive Summary

This is the Final Report for TO4203. In this project we investigated the effect of trucks, manually driven as well as with different Adaptive Cruise Control (ACC) systems in mixed traffic on the environment and traffic flow characteristics. We used driver models to simulate human driving and validated truck dynamical models for simulations and ACC design. Experiments involving actual vehicles are carried out in order to validate the models used. Emissions models for passenger vehicles and trucks developed by the group of Professor Matthew Barth of the University of California at Riverside are used to study the effect of trucks in mixed traffic on the fuel economy and pollution. A new ACC design for trucks is developed that has better properties than existing ones with respect to impact on the environment and performance.

The main findings of this project are as follows:

1. The sluggish dynamics of trucks whether manual or ACC due to limited acceleration and speed capabilities make their response to disturbances caused by lead passenger vehicles smooth. The vehicles following the truck are therefore presented with a smoother speed trajectory to track. This filtering effect of trucks is shown to have beneficial effects on fuel economy and pollution. The quantity of these benefits depends very much on the level of the disturbance and scenario of maneuvers. For example if the response of the truck is too sluggish relative to the speed of the lead vehicle then a large intervehicle spacing may be created inviting cut ins from neighboring lanes. These cut-ins create additional disturbances with negative effects on fuel economy and pollution. Situations can be easily constructed where the benefits obtained due to the filtering effect of trucks are eliminated due to disturbances caused by possible cut-ins. Furthermore cut-ins are shown to increase travel time for the vehicles in the original traffic stream.
2. The ACC trucks improve performance as they are designed to respond smoothly during vehicle following while maintaining safe intervehicle spacings. The spacing rule adopted influences the performance and response of the ACC truck. For the same spacing rule however different ACC designs behave in a very similar manner. The new ACC design developed, analyzed and tested under this project is shown to have better filtering properties than existing ones leading to improved benefits for fuel economy and pollution during traffic disturbances. Furthermore the new ACC design provides a smooth response and filters oscillations that may appear in the speed response of the lead vehicle.
3. The behavior of trucks in mixed traffic on the macroscopic level is analyzed and found to depend on a particular number that characterizes the ratio of the time headway used by trucks versus that of the passenger vehicles. For relatively low ratios the presence of trucks appears to improve the traffic flow characteristics whereas for high ratios the traffic flow of mixed traffic becomes unstable at lower traffic densities and at lower traffic flows compared with traffic with no trucks. In practice for safety reasons and due to limited acceleration and speed capabilities of trucks this ratio is large most of the time leading to the conclusion that trucks will tend to make traffic flow more unstable at lower

traffic densities and at lower traffic flows. The use of ACC however will reduce this ratio and improve the traffic flow characteristics.

4. The limited experiments performed validated our simulation models at least on the microscopic level. In addition they demonstrated that our new ACC design works in real time and under actual driving conditions in a satisfactory manner. Additional experiments of larger scale are essential in order to validate the results of the emission models as well as some of the macroscopic phenomena predicted by simulations and the fundamental diagram.

TABLE OF CONTENTS

LIST OF FIGURES	V
LIST OF TABLES	VIII
1 INTRODUCTION	I
2 VEHICLE MODELS	4
2.1 Truck Dynamics	4
2.2 Human Driver Models	4
2.2.1 <i>Human driver model for passenger vehicles</i>	4
2.2.2 <i>Human driver model for heavy trucks</i>	6
2.2.3 <i>String Stability</i>	8
3 ADAPTIVE CRUISE CONTROL DESIGNS FOR HEAVY TRUCKS	11
3.1 Simplified Model for Control Design	11
3.2 ACC Design	12
3.2.1 <i>Control Design for Speed Tracking</i>	12
3.2.1 <i>Control Design for Vehicle Following</i>	14
3.3 Modified ACC Design for Heavy Trucks	20
3.3.1 <i>Modifications in Speed Tracking Control</i>	20
3.3.2 <i>Modifications in Vehicle Following Control</i>	21
3.4 Simulations	27
3.4.1 <i>Low Acceleration Maneuvers</i>	28
3.4.2 <i>High Acceleration Maneuvers</i>	34
3.4.3 <i>High Acceleration Maneuvers with Oscillations</i>	40
3.5 Experimental Testing	44
3.5.1 <i>Low Acceleration Maneuvers</i>	44
3.5.2 <i>High Acceleration Maneuvers</i>	49
3.5.3 <i>Model Validation</i>	54
4 IMPACT OF HEAVY TRUCKS ON MIXED TRAFFIC	57
4.1 Emission and Fuel Consumption	57
4.1.1 <i>Emission Models for Passenger Vehicles and Heavy Trucks</i>	57
4.1.2 <i>Vehicle Following Disturbances</i>	58
4.1.3 <i>Lane Change Effect</i>	62
4.2 Macroscopic Traffic Flow Analysis	64
4.2.1 <i>Fundamental Flow-Density Diagram</i>	64
4.2.1.1 <i>Manual/ACC Traffic without Heavy Trucks</i>	65
4.2.1.2 <i>Manual/ACC Traffic with Heavy Trucks</i>	69
4.2.2 <i>Shock Waves Analysis</i>	81
5 CONCLUSIONS	84
ACKNOWLEDGMENT	85
APPENDIX : TRUCK LONGITUDINAL MODEL	86
REFERENCES	89

LIST OF FIGURES

Figure 1. Interconnected system of vehicles following each other in a single lane.....	5
Figure 2. Block diagram of the Pipes' model	5
Figure 3. Block diagram of the Bando's model.....	6
Figure 4. Diagram of the truck following mode	15
Figure 5. The nonlinear filter used in the speed tracking mode.....	20
Figure 6. Region 1 and Region 2 in the $\delta - v_r$ plane	21
Figure 7. The nonlinear filter used in the vehicle following mode.....	22
Figure 8. Block diagram of the new ACC system	25
Figure 9. Flow diagram of the new ACC system.....	26
Figure 10. Low acceleration: (a) speed responses and (b) separation error responses of the vehicles in string 1 (all the vehicles are manually driven passenger vehicles).....	29
Figure 11. Low acceleration: (a) speed responses and (b) separation error responses of the vehicles in string 2 (the second vehicle is a manually driven heavy truck).....	29
Figure 12. Low acceleration: (a) speed responses and (b) separation error responses of the vehicles in string 3 (the second vehicle is an ACC truck with the nonlinear spacing rule), (c) fuel response and (d) engine torque response of the ACC truck	30
Figure 13. Low acceleration: (a) speed responses and (b) separation error responses of the vehicles in string 4 (the second vehicle is an ACC truck with the quadratic spacing rule), (c) fuel response and (d) engine torque response of the ACC truck	31
Figure 14. Low acceleration: (a) speed responses and (b) separation error responses of the vehicles in string 5 (the second vehicle is an ACC truck with the constant time headway spacing rule), (c) fuel response and (d) engine torque response of the ACC truck	32
Figure 15. Low acceleration: (a) speed and separation error responses of the vehicles in string 6 (the second vehicle is an ACC truck with the new controller), (c) fuel response and (d) engine torque response of the ACC truck.....	33
Figure 16. High acceleration: (a) speed responses and (b) separation error responses of the vehicles in string 1 (all the vehicles are manually driven passenger vehicles)...	35
Figure 17. High acceleration: (a) speed responses and (b) separation error responses of the vehicles in string 2 (the second vehicle is a manually driven heavy truck).....	35
Figure 18. High acceleration: (a) speed responses and (b) separation error responses of the vehicles in string 3 (the second vehicle is an ACC truck with the nonlinear spacing rule), (c) fuel response and (d) engine torque response of the ACC truck ..	36
Figure 19. High acceleration: (a) speed responses and (b) separation error responses of the vehicles in string 4 (the second vehicle is an ACC truck with the quadratic spacing rule), (c) fuel response and (d) engine torque response of the ACC truck ..	37
Figure 20. High acceleration: (a) speed responses and (b) separation error responses of the vehicles in string 5 (the second vehicle is an ACC truck with the constant time headway spacing rule), (c) fuel response and (d) engine torque response of the ACC truck	38
Figure 21. High acceleration: (a) speed responses and separation error responses of the vehicles in string 6 (the second vehicle is an ACC truck with the new controller), (c) fuel response and (d) engine torque response of the ACC truck	39

Figure 22. High acceleration with oscillations: (a) speed responses and (b) separation error responses of the vehicles in string 1 (all the vehicles are manually driven passenger vehicles)	41
Figure 23. High acceleration with oscillations: (a) speed responses and (b) separation error responses of the vehicles in string 2 (the second vehicle is a manually driven heavy truck)	41
Figure 24. High acceleration with oscillations: (a) speed responses and (b) separation error responses of the vehicles in string 3 (the second vehicle is an ACC truck with the nonlinear spacing rule).....	42
Figure 25. High acceleration with oscillations: (a) speed responses and (b) separation error responses of the vehicles in string 4 (the second vehicle is an ACC truck with the quadratic spacing rule).....	42
Figure 26. High acceleration with oscillations: (a) speed responses and (b) separation error responses of the vehicles in string 5 (the second vehicle is an ACC truck with the constant time headway spacing rule).....	43
Figure 27. High acceleration with oscillations: (a) speed responses and separation error responses of the vehicles in string 6 (the second vehicle is an ACC truck with the new controller).....	43
Figure 28. Low acceleration (experiment data): (a) speeds of the three vehicles, (b) separation error and (c) engine torque responses of the ACC truck with the nonlinear spacing rule.....	45
Figure 29. Low acceleration (experiment data): (a) speeds of the three vehicles, (b) separation error and (c) engine torque responses of the ACC truck with the quadratic spacing rule.....	46
Figure 30. Low acceleration (experiment data): (a) speeds of the three vehicles, (b) separation error and (c) engine torque responses of the ACC truck with the constant time headway spacing rule.....	47
Figure 31. Low acceleration (experiment data): (a) speeds of the three vehicles, (b) separation error and (c) engine torque responses of the ACC truck with the new controller.....	48
Figure 32. High acceleration (experiment data): (a) speeds of the three vehicles, (b) separation error and (c) engine torque responses of the ACC truck with the nonlinear spacing rule.....	50
Figure 33. High acceleration (experiment data): (a) speeds of the three vehicles, (b) separation error and (c) engine torque responses of the ACC truck with the quadratic spacing rule.....	51
Figure 34. High acceleration (experiment data): (a) speeds of the three vehicles, (b) separation error and (c) engine torque responses of the ACC truck with the constant time headway spacing rule.....	52
Figure 35. High acceleration (experiment data): (a) speeds of the three vehicles, (b) separation error and (c) engine torque responses of the ACC truck with the new controller.....	53
Figure 36. Model validation: (a) speed responses of the three vehicles (the second is ACC_C) and (b) engine torque responses of ACC_C in experiment and simulation	55

Figure 37. Model validation: (a) speed responses of the three vehicles (the second is ACC_N) and (b) engine torque responses of ACC_N in experiment and simulation	56
Figure 38. Diagram of the CMEM model.....	57
Figure 39. Responses of the vehicles in string 6 in high acceleration maneuvers with three cut-in vehicles: (a) speed responses and (b) separation error responses.....	63
Figure 40. Fundamental flow-density diagrams of the manual traffic and the ACC traffic	67
Figure 41. Mixed traffic with passenger vehicles and heavy trucks.....	69
Figure 42. Fundamental flow-density diagrams of the manual traffics with/without heavy trucks ($r_{hm} = r_L$)	74
Figure 43. Fundamental flow-density diagrams of the manual traffics with/without heavy trucks ($r_{hm} < r_L$)	75
Figure 44. Fundamental flow-density diagrams of the manual traffics with/without heavy trucks (one truck is treated as r_L passenger vehicles, $r_{hm} < r_L$).....	76
Figure 45. Fundamental flow-density diagrams of the manual traffics with/without heavy trucks ($r_{hm} > r_L$)	77
Figure 46. Fundamental flow-density diagrams of the manual traffics with/without heavy trucks (one truck is treated as r_L passenger vehicles, $r_{hm} > r_L$).....	78
Figure 47. Fundamental flow-density diagrams of the ACC traffic with/without heavy trucks ($r_{ha} < r_L$).....	80
Figure 48. Illustration of shock wave in transportation traffic	82

LIST OF TABLES

Table 1. Travel time, fuel and emission benefits of the 8 passenger vehicles following the truck in a string of 10 vehicles for low acceleration maneuvers of the lead vehicle (no cut-ins).....	59
Table 2. Fuel and emission benefits of the heavy truck during low acceleration maneuvers of the lead vehicle (no cut-ins).....	59
Table 3. Travel time, fuel and emission benefits of the 8 passenger vehicles following the truck in a string of 10 vehicles for high acceleration maneuvers of the lead vehicle (no cut-ins).....	60
Table 4. Fuel and emission benefits of the heavy trucks in high acceleration maneuvers (no cut-ins).....	61
Table 5. Travel time, fuel and emission benefits of the 8 passenger vehicles following the truck in a string of 10 vehicles for high acceleration maneuvers with oscillations of the lead vehicle (no cut-ins).....	61
Table 6. Fuel and emission benefits of the trucks in high acceleration maneuvers with oscillations (no cut-ins).....	62
Table 7. Travel time, fuel and emission data of the 8 passenger vehicles following ACC_NEW in high acceleration maneuvers, without cut-in(s) and with three cut-ins	64

1 INTRODUCTION

During the last decade, extensive studies related to vehicle automation have been done to improve safety and efficiency of vehicle following. In addition to California's Intelligent Transportation System (ITS) program led by Partners for Advanced Transit and Highways (PATH), the US DOT National Automated Highway System Consortium (NAHSC) and the Intelligent Vehicle Initiative (IVI), almost every major automobile company has developed or is currently developing automatic controllers for passenger vehicles and trucks, which is the first significant step towards vehicle automation. In most countries such as USA, Europe and Japan, the Intelligent Cruise Control (ICC) or adaptive cruise control (ACC) or active control system where a vehicle can follow the vehicle in front in a single lane automatically is already available for some passenger vehicles.

It is envisioned that automation in heavy trucks is more of a near term reality than in its counterpart passenger vehicles. A number of truck companies experimented with heavy truck automation. DaimlerChrysler has already developed automatic vehicle following control systems for heavy trucks, "electronic draw bar" system, based on electronic sensors used for things such as brake-by-wire and collision avoidance systems [19]. Others include the Eaton-VORAD Collision Avoidance System which allows a truck to perform automatic vehicle following maintaining a safe time headway in traffic flow [16]. Lateral controllers like the Rapidly Adapting Lateral Position Handler (RAPLH) are used to steer buses/trucks along winding roads and change lanes to pass slower vehicles [16]. Another system for detecting lane departure developed by Odetics ITS of Anaheim, California has been announced as an option on the Mercedes-Benz Actros truck/tractor in Europe, and is about to be introduced as an option by Mercedes' North American counterpart, Freightliner [16]. Furthermore, THOMSON-SCF DETEXIS, a company formed by an alliance between THOMSON-SCF and DASSAULT Electronique is currently engaged in developing onboard electronics for advanced automotive products such as Adaptive Cruise Control (ACC) [32]. At PATH, there have been several research efforts on truck automation. A number of different longitudinal controllers, proposed and tested in [28, 29] with either linear or nonlinear spacing policies, allow automatic vehicle following in the longitudinal direction. It has been shown that the control strategies satisfy individual stability and string stability for a platoon of trucks. In the case of lateral control of heavy trucks, classical loop-shaping, H-infinity loop-shaping and sliding mode control methods have been tested and verified by experiments in [10].

The environmental performance of these automatic control systems as they begin to penetrate into the transportation system is very important. The expected benefits and positive effects once validated by analysis and experiments will help accelerate the deployment of automated heavy trucks as well as other intelligent vehicles and concepts of Automated Highway Systems (AHS). In [4, 5] it has been shown that the smooth response of the ACC vehicles, designed for passenger comfort, significantly reduces fuel consumption and levels of pollutants during the presence of traffic disturbances. It has

been shown that the presence of 10% ICC vehicles in the highway traffic lowers the fuel consumption and pollution levels by as much as 8% and 3.8% to 47.3% respectively during traffic disturbance scenarios [4, 5]. Other studies have been done that indicate the potential impact of Advanced Public Transportation Systems (APTS) on air quality and fuel economy, which conclude that transit buses produce less hydrocarbon (HC) and carbon monoxide (CO) emissions than autos on a passenger-mile basis [15]. In [12] different Intelligent Transportation Technologies (ITS) have been discussed that have the potential to improve air quality, including reduction of unnecessary “stop and go” type of traffic.

In this report, we evaluated the performance of different vehicle following controllers (ACC) currently available for heavy trucks using microscopic simulations. A new ACC controller is designed to provide better performance on the microscopic level with beneficial effects on fuel economy and pollution. The current and new ACC controllers are evaluated using extensive simulations. Experiments with actual vehicles are used to demonstrate the operation of the new ACC controller in real time and to validate our simulation models. Microscopic as well as macroscopic analyses coupled with simulations are used to investigate the impact of trucks in mixed traffic with passenger vehicles. The emission models for passenger vehicles and trucks developed by Professor’s Matthew Barth of the university of California at Riverside are used to evaluate the impact of trucks on emissions and fuel economy. Our main findings are the following:

1. The sluggish dynamics of trucks whether manual or ACC due to limited acceleration and speed capabilities make their response to disturbances caused by lead passenger vehicles smooth. The vehicles following the truck are therefore presented with a smoother speed trajectory to track. This filtering effect of trucks is shown to have beneficial effects on fuel economy and pollution. The quantity of these benefits depends very much on the level of the disturbance and scenario of maneuvers. For example if the response of the truck is too sluggish relative to the speed of the lead vehicle then a large intervehicle spacing may be created inviting cut-ins from neighboring lanes. These cut-ins create additional disturbances with negative effects on fuel economy and pollution. Situations can be easily constructed where the benefits obtained due to the filtering effect of trucks are eliminated due to disturbances caused by possible cut-ins. Furthermore cut-ins are shown to increase travel time for the vehicles in the original traffic stream.
2. The ACC trucks improve performance as they are designed to respond smoothly during vehicle following while maintaining safe intervehicle spacings. The spacing rule adopted influences the performance and response of the ACC truck. For the same spacing rule however different ACC designs behave in a very similar manner. The new ACC design developed, analyzed and tested under this project is shown to have better filtering properties than existing ones leading to improved benefits for fuel economy and pollution during traffic disturbances. Furthermore the new ACC design provides a smooth response and filters oscillations that may appear in the speed response of the lead vehicle.

3. The behavior of trucks in mixed traffic on the macroscopic level is analyzed and found to depend on a particular number that characterizes the ratio of the time headway used by trucks versus that of the passenger vehicles. For relatively low ratios the presence of trucks appears to improve the traffic flow characteristics whereas for high ratios the traffic flow of mixed traffic becomes unstable at lower traffic densities and at lower traffic flows compared with traffic with no trucks. In practice for safety reasons and due to limited acceleration and speed capabilities of trucks this ratio is large most of the time leading to the conclusion that trucks will tend to make traffic flow more unstable at lower traffic densities and at lower traffic flows. The use of ACC however will reduce this ratio and improve the traffic flow characteristics.

4. The limited experiments performed validated our simulation models at least on the microscopic level. In addition they demonstrated that our new ACC design works in real time and under actual driving conditions in a satisfactory manner. Additional experiments of larger scale are essential in order to validate the results of the emission models as well as some of the macroscopic phenomena predicted by simulations and the fundamental diagram.

2 VEHICLE MODELS

2.1 Truck Dynamics

The longitudinal dynamics of a heavy truck can be characterized by a set of differential equations, algebraic relations and look-up tables. In this report, the truck model used for simulations is taken from [29, 30] and is described for completeness in the Appendix. This model contains six states and is detailed enough to capture all the important longitudinal dynamics of a truck. Among the six states, the dominant state is the one associated with the truck longitudinal speed v^* , which is determined by

$$\dot{v} = \frac{F_t - F_a - F_r}{m} \quad (2-1)$$

where m is the vehicle mass, F_t is the tractive tire force, F_a is the aerodynamic drag force, and F_r is the rolling friction force. In (2-1), F_a is equal to $c_a v^2$, where c_a is the aerodynamic drag coefficient, and F_r is equal to $c_r mg/h_w$, where c_r is the rolling friction coefficient, h_w is the radius of the front wheels, g is the gravity constant. The brake/fuel commands are incorporated in the differential and algebraic equations that determine the tire force F_t . As in practice, in our analysis and simulations the fuel and brake commands are applied during separate time intervals.

2.2 Human Driver Models

2.2.1 Human driver model for passenger vehicles

In our study, the Pipes' vehicle following model is chosen among several other vehicle following models as it simulates slinky type effects that are often observed in actual vehicle following. Therefore, as in previous studies [4, 5], we find it to be the most appropriate human driver model for the type of simulations and experiments we performed. The Pipes' model was first proposed by Pipes [20] and later validated by Chandler [7]. It is a linear follow-the-leader model based on the vehicle following theory that pertains to the single lane dense traffic with no passing and assumes that each driver reacts to the stimulus from the vehicle ahead.

Suppose that the i th vehicle among the vehicle string shown in Figure 1 is manually driven. The driver adjusts the speed of the i th vehicle in a way described as

* In this report, "speed" always represents "longitudinal speed".

$$v_i(t) = \frac{1}{h_{cm}} [x_{i-1}(t-\tau) - x_i(t-\tau) - L_c] \quad (2-2)$$

where $h_{cm} > 0$ is the time headway used by the driver, L_c is the passenger vehicle length, $x_i(t)$ and $v_i(t)$ are the position and speed of the i th vehicle at time t , respectively, and τ is the driver's response time. By differentiating both sides of (2-2), the Pipes' model can be rewritten as

$$a_i(t) = K[v_{i-1}(t-\tau) - v_i(t-\tau)] \quad (2-3)$$

where v_{i-1} and v_i are the speeds of the $i-1$ th and i th vehicles, respectively, a_i is the acceleration of the i th vehicle and $K = \frac{1}{h_{cm}}$ is the sensitivity factor.

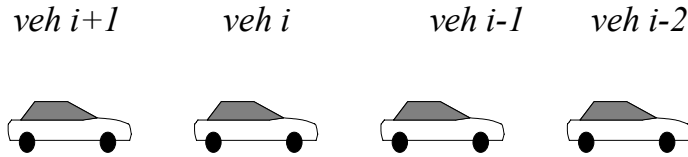


Figure 1. Interconnected system of vehicles following each other in a single lane

The transfer function of the Pipes' model, shown in Figure 2, is given by

$$G_p(s) = \frac{v_i}{v_{i-1}} = \frac{Ke^{-\tau s}}{s + Ke^{-\tau s}} \quad (2-4)$$

with $\tau = 1.5\text{sec}$ and $K = 0.37\text{sec}^{-1}$.

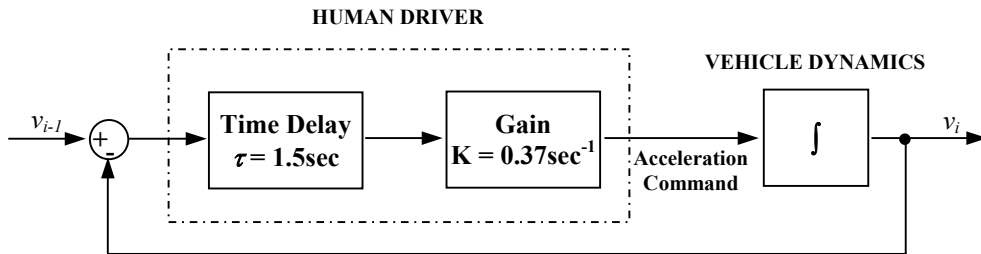


Figure 2. Block diagram of the Pipes' model

2.2.2 Human driver model for heavy trucks

The human driver model for heavy trucks used in our study is proposed by Bando et al [1]. In this model, the driver of the vehicle controls the acceleration in such a way that he/she maintains an optimal safe speed according to the following distance to the preceding vehicle. The model has the following form:

$$\ddot{x}_i(t) = K_a (V(x_{i-1}(t - \tau_t) - x_i(t - \tau_t)) - \dot{x}_i(t)) \quad (2-5)$$

where τ_t is a time delay, K_a is a positive gain, $x_{i-1}(t)$ and $x_i(t)$ are the positions of the $i-1$ th vehicle and the i th vehicle in a vehicle string, and $V(\bullet)$ is the desired speed as a function of the vehicle separation distance. The diagram of the Bando's model is shown in Figure 3. In our subsequent analysis and in Figure 3, $\Delta x_i(t) = x_{i-1}(t) - x_i(t)$ denotes the separation distance between the $i-1$ th and the i th vehicles.

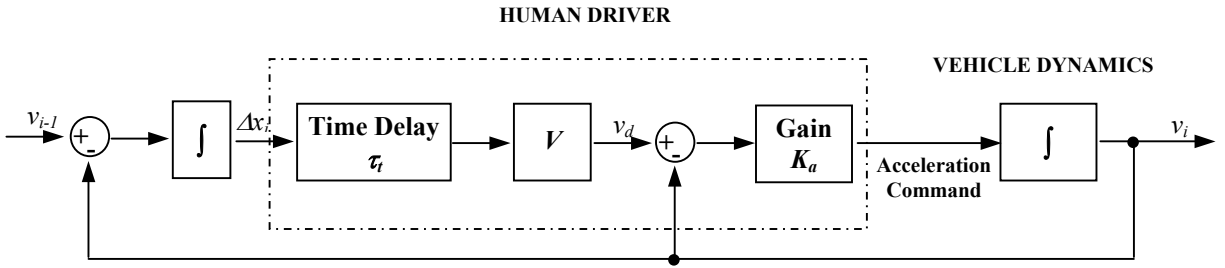


Figure 3. Block diagram of the Bando's model

The desired speed chosen by the driver is modeled as a non-decreasing function of the intervehicle spacing, such that for small following distances it becomes small, and gradually increases with a growing distance, but does not exceed some maximum value assessed as safe by the driver. Therefore, the desired speed $V(\Delta x_i)$ has the following properties [1]: (i) $V(\Delta x_i) = 0$ for $\Delta x_i < s_0$, where s_0 is the intervehicle spacing corresponding to the jam density, (ii) $V(\Delta x_i)$ is an increasing function, and (iii) $\lim_{\Delta x_i \rightarrow \infty} V(\Delta x_i) = V_\infty$ where V_∞ is some maximum safe speed that the driver maintains in a free moving traffic. According to this model, for any intervehicle spacing, there exists a safe speed that the driver tries to achieve.

If we assume that the truck driver attempts to maintain a constant time headway during driving, then the desired speed is set by

$$V(\Delta x_i) = \max \left\{ 0, \frac{\Delta x_i - s_0}{h_{tm}} \right\} \quad (2-6)$$

where h_m is the time headway used by the truck driver. If we take a further look at the truck driver model described by (2-5) and (2-6), we can see that it is closely related to the Pipes' model. Without confusion, we use τ to substitute τ_i in the Bando's model. From

$$\Delta x_i(t) = \int_0^t (v_{i-1}(\lambda) - v_i(\lambda)) d\lambda + s_0 \quad (2-7)$$

and (2-5), we get

$$sv_i - v_i(0) = K_a \left[\frac{e^{-s\tau}}{s} (v_{i-1} - v_i + s_0) - h_m v_i \right] \quad (2-8)$$

If we consider the desired speed (2-6) as $V(\Delta x_i) = \frac{\Delta x_i - s_0}{h_m}$, then

$$v_i = \frac{1}{s^2 + K_a h_m s + K_a e^{-s\tau}} \left[K_a e^{-s\tau} (v_{i-1} + s_0) + sv_i(0) \right] \quad (2-9)$$

With $K_a \rightarrow \infty$, (2-9) becomes

$$v_i = \frac{\frac{1}{h_m} e^{-s\tau}}{s + \frac{1}{h_m} e^{-s\tau}} (v_{i-1} + s_0) \quad (2-10)$$

Comparing (2-10) with (2-4), it becomes clear that the Pipes' model is a special case of the Bando's model.

In our model, the acceleration for the manually driven truck is given by

$$\ddot{x}_i(t) = \begin{cases} A_{\min}, & \text{if } K_a (V(x_{i-1}(t-\tau) - x_i(t-\tau)) - \dot{x}_i) < A_{\min} \\ A_{\max}, & \text{if } K_a (V(x_{i-1}(t-\tau) - x_i(t-\tau)) - \dot{x}_i) > A_{\max} \\ K_a (V(x_{i-1}(t-\tau) - x_i(t-\tau)) - \dot{x}_i), & \text{otherwise} \end{cases} \quad (2-11)$$

where A_{\min} and A_{\max} are the minimum acceleration (i.e. maximum deceleration) and maximum acceleration respectively the truck is capable to achieve, and V is taken as in (2-6). In our simulations, we take $K_a = 0.8 \text{sec}^{-1}$, which is recommended in [18]. The time delay τ_i is taken as 1.0 second, which is shorter than the delay in the Pipes' model. The reason is that the truck driver sits high, views traffic far ahead and makes a decision faster than drivers in passenger vehicles. The time headway h_m is set as 3.0 seconds, which is larger than that used in the Pipes' model for passenger vehicles. The reason being that the truck has lower braking acceleration capabilities than passenger vehicles

and truck drivers need to maintain longer headways for safety considerations. We put $s_0 = 6.0m$ to account for the intervehicle spacing at zero or very low speeds.

2.2.3 String Stability

One important issue involved in vehicle following control is *string stability* [4, 5, 21, 24]. String stability in a platoon or string of vehicles implies that the intervehicle spacing, speed and acceleration errors of an individual vehicle in the vehicle string does not get amplified as it propagates upstream [4]. A platoon composed of M vehicles, in Figure 1, can be modeled as

$$v_i = G_i(s)v_{i-1} \quad (2-12)$$

where $2 \leq i \leq M$, v_i is the speed of the i th vehicle and $G_i(s)$ is a proper stable transfer function that represents the input-output behavior of the i th vehicle. The speed error v_r , acceleration error a_r and separation error δ for the i th vehicle are defined as

$$\begin{cases} v_{ri} = v_{i-1} - v_i \\ a_{ri} = a_{i-1} - a_i \\ \delta_i = x_{ri} - s_{di} \end{cases} \quad (2-13)$$

where x_{ri} is the separation distance and s_{di} is the desired separation distance between the $i-1$ th and the i th vehicles.

Definition 2.1 [4]: A platoon is said to be *string stable* if

$$\begin{cases} \|v_{ri}\|_p \leq \|v_{ri-1}\|_p \\ \|a_{ri}\|_p \leq \|a_{ri-1}\|_p, \\ \|\delta_i\|_p \leq \|\delta_{i-1}\|_p \end{cases} \quad \forall p \in [1, +\infty], \forall i \text{ with } 2 \leq i \leq M \quad (2-14)$$

Theorem 2.1 (String Stability) [4]: The class of interconnected systems of vehicles following each other in a single lane without passing is string stable if and only if the impulse response $g_i(t)$ of the error propagation transfer function for each individual vehicle in this class satisfies

$$\|g_i\|_1 \leq 1 \quad \forall i \text{ with } 2 \leq i \leq M \quad (2-15)$$

Theorem 2.2: Suppose the error propagation transfer function $G_i(s)$ is proper and stable with $|G_i(0)| \leq 1$. The interconnected system is string stable if $G_i(s)$ has the pole-zero interlacing property [8].

Proof: Suppose $G_i(s)$ is a proper stable transfer function with the pole-zero interlacing property. It can be expressed as

$$G_i(s) = K \frac{\prod_{j=1}^{n-1} (s - z_j)}{\prod_{k=1}^n (s - p_k)} \quad (2-16)$$

with $p_n < z_{n-1} < p_{n-1} < z_{n-2} < \dots < z_1 < p_1 < 0$. Hence we can express $G(s)$ as

$$G_i(s) = \sum_{k=1}^n \frac{K_k}{(s - p_k)} \quad (2-17)$$

where $K_1, K_2 \dots K_n$ have the same sign. This implies the impulse response of $G_i(s)$, $g_i(t)$, doesn't change sign. Hence,

$$\|g\|_1 = \int_0^{\infty} |g(t)| dt = \left| \int_0^{\infty} g(t) e^{-0t} dt \right| = |G(0)| \leq 1 \quad (2-18)$$

Theorem 2.1 implies that the interconnected system is string stable. □

Generally speaking, it is difficult to judge whether an interconnected system is string stable or not unless we are given the numerical form of the error transfer functions. In this study, we will pay more attention to a special case of string stability: L_2 string stability. L_2 string stability can be defined similarly to (2-14) with the only difference: $p = 2$. It means that the energy (represented by the L_2 norm) of the output error is not larger than the energy of the input error. If the error transfer function in an interconnected system is $G_e(s)$, L_2 string stability is equivalent to $\|G_e(j\omega)\|_{\infty} \leq 1$ [4], where $\|G_e(j\omega)\|_{\infty}$ is defined as $\sup_{\omega} |G_e(j\omega)|$. Since we know [8]

$$\|G_e(j\omega)\|_{\infty} \leq \|g_e\|_1 \quad (2-19)$$

the condition to judge L_2 string stability, $\|G_e(j\omega)\|_{\infty} \leq 1$, is conservative compared to (2-15).

We investigate the string stability of a string of manual vehicles closely following each other in a single lane using the human driver models that have been presented. The string stability theorem is used to examine whether the driver models considered belong to the class of systems that guarantee string stability. We assume that all vehicles in the string have identical input/output characteristics. It is easy to see that

$$\frac{\delta_i}{\delta_{i-1}} = \frac{v_{ri}}{v_{ri-1}} = \frac{a_{ri}}{a_{ri-1}} = \frac{v_i}{v_{i-1}} = G_e(s) = G_i(s) \quad (2-20)$$

For the Pipes' model given in (2-4) with $\tau = 1.5$ and $K = 0.37$, we obtain

$$G_i(s) = G_p(s) = \frac{0.37e^{-1.5s}}{s + 0.37e^{-1.5s}} \quad (2-21)$$

As shown in [4], $|G_i(j\omega)| > 1$, for some small frequencies (for example, $|G_i(0.3j)| \approx 1.025$). This means $\|G_e(j\omega)\|_\infty > 1$, and the Pipes' model does not guarantee L_2 string stability. String stability as defined in Definition 2.1 cannot be satisfied, either. Pipes' model was validated in practice in numerous experiments. It was shown that, among other examined vehicle following models, this model shows the closest resemblance to actual human driving that is characterized by an oscillatory behavior and 'slinky-type' effects (string instability), which are often observed in practice [4].

For the Bando's model given in (2-11), if there is no acceleration or speed limits, we have

$$G_i(s) = \frac{v_i}{v_{i-1}} = \frac{0.8e^{-s}}{s^2 + 2.4s + 0.8e^{-s}} \quad (2-22)$$

It can be shown that $|G_i(j\omega)| < 1$ for any finite ω , $\|G_i(j\omega)\|_\infty = 1$ but $\|g_i\|_1 > 1$, which means it can only guarantee L_2 string stability. If we consider acceleration limits for a heavy truck, we expect the slinky effect to be more serious than that of a passenger vehicle, since the truck cannot regulate its speed fast enough due to limited acceleration. We use the above human driver models to simulate manual driving in the subsequent sections of the report.

3 ADAPTIVE CRUISE CONTROL DESIGNS FOR HEAVY TRUCKS

The Adaptive Cruise Control (ACC) system is an extension of the conventional Cruise Control (CC) system. In addition to the autonomous speed regulation provided by the conventional CC systems, the ACC system provides the intelligent function that enables the ACC vehicle to adjust its speed automatically in order to maintain a desired intervehicle spacing between itself and a moving preceding vehicle or obstacle in the same lane. In this section, we present the ACC designs and modifications based on fuel economy and emission considerations for heavy trucks. Simulations and experiments are carried out to compare the behaviors of heavy trucks with different ACC controllers.

An ACC vehicle operates in the mode of speed tracking or vehicle following. The speed tracking mode is active when the lane is clear, i.e. no object is detected by the forward-looking sensor installed on the vehicle. Otherwise, the vehicle following mode is active and the ACC system adjusts the vehicle speed to maintain a desired spacing from the vehicle or obstacle ahead. The control objectives in these two modes are different, which indicates the controllers employed in the two modes should be considered separately. However, the control constraints are the same in these two modes. The control objectives should be achieved under the following two constraints [14]:

- C1. $a_{\min} \leq \dot{v} \leq a_{\max}$, where a_{\min} and a_{\max} are specified.
- C2. The absolute value of jerk defined as $|\ddot{v}|$ should be small.

The first constraint arises from the inability of the truck to generate high accelerations and from driver comfort and safety considerations. For example, in most ACC designs emergency braking is a task given to the driver. This means that the ACC system will activate braking up to a certain deceleration and the driver is expected to take over and complete the emergency stopping. The second constraint is for driver comfort. While this constraint is more crucial in passenger vehicles it would be desirable to have in trucks too.

3.1 Simplified Model for Control Design

The longitudinal model discussed in the previous section is sixth-order and highly nonlinear, thus not suitable for control design. Since the mode associated with the longitudinal speed is much slower than those associated with the other five states, the longitudinal truck model can be approximated as a first-order nonlinear system:

$$\dot{v} = f(v, u, \tau) \quad (3-1)$$

where v is the longitudinal speed, u is the fuel/brake command and τ represents the negligible fast dynamics. This nonlinear model can be linearized around operating points corresponding to steady state, i.e.

$$\dot{v} = -a(v - v_d) + b(u - u_d) + d \quad (3-2)$$

where v_d is the desired steady state speed, u_d is the corresponding steady state fuel command, d is the modeling uncertainty, and a and b are constant parameters that depend on the operating point, i.e. the steady state values of the vehicle speed and load torque. If there is no shift of gears, a and b are positive. In our analysis, we always assume a and b are positive since gear shift is a short time transient activity. For a given vehicle, the relation between v_d and u_d can be described by a look-up table, or by a 1-1 mapping continuous function

$$v_d = f_u(u_d) \quad (3-3)$$

In our analysis, we assume $f_u(u_d)$ is differentiable and

$$m_u \leq \frac{d}{du_d} f_u(u_d) \leq M_u \quad (3-4)$$

Hence, the simplified truck model used for ACC design is described by (3-2) - (3-4).

3.2 ACC Design

3.2.1 Control Design for Speed Tracking

In the speed tracking mode, the ACC system should always regulate the vehicle speed v close to the desired speed v_d set by the driver or by the roadway in an advanced vehicle highway system [27]. The control objective can be expressed as

$$\lim_{t \rightarrow \infty} e_v(t) = 0 \quad (3-5)$$

where $e_v(t) = v_d(t) - v(t)$.

Lemma 3.1: For the system represented in (3-2), (3-3) and (3-4), the following controller

$$u = k_p e_v + k_i \frac{1}{s} e_v + k_d \frac{s}{\frac{1}{N}s + 1} e_v \quad (3-6)$$

where k_p , k_i , k_d and N are some positive parameters, can stabilize the closed-loop system and guarantee that $e_v(t)$ converges exponentially fast to the residual set

$$E_v = \left\{ e_v \in R \left\| e_v \right\| \leq C_1 \cdot \|\dot{v}_d(t)\|_\infty + C_2 \cdot \|\dot{d}(t)\|_\infty \right\} \quad (3-7)$$

where $C_1, C_2 > 0$ are some constants. Furthermore, if v_d and d are constant, then $e_v(t)$ converges to zero exponentially fast.

Proof: Using (3-6), the closed-loop system is

$$e_v(s) = \frac{s^2(s+N)}{\Delta(s)} v_d(s) - \frac{s(s+N)[d(s) - bu_d(s)]}{\Delta(s)} \quad (3-8)$$

where $\Delta(s) = s^3 + [a + bk_p + N(1 + bk_d)]s^2 + [bk_i + N(a + bk_p)]s + Nbk_i$. The initial conditions are ignored since they do not affect stability and steady state performance. Recall that a and b are positive and k_p, k_i, k_d and N are also designed to be positive, thus all the coefficients in $\Delta(s)$ are positive. From Routh's stability criterion, $\Delta(s)$ is Hurwitz if and only if

$$[a + bk_p + N(1 + bk_d)] \cdot [bk_i + N(a + bk_p)] > Nbk_i \quad (3-9)$$

or equivalently,

$$[a + bk_p + Nbk_d] \cdot [bk_i + N(a + bk_p)] + N^2(a + bk_p) > 0 \quad (3-10)$$

Since (3-10) always holds, the closed-loop system is always stable. Rewrite the closed-loop system as

$$e_v(s) = G_1(s)\dot{v}_d(s) + G_2(s)[bu_d(s) - \dot{d}(s)] + R(s) \quad (3-11)$$

where $\dot{v}_d(s)$, $\dot{u}_d(s)$ and $\dot{d}(s)$ denotes the Laplace transforms of $\dot{v}_d(t)$, $\dot{u}_d(t)$ and $\dot{d}(t)$, respectively, and $R(s)$ denotes the terms related to initial conditions ignored in (3-8). Hence

$$e_v(t) = \int_0^t g_1(\tau)\dot{v}_d(t-\tau)d\tau + \int_0^t g_2(\tau)[bu_d(t-\tau) - \dot{d}(t-\tau)]d\tau + r(t) \quad (3-12)$$

where $g_1(t)$, $g_2(t)$ and $r(t)$ are the inverse Laplace transforms of $G_1(s)$, $G_2(s)$ and $R(s)$, respectively, and $r(t)$ consists of terms that converge to zero exponentially fast. Since the system is stable, $g_1(t), g_2(t) \in L_1$ [8]. It follows from (3-12) that

$$\|e_v(t)\| \leq \|g_1(t)\|_1 \|\dot{v}_d(t)\|_\infty + b \|g_2(t)\|_1 \|\dot{u}_d(t)\|_\infty + \|g_2(t)\|_1 \|\dot{d}(t)\|_\infty + |r(t)| \quad (3-13)$$

Using the assumption in (3-4) and taking $C_1 = \|g_1(t)\|_1 + \frac{b}{m_u} \|g_2(t)\|_1$ and $C_2 = \|g_2(t)\|_1$, it follows that $e_v(t)$ converges exponentially fast to the residual set given by (3-7). Furthermore, if v_d and d are constants, it follows from (3-7) that $e_v(t)$ converges to zero exponentially fast. □

According to (3-6), a fuel command is issued when u is positive, while the brake is activated when $u < -u_0$ ($u_0 > 0$ is a constant). If $-u_0 \leq u \leq 0$, the brake system is inactive and the fuel system is operating as in idle speed. This is a simple switch logic that prevents frequent chattering between the fuel and brake actuators. In [29], an alternative approach is used to deal with the same problem. In the work of [29] the control effort u is multiplied by a fixed gain whenever u is negative in order to deal with the different actuator limits.

In the previous ACC or CC designs no effort has been made to meet the control constraints **C1**, **C2** directly and prevent saturation. The reason is that in these designs it has been assumed that the desired speed is a constant or a slowly increasing signal set by the driver. Hence the constraints will not be violated. However, if the desired speed is set by the roadside control system in a future architecture [27], then v_d may differ much from v at some points in time and the constraints may be violated. We will address this issue in a subsequent section on modifications of the ACC controller.

3.2.1 Control Design for Vehicle Following

In the vehicle following mode, the ACC system regulates the vehicle speed so that it follows the preceding vehicle by maintaining a desired intervehicle spacing and a steady state speed that doesn't exceed the allowable speed limit V_{\max} . The control objective is to regulate the vehicle speed v_f to track the speed of the preceding vehicle v_l , as long as $v_l \leq V_{\max}$ while maintaining a vehicle separation x_r as close to the desired spacing s_d as possible, as shown in Figure 4. With the time headway policy, the desired intervehicle spacing is given by

$$s_d = s_0 + hv_f \quad (3-14)$$

where s_0 is a fixed safety intervehicle spacing to avoid vehicle contact at low or zero speeds and h is the time headway. In most applications, h is a positive constant. The control objective in the vehicle following mode can be expressed as

$$v_r \rightarrow 0, \delta \rightarrow 0 \text{ as } t \rightarrow \infty \quad (3-15)$$

where $v_r = v_l - v_f$ is the relative speed and $\delta = x_r - s_d$ is the separation error. In practice, this control objective may not be met exactly when v_l varies considerably, or in the presence of sensor noise, modeling errors, delays and other imperfections. The ACC system should be designed to be robust with respect to these imperfections so that δ remains non-negative most of the time. If δ becomes negative, it means the intervehicle spacing x_r is less than the desired s_d and the vehicle may be violating the vehicle following safety separation. The safety separation can be chosen to account for possible imperfections so that small negative values for δ do not violate safety.

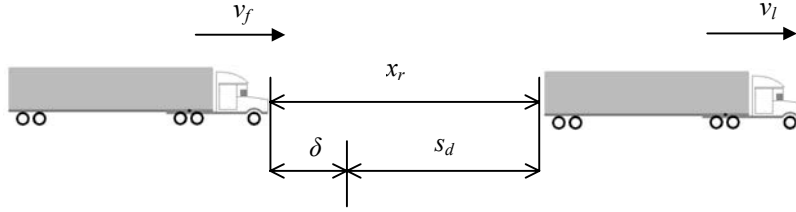


Figure 4. Diagram of the truck following mode

The simplified longitudinal model similar to that shown in (3-2) is used for the control design for the vehicle following mode. However, in this mode, the desired steady state speed is equal to v_l , the speed of the lead vehicle. Hence the longitudinal model in (3-1) can be linearized along the lead vehicle's speed trajectory v_l and the corresponding steady state fuel command u_d when v_l is a constant or varies slowly. The simplified linear model is

$$\dot{v}_f = -a(v_f - v_l) + b(u - u_d) + d \quad (3-16)$$

where $u_d = f_u^{-1}(v_l)$. The explanations for a , b and d are the same as before.

Lemma 3.2: For the system represented in (3-16), (3-3) and (3-4), the following controller

$$u = k_p(v_r + k\delta) + k_i \frac{1}{s}(v_r + k\delta) + k_d \frac{s}{\frac{1}{N}s + 1}(v_r + k\delta) \quad (3-17)$$

where $k > 0$, can stabilize the closed-loop system if the positive control parameters k_p , k_i , k_d and N are chosen properly. Furthermore v_r and δ converge exponentially fast to the residual set

$$E_{v\delta} = \left\{ v_r \in R, \delta \in R \left| \begin{aligned} |v_r| &\leq C_1 \cdot \|\dot{v}_l(t)\|_\infty + C_2 \cdot \|\dot{d}(t)\|_\infty \\ \text{and } |\delta| &\leq C_3 \cdot \|\dot{v}_l(t)\|_\infty + C_4 \cdot \|\dot{d}(t)\|_\infty \end{aligned} \right. \right\} \quad (3-18)$$

for some finite constants $C_i > 0$, $i = 1, 2, 3, 4$. Furthermore, if v_l and d are constants, then $v_r \rightarrow 0$ and $\delta \rightarrow 0$ exponentially fast.

Proof: Using (3-17), we obtain

$$v_f(s) = \frac{\Gamma_1(s) - \Gamma_1^*(s)}{\Gamma(s) - \Gamma^*(s)} v_l(s) + \frac{s^2}{\Gamma(s) - \Gamma^*(s)} (d(s) - bu_d(s)) \quad (3-19)$$

where $\Gamma(s) = [1 + bkk_d(1 + kh)]s^3 + [a + bkk_d + bkp(1 + kh)]s^2 + [bkk_p + bki(1 + kh)]s + bkk_i$, $\Gamma^*(s) = \frac{bkk_d[(1 + kh)s + k]s^3}{s + N}$, $\Gamma_1(s) = bkk_d s^3 + (a + bkk_d + bkp)s^2 + (bki + bkk_p)s + bkk_i$, and $\Gamma_1^*(s) = \frac{bkk_d(s + k)s^3}{s + N}$. We have assumed $x_r(0) = s_0$ and ignored all the other initial states since they will not affect stability and system performance at steady state. The system in (3-19) is stable if $\Gamma(s)$ is Hurwitz and

$$\left| \frac{\Gamma^*(s)}{\Gamma(s)} \right|_{s=j\omega} < 1, \forall \omega \in [0, +\infty) \quad (3-20)$$

Express $\Gamma(s)$ as $\Gamma(s) = a_3s^3 + a_2s^2 + a_1s + a_0$. The four coefficients in $\Gamma(s)$ are all positive, since k_p , k_i , k_d and k are positive constants. From Routh's stability criterion, $\Gamma(s)$ is Hurwitz if and only if

$$a_1a_2 > a_0a_3 \quad (3-21)$$

or equivalently

$$[a + bkp(1 + kh)] \cdot [k_i(1 + kh) + kkp] + bkk_d k_p - kki > 0 \quad (3-22)$$

Obviously, there always exist constants k_p , k_i and k_d satisfying (3-22). For example, if we fix k_i and k_d , (3-22) is satisfied by choosing k_p large. If we rewrite $\frac{\Gamma^*(s)}{\Gamma(s)}$ as

$$\frac{b_3s^3 + b_2s^2}{a_3s^3 + a_2s^2 + a_1s + a_0} \cdot \frac{s}{s + N}, \text{ then (3-20) is equivalent to}$$

$$\begin{aligned} & (a_3^2 - b_3^2)\omega^8 + (N^2a_3^2 + a_2^2 - 2a_1a_3 - b_2^2)\omega^6 + (a_1^2 - 2a_0a_2 + N^2a_2^2 - 2N^2a_1a_3)\omega^4 \\ & (a_0^2 + N^2a_1^2 - 2N^2a_0a_2)\omega^2 + N^2a_0^2 > 0 \end{aligned} \quad (3-23)$$

for all $\omega \in [0, \infty)$. Since $a_3^2 - b_3^2 > 0$, one sufficient condition for (3-23) to be satisfied is that

$$a_1^2 - 2a_0a_2 \geq 0 \text{ and } a_2^2 - 2a_1a_3 - b_2^2 \geq 0 \quad (3-24)$$

It is trivial to see that (3-24) is satisfied by choosing k_p large for any fixed values of k_d and k_i . It follows that if the controller parameters k_p , k_i , k_d and N are chosen to satisfy (2-21) and (2-23), the closed-loop system is stable.

With (3-19) and $\delta(s) = -\frac{hs+1}{s}v_f(s) + \frac{1}{s}v_l(s)$ (s_0 is canceled by $x_r(0)$), we can show that v_r and δ converge exponentially fast to the residual set $E_{v,\delta}$ by following the same approach used in the proof of Lemma 3.1. If v_l are d are constants, (3-18) implies that $v_r \rightarrow 0$ and $\delta \rightarrow 0$ exponentially fast. □

If we assume that a vehicle string contains only trucks and all of them have identical input/output characteristics, then from (2-20), we can show that all the error transfer functions are the same as the speed transfer function $G_v(s)$. If the lead vehicle speed varies slowly around some point, the values of a and b in (3-16) can be viewed as constants, and the speed transfer function inside the string is described by

$$\frac{v_f}{v_l} = G_v(s) = \frac{\Gamma_1(s) - \Gamma_1^*(s)}{\Gamma(s) - \Gamma^*(s)} \quad (3-25)$$

We rewrite this transfer function as

$$G_v(s) = \frac{b_3s^3 + b_2s^2 + b_1s + b_0}{s^4 + a_3s^3 + a_2s^2 + a_1s + a_0} \quad (3-26)$$

where

$$\begin{aligned} b_3 &= Nbk_d + a + bk_p \\ b_2 &= N(a + bkk_d + bk_p) + (bk_i + bkk_p) \\ b_1 &= N(bk_i + bkk_p) + bkk_i \\ b_0 &= Nbk_i \\ a_3 &= N[1 + bk_d(1 + kh)] + [a + bk_p(1 + kh)] \end{aligned}$$

$$\begin{aligned}
a_2 &= N[a + bkk_d + bk_p(1 + kh)] + [bk_i(1 + kh) + bkk_p] \\
a_1 &= N[bk_i(1 + kh) + bkk_p] + bkk_i \\
a_0 &= Nbkk_i
\end{aligned}$$

Lemma 3.3: The system represented by (3-3), (3-4), (3-16) and (3-17) can be made L_2 string stable if the controller parameters k_p , k_i , k_d and N are properly chosen.

Proof: The system is L_2 string stable if and only if $\|G_v(j\omega)\|_\infty \leq 1$, or equivalently

$$\frac{(-b_3\omega^3 + b_1\omega)^2 + (-b_2\omega^2 + b_0)^2}{(-a_3\omega^3 + a_1\omega)^2 + (\omega^4 - a_2\omega^2 + a_0)^2} \leq 1, \forall \omega \in [0, +\infty) \quad (3-27)$$

After some algebraic calculations, we can show (3-27) is equivalent to

$$\begin{aligned}
\omega^6 + (a_3^2 - b_3^2 - 2a_2)\omega^4 + (a_2^2 - b_2^2 - 2a_1a_3 + 2b_1b_3 + 2a_0)\omega^2 \\
+ (a_1^2 - b_1^2 - 2a_0a_2 + 2b_0b_2) \geq 0
\end{aligned} \quad (3-28)$$

for all $\omega \in [0, +\infty)$. It is easy to show that $a_1^2 - b_1^2 - 2a_0a_2 + 2b_0b_2 > 0$. Hence one sufficient condition for (3-28) to hold is

$$a_3^2 - b_3^2 - 2a_2 \geq 0 \text{ and } a_2^2 - b_2^2 - 2a_1a_3 + 2b_1b_3 + 2a_0 \geq 0 \quad (3-29)$$

Any set of parameters that provides system stability and satisfies (3-29) can guarantee L_2 string stability. One can verify that if k_i and k_d are fixed, then (3-29) holds for large k_p and N . Therefore the truck platoon is L_2 string stable. \square

In the above analysis, h and k are both constants. In [6], the desired intervehicle spacing is taken as

$$s_d = s_0 + h_1v_f + h_2v_f^2 \quad (3-30)$$

where h_1 and h_2 are positive constants. We refer to (3-30) as the quadratic spacing policy. In fact, the time headway employed in the quadratic spacing policy is $h_1 + h_2v_f$. Suppose the lead vehicle operates around a nominal speed v_{i0} . Then the time headway used by the following vehicle can be approximated by $h_1 + h_2v_{i0}$. Hence the above analysis for stability and string stability is applicable to the quadratic spacing policy for small perturbations around the nominal speed v_{i0} . In [28], the time headway h and the control parameter k are chosen as

$$\begin{cases} h = \text{sat}(h_0 - c_h v_r) \\ k = c_k + (k_0 - c_k)e^{-\sigma\delta^2} \end{cases} \quad (3-31)$$

where h_0 , c_h , k_0 , c_k and σ are positive constants to be designed (with $c_k < k_0$) and the saturation function $\text{sat}(\bullet)$ has an upper bound 1 and a lower bound 0. If we set c_h and σ to be zero, then $h = h_0$ and $k = k_0$, which implies the linear spacing policy involving the constant h and k is a special case of the nonlinear spacing policy with variable h and k in (3-31). With linearization, we can repeat the previous analysis for local stability and string stability for the nonlinear spacing policy. Detailed information can be found in [28, 31]. Other choices of spacing rules based on traffic flow characteristics can be found in [23].

In this report, we will present the simulation results with the PID type controller (3-17) for different spacing policies. Other control methodologies, such as sliding mode control and adaptive control, can be easily designed based on the linearized model in (3-16). Simulation results indicate that for a given heavy truck, its transient speed response characteristics depend on the spacing rule used, i.e. how the time headway h and the control parameter k are chosen. In other words, for the same spacing rule, different controllers exhibit similar behavior as long as they are designed properly.

There are several practical issues associated with the application of the controller (3-17). To guarantee that the constraints **C1**, **C2** are not violated, we should avoid the generation of high or fast varying control signals. Such high or fast varying control signals can be generated by the control law (3-17) if the lead vehicle accelerates rapidly or changes lanes creating a large spacing error or the truck switches to a new target with large initial spacing error. In [28], these practical situations have not all been addressed as the emphasis was on following another lead truck whose acceleration profiles are also limited. The control parameter k shown in (3-31) is proposed in [28] to eliminate the adverse effect of large separation error. However, in the mixed traffic case considered in our research, the lead vehicle may be a passenger vehicle and we must consider how to deal with the situation in which the lead vehicle speeds up with acceleration not attainable by the following truck. In [14], a nonlinear filter is used to smooth the speed trajectory of the lead vehicle, and $\text{sat}(\delta)$ is used instead of δ to eliminate the adverse effect of large separation error. These modifications worked well for the passenger vehicle case. However, in the heavy truck case, fast increasing v_l may also lead to fast increasing δ since the heavy truck can only accelerate slowly. This indicates that δ should also be smoothed before being passed into the control system. Furthermore, in this situation, the temporary separation error could be very large, and it may take long time for the truck to catch the preceding vehicle. If we simply use $\text{sat}(\delta)$ for the controller (3-17), any changes in v_l will affect the control signal when $\delta > \text{sat}(\delta)$, while some changes in v_l may be ignored. In the following section we modify the ACC controller to address these issues in addition to others.

3.3 Modified ACC Design for Heavy Trucks

High accelerations are not achievable by heavy trucks due to the inherent low actuation-to-weight ratio and fuel system saturation. This means heavy trucks cannot tightly track a rapidly increasing speed or follow a rapidly accelerating passenger vehicle especially when their loads are heavy. The ACC control system discussed in the previous subsection must be modified to take this fact into account.

3.3.1 Modifications in Speed Tracking Control

For the speed tracking case, the reference speed trajectory must be modified to correspond to accelerations achievable by the heavy trucks in order to avoid saturation of the fuel system. This point can be realized by passing the desired speed trajectory through the nonlinear filter shown in Figure 5 to generate a smooth reference signal v_{ref} , and forcing the truck to track v_{ref} . In the nonlinear filter, p is a positive constant, and the saturation function is used to limit the varying rate of v_{ref} . The upper and lower bounds of the saturation function, a_{max} and a_{min} , are chosen in a way the driver feels comfortable and the fuel and brake saturations are avoided when the heavy truck tightly follows v_{ref} . These two bounds can be selected according to vehicle dynamics or experimental results, and they are functions of the reference speed v_{ref} and load weight. This nonlinear filter was first used in [14] for the design of ACC systems for passenger vehicles. The controller for speed tracking used in the new ACC system has the same form as (3-6) with v_d replaced by v_{ref} , and Lemma 3.1 can be applied with the same substitution. If v_d is a constant, then $\lim_{t \rightarrow \infty} v_{ref}(t) = v_d$ and the control objective in (3-5) can still be achieved. In our simulations, k_d is set to be zero since v_{ref} will only vary in a smooth way and the approximated differential term is no longer important for performance.

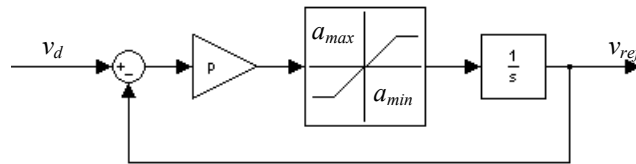


Figure 5. The nonlinear filter used in the speed tracking mode

3.3.2 Modifications in Vehicle Following Control

In the vehicle following case, the controller should be modified so that the control objective in (3-15) is still achievable and the truck satisfies the constraints **C1**, **C2**. With constant h and k , it is easy to show that

$$v_r \rightarrow 0, \delta \rightarrow 0 \text{ as } t \rightarrow \infty \Leftrightarrow v_r + k\delta \rightarrow 0 \text{ as } t \rightarrow \infty \quad (3-32)$$

The control objective in (3-15) can therefore be stated as $v_r + k\delta \rightarrow 0$. This objective is equivalent to

$$v_f \rightarrow v_l + k\delta \text{ as } t \rightarrow \infty \quad (3-33)$$

This indicates that the vehicle following mode can be viewed as a special speed tracking mode, in which the desired speed v_d is equal to $v_l + k\delta$.

Since v_d may vary faster than a truck can track, we can employ a nonlinear filter similar to that in Figure 5 to generate a smooth signal v_{ref} to be tracked. By regulating the truck's speed towards v_{ref} , the ACC system forces the truck to follow the preceding vehicle in a safe and comfortable way, and the control objective in (3-33) is still achievable. As shown in Figure 6, the dashed line represents $v_r + k\delta = 0$, where the control objective in (3-33) is achieved. All the trajectories in this plane should be regulated towards this line and finally reach the original point if the speed of the lead vehicle is a constant. The solid line in Figure 6 represents $v_r + k\delta = -B$, where B is a positive constant. The whole plane is split into two regions by this solid line: the area above represents the safe region (region 1), while the area below represents the unsafe region (region 2). The reference speed v_{ref} is generated depending on which region v_r and δ are located.

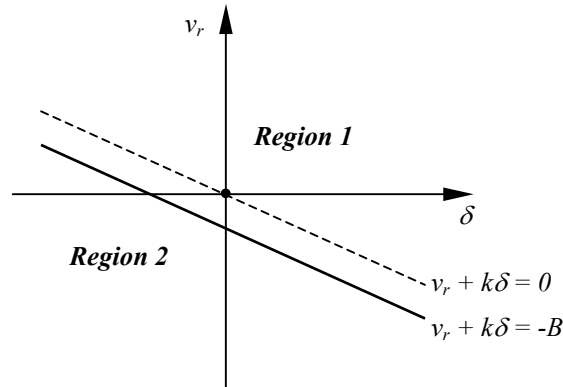


Figure 6. Region 1 and Region 2 in the $\delta - v_r$ plane

In region 1, $v_r + k\delta > -B$ means the vehicle separation distance is safe for the truck. If the truck tries to tightly track the desired speed $v_d = v_l + k\delta$, its speed may be regulated much higher than v_l and its fuel system may be saturated. In this case the nonlinear filter shown in Figure 7 is used to generate a smooth reference speed, v_{ref} , to be tracked instead of v_d . This nonlinear filter limits \dot{v}_{ref} between a_{max} and a_{min} , and prevents regulating v_{ref} higher than V_{max} or too higher than v_l . In some situations, when δ is large, it can ignore some changes in v_l and generate constant reference speed. These points are realized with the use of the saturation function and the following function

$$f(z, v_{ref}, v_l) = \begin{cases} z, & \text{if } v_{ref} = V_{max}, v_{ref} \leq v_l + M_v \text{ and } z < 0; \\ & \text{or } v_{ref} < V_{max} \text{ and } v_{ref} < v_l + m_v; \\ & \text{or } v_{ref} < V_{max}, v_l + m_v \leq v_{ref} \leq v_l + M_v \text{ and } z < 0 \\ 0, & \text{if } v_{ref} = V_{max}, v_{ref} \leq v_l + M_v \text{ and } z \geq 0; \\ & \text{or } v_{ref} < V_{max}, v_l + m_v \leq v_{ref} \leq v_l + M_v \text{ and } z \geq 0; \\ a_{min}, & \text{if } v_{ref} > v_l + M_v \end{cases} \quad (3-34)$$

where z is the signal after the acceleration limiter (the saturation function in Figure 7), and m_v and M_v are design parameters with $0 < m_v < M_v$. Obviously, with (3-34), the nonlinear filter will never generate a reference speed over V_{max} . Let's assume that there is no speed limit (V_{max} is infinite). When $v_{ref} < v_l + m_v$, which means the reference speed for the following vehicle is not too large, v_{ref} can vary with any rate that lies between a_{max} and a_{min} . If v_l increases and stays at some constant value, then from (3-34), it can be seen that v_{ref} will never exceed $v_l + m_v$, which means the follower's speed could hardly exceed $v_l + m_v$. If for some reason (the preceding vehicle slows down later or there is a cutting-in vehicle), $v_l + m_v \leq v_{ref} \leq v_l + M_v$ is satisfied, then v_{ref} decreases when $v_{ref} > v_l + k\delta$, or remains constant when $v_{ref} \leq v_l + k\delta$. In the last case, when $v_{ref} > v_l + M_v$, v_{ref} decreases with the deceleration a_{min} to avoid large relative speed.

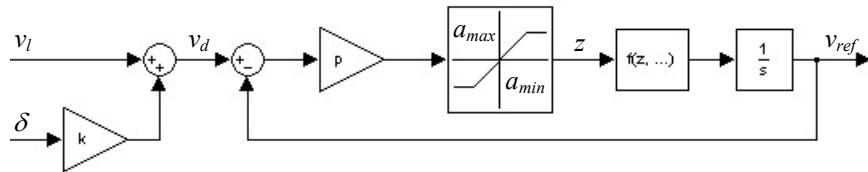


Figure 7. The nonlinear filter used in the vehicle following mode.

In region 2, $v_r + k\delta \leq -B$ indicates that the truck is too close to the preceding vehicle and it is in the unsafe region. The same nonlinear filter as used in region 1 is employed to generate a smooth reference speed. However, in this region the absolute values used for a_{\min} are larger than those used in region 1. In other words, v_{ref} is allowed to decrease faster in order to guarantee safety.

The key idea of the new ACC system is to generate smooth reference speed trajectory v_{ref} with the nonlinear filters shown in Figure 5 and 7, and regulate the truck's speed towards it. The acceleration filter function in (3-34) is employed to prevent v_{ref} from being regulated to a value higher than V_{\max} or much higher than v_l , and reject some changes in v_l when δ is large (see simulations in Section 3.4.3). The ACC controller employed here is

$$u = k_p (v_{ref} - v) + k_i \frac{1}{s} (v_{ref} - v) \quad (3-35)$$

v_{ref} used in (3-35) is generated from either the nonlinear filter in Figure 5 or the nonlinear filter in Figure 7 depending on the mode of operation. We no longer use the approximated derivative term in the controller since v_{ref} always changes smoothly.

Lemma 3.4: For the system represented in (3-16), (3-3) and (3-4), the controller (3-35) can locally stabilize the closed-loop system if the control parameters k_p , k_i and p are chosen properly. If v_l and d are constants with $v_l < V_{\max}$, then $x_e = [0, 0, 0, 0]^T$ is uniformly asymptotically stable, where the state vector $x = [x_1, x_2, x_3, x_4]^T$ is defined as $x_1 = v_l - v_f$, $x_2 = \delta$, $x_3 = v_{ref} - v_f$ and $x_4 = \int_0^t (v_{ref} - v_f) d\tau - \frac{u_d}{k_i} + \frac{d}{bk_i}$.

Proof: (a) Suppose the acceleration limiter and the function (3-34) are removed from the nonlinear filter in Figure 7. We have

$$v_{ref}(s) = \frac{P}{s+p} (v_l(s) + k\delta(s)) \quad (3-36)$$

From (3-16) and (3-36), we obtain

$$v_f(s) = \frac{\Omega_1(s) - \Omega_1^*(s)}{\Omega(s) - \Omega^*(s)} v_l(s) + \frac{s^2}{\Omega(s) - \Omega^*(s)} (d(s) - bu_d(s)) \quad (3-37)$$

where $\Omega(s) = s^3 + [a + bk_p(1 + kh)]s^2 + [bkk_p + bk_i(1 + kh)]s + bkk_i$ is the same as $\Gamma(s)$ in (3-19) with $k_d = 0$, $\Omega_1(s) = (a + bk_p)s^2 + (bk_i + bkk_p)s + bkk_i$ is the same as $\Gamma_1(s)$ in (3-

19) with $k_d = 0$, $\Omega^*(s) = \frac{b(k_p s + k_i)(khs + k)s}{s + p}$ and $\Omega_1^*(s) = \frac{b(k_p s + k_i)(s + k)s}{s + p}$. The system in (3-37) is stable if $\Omega(s)$ is Hurwitz and

$$\left| \frac{\Omega^*(s)}{\Omega(s)} \right|_{s=j\omega} < 1, \forall \omega \in [0, +\infty) \quad (3-38)$$

Similar to the proof for Lemma 3.2, $\Omega(s)$ is Hurwitz if and only if

$$[a + bk_p(1 + kh)] \cdot [k_i(1 + kh) + kk_p] - kk_i > 0 \quad (3-39)$$

Obviously, there always exist constants k_p and k_i satisfying (3-39). After we have chosen k_p and k_i based on (3-39), we need to check the condition (3-38). It is true that

$$\left| \frac{b(k_p s + k_i)(khs + k)}{\Omega(s)} \right|_{s=j\omega} < \infty \quad \text{and} \quad \left| \frac{s}{s + p} \right|_{s=j\omega} < 1 \quad \text{for all } \omega \in [0, \infty), \quad \text{and}$$

$$\lim_{\omega \rightarrow \infty} \left| \frac{b(k_p s + k_i)(khs + k)}{\Omega(s)} \right| = 0. \quad \text{Hence, for large } p, \text{ (3-38) holds and the closed-loop system}$$

is stable. If v_i and d are constants, it is easy to show that $x_e = [0, 0, 0, 0]^T$ is uniformly asymptotically stable in the large [13].

(b) Using the controller with the nonlinear filter described in Figure 7, the closed-loop system is described by

$$\dot{x} = Ax + f_0 + f_1(x) \quad (3-40)$$

where

$$f_1(x) = [0, 0, f(z, v_{ref}, v_i) - p(x_1 + kx_2 - x_3), 0]^T \quad (z = \text{sat}(p(x_1 + kx_2 - x_3))),$$

$$f_0 = [\dot{v}_i, 0, 0, 0]^T, \text{ and}$$

$$A = \begin{bmatrix} -a & 0 & -bk_p & -bk_i \\ 1 - ah & 0 & -bk_p h & -bk_i h \\ p - a & kp & -bk_p - p & -bk_i \\ 0 & 0 & 1 & 0 \end{bmatrix}$$

$f_1(x) = [0, 0, 0, 0]^T$ leads to the case discussed in part (a). In the proof for part (a) we have shown that A is stable when k_p , k_i and p are chosen properly. It is easy to verify that $f_1(x) = 0$ when $|x|$ is sufficiently small. Hence the closed-loop system is locally stable when the control parameters are properly chosen. If v_i and d are constants with $v_i < V_{\max}$,

then it can be verified that $x_e = [0,0,0,0]^T$ is the only equilibrium point of (3-40), and it is uniformly asymptotically stable according to Theorem 3.4.5 in [13]. □

Remark: Even though we can only show uniform asymptotic stability, our simulation results indicate that $x_e = [0,0,0,0]^T$ is asymptotically stable in the large (when $v_l < V_{\max}$).

In the ACC system, the two sub-systems for fuel and brake cannot be active at the same time. Since only one control effort u is used to generate two inputs for the two sub-systems, we design the logic that dictates the switching between the brake and fuel systems in a way that prevents chattering. The following switching rules are incorporated in the ACC system:

In the vehicle following mode:

S1. If the separation distance x_r is larger than x_{\max} ($x_{\max} > 0$ is a design constant), then the fuel system is on.

S2. If the separation distance x_r is smaller than x_{\min} ($x_{\min} > 0$ is a design constant), then the brake system is on.

S3. If $x_{\min} \leq x_r \leq x_{\max}$, then the fuel system is on when $u > 0$, while the brake system is on when $u < -u_0$ ($u_0 > 0$ is a positive constant). When $-u_0 \leq u \leq 0$, the brake is off and the fuel system is operating as in idle speed.

In the speed tracking mode:

S4. The fuel system is on when $u > 0$, while the brake system is on when $u < -u_0$. When $-u_0 \leq u \leq 0$, the brake is off and the fuel system is operating as in idle speed.

S1 and **S2** in the vehicle following mode are used to avoid unnecessary activities of the brake or fuel systems when the vehicle separation is large or small enough. They are similar to those used in [14]. When the controller is switched from speed tracking to vehicle following, the reference speed v_{ref} should also be properly set to avoid large control effort jumps.

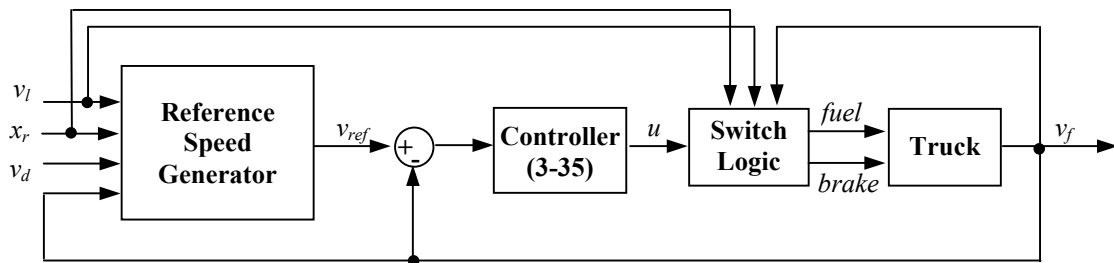


Figure 8. Block diagram of the new ACC system

Figures 8 and 9 show the block diagram and flow diagram of the new ACC system, respectively.

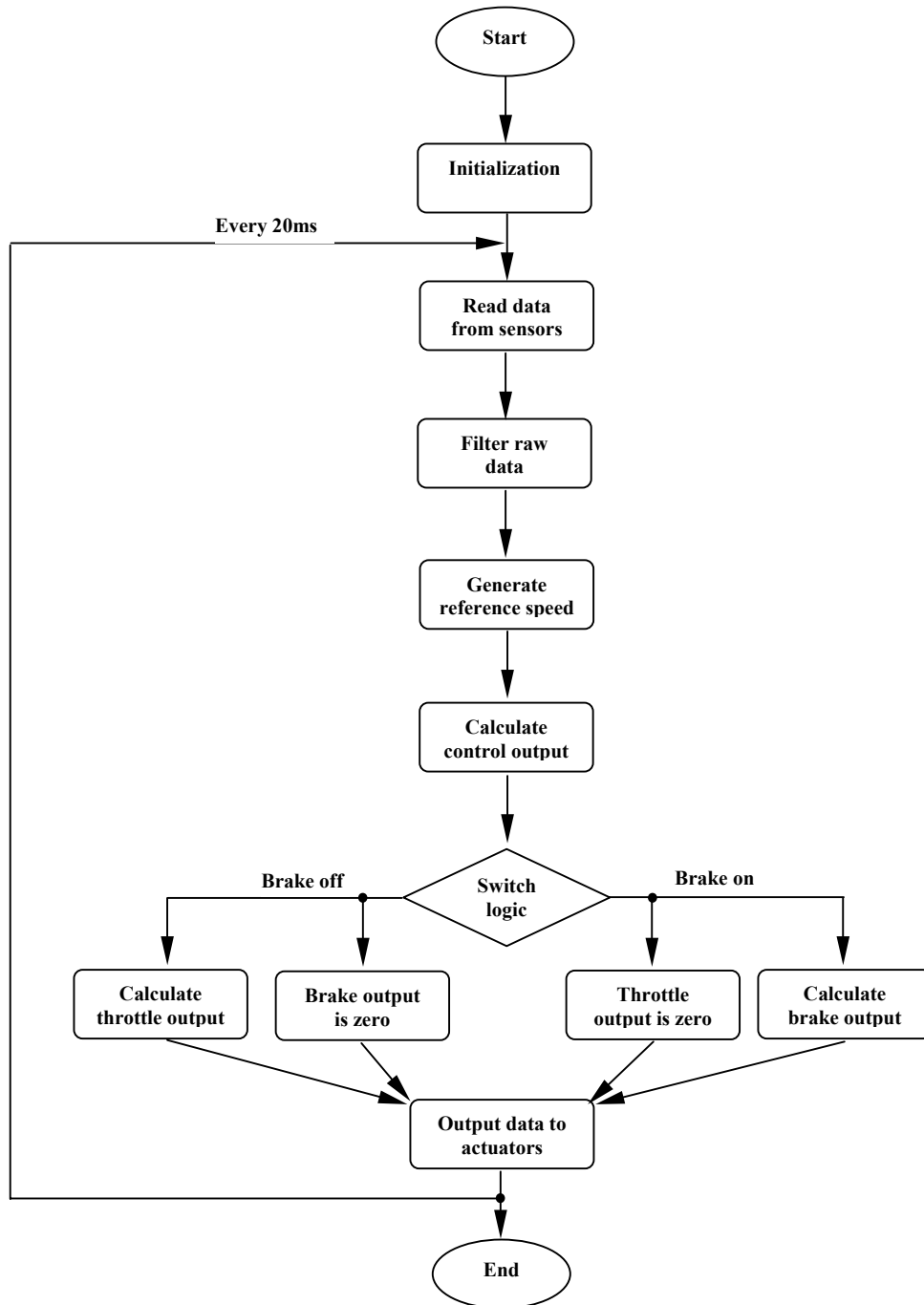


Figure 9. Flow diagram of the new ACC system

3.4 Simulations

Simulations are carried out with Matlab/Simulink to study the effects of heavy trucks on mixed traffic. We use simulation results to investigate how a heavy truck would affect the speed and separation responses of the following passenger vehicles. In the next section, these simulation results are used to analyze the effects of these responses on fuel consumption and emissions.

We use simulations to investigate and compare the behavior of six vehicle strings, each containing ten vehicles. In vehicle string 1, all the ten vehicles are passenger vehicles (modeled using the Pipes' model (2-4)). Vehicle strings 2, 3, 4, 5 and 6 are almost the same as vehicle string 1, but their second vehicle is replaced by a manually driven truck (modeled using the modified Bando's model in (2-11), an ACC truck with the nonlinear spacing policy in (3-31), an ACC truck with the quadratic spacing policy, an ACC truck with the constant time headway policy and an ACC truck with the newly developed controller, respectively. The truck dynamics used in the simulations are described in the Appendix. For easy reference, we will use ACC_N, ACC_Q, ACC_C and ACC_NEW to represent ACC trucks with nonlinear spacing rule, quadratic spacing rule, constant time headway rule and the newly developed controller, respectively.

In each set of simulations, the lead passenger vehicle operates with the same speed trajectory and all the other vehicles are following their preceding ones. The simulation parameters for manual vehicles are the same as those presented in Section 2, and the parameters for ACC trucks are chosen as:

ACC_N: $h_0=1.6\text{s}$, $k_0=1\text{s}^{-1}$, $c_h=0.2\text{s}$, $c_k=0.5\text{s}^{-1}$, $\sigma=0.1\text{m}^{-2}$ and $s_0=6.0\text{m}$

ACC_Q: $h_1=0.8\text{s}$, $h_2=0.03\text{s}^2/\text{m}$, $k=0.2\text{s}^{-1}$ and $s_0=6.0\text{m}$

ACC_C: $h=1.6\text{s}$, $k=0.2\text{s}^{-1}$ and $s_0=6.0\text{m}$

ACC_NEW: $h=1.6\text{s}$, $k=0.2\text{s}^{-1}$, $s_0=6.0\text{m}$, $p=10\text{s}^{-1}$, $m_v=2.0\text{m/s}$, $M_v=8.0\text{m/s}$, and a_{\max} and a_{\min} are acceleration limits chosen based on the capabilities of the truck and desired driver comfort considerations.

In the simulations, the truck weight is fixed at 20 tons, and the parameters for the ACC controllers are tuned for each truck to achieve good performance. A low-pass filter is placed after each ACC controller to limit the change rate of control effort. In ACC_N, ACC_Q and ACC_C, the velocity of the preceding vehicle, v_l , is not fed into the ACC systems directly. It is processed with the nonlinear filter shown in Figure 5, and the acceleration bounds in the nonlinear filter are chosen to be 1.0m/s^2 and -2.0m/s^2 . These two bounds are chosen based on driving comfort. The filtered velocity is fed into the ACC systems. We also use $\text{sat}(\delta)$ instead of δ in ACC_Q and ACC_C to eliminate the adverse effect of large separation errors. These techniques were used in [14] for the ACC passenger vehicle. In our simulations, we assume that the ranging sensor installed on ACC trucks to measure inter vehicle distance and relative speed has a maximum operating range of 120 meters. If the vehicle separation distance is larger than 120

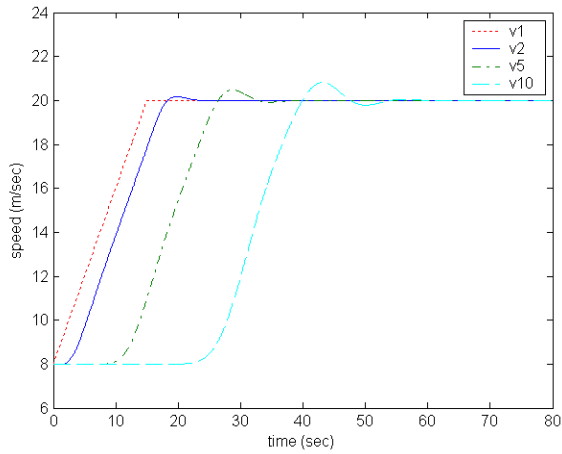
meters, the ACC system will switch from the vehicle following mode to the speed tracking mode.

3.4.1 Low Acceleration Maneuvers

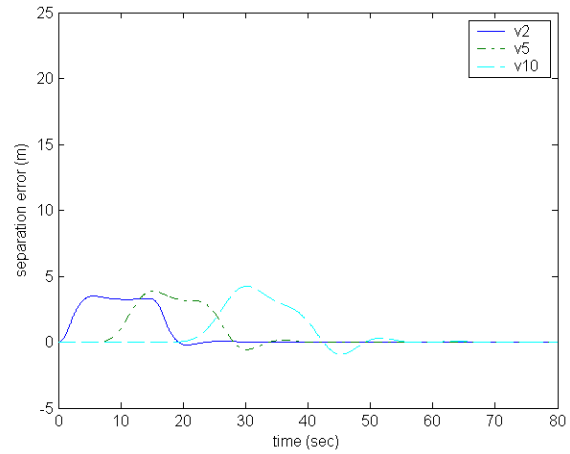
In these simulations, the lead passenger vehicle accelerates from 8m/s to 20m/s with a constant acceleration of 0.8m/s^2 , and then cruises at a constant speed. The 0.8m/s^2 acceleration is easily achievable by passenger vehicles but it is larger than the maximum acceleration a heavy truck could achieve with the particular trailer mass used in the simulations. When the lead passenger vehicle increases its speed with accelerations much smaller than 0.8m/s^2 , a heavy truck can easily follow the preceding vehicle. The five different trucks will behave similarly to a passenger vehicle. However, if the lead passenger vehicle increases its speed faster than 0.8m/s^2 , the responses of the five trucks with different ACC systems are different.

Figures 10(a) and (b) show the speed and separation error responses in vehicle string 1 (all manually driven passenger vehicles), and Figures 11(a) and (b) show the speed and separation error responses in vehicle string 2 (manually driven passenger vehicles with the second vehicle in the string being a manually driven truck). The response labeled by “ v_i ” corresponds to the i th vehicle in the string. These figures indicate that the manually driven truck behavior is similar to that of the second passenger vehicle in vehicle string 1. The truck however has to reach its maximum acceleration limit in order to follow the preceding vehicle, leading to a slightly larger overshoot in the speed response. Furthermore, the maximum transient separation error of the truck is slightly larger than that of the second passenger vehicle in vehicle string 1,

Figures 12, 13, 14 and 15 show the speed, separation error and truck fuel and engine torque responses in vehicle string 3, 4, 5 and 6, respectively. The vehicle following controllers in ACC_N, ACC_Q and ACC_C tend to generate large control efforts in the presence of large speed and separation errors, which easily leads to fuel system saturation. This point can be seen from the fuel responses in Figures 12, 13 and 14. Within the three controller, the one in ACC_N behaves the most aggressively, due to its variable time headway. However, the newly developed ACC controller regulates the truck’s speed towards a smooth reference speed generated by the nonlinear filter in Figure 7. Therefore, its fuel system and engine torque response in a smooth way. The fuel saturation is avoided in Figure 15(c) and the truck’s acceleration is kept within the desired acceleration limits a_{\max} and a_{\min} . The adverse effect caused by the new ACC controller is that it makes the heavy truck more sluggish, and the separation error is larger than those of the other ACC trucks until the truck catches up with the lead vehicle.

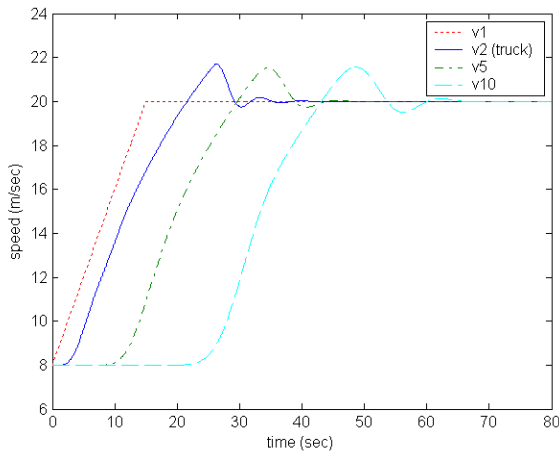


(a)

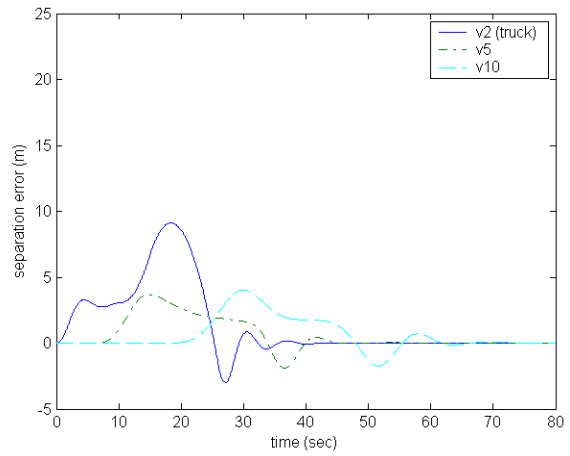


(b)

Figure 10. Low acceleration: (a) speed responses and (b) separation error responses of the vehicles in string 1 (all the vehicles are manually driven passenger vehicles)

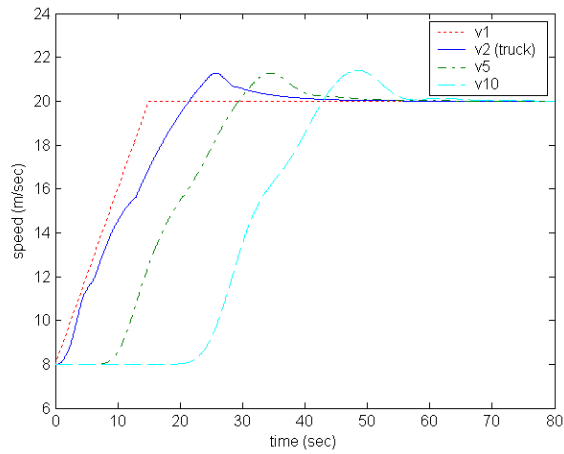


(a)

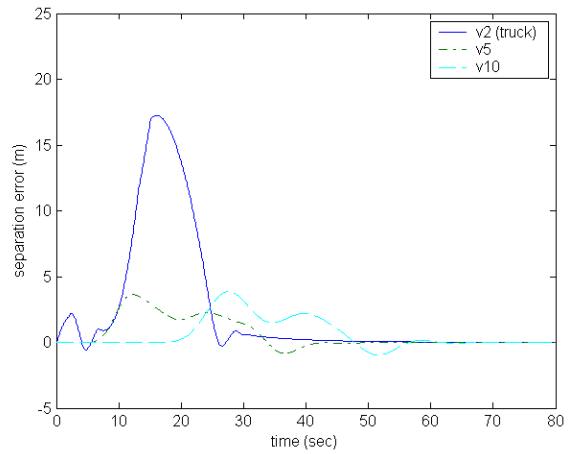


(b)

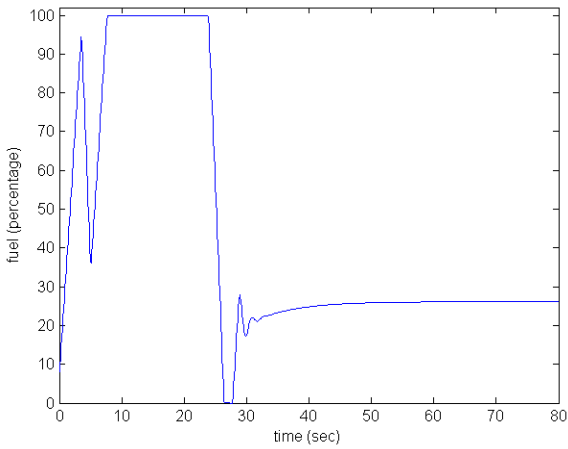
Figure 11. Low acceleration: (a) speed responses and (b) separation error responses of the vehicles in string 2 (the second vehicle is a manually driven heavy truck)



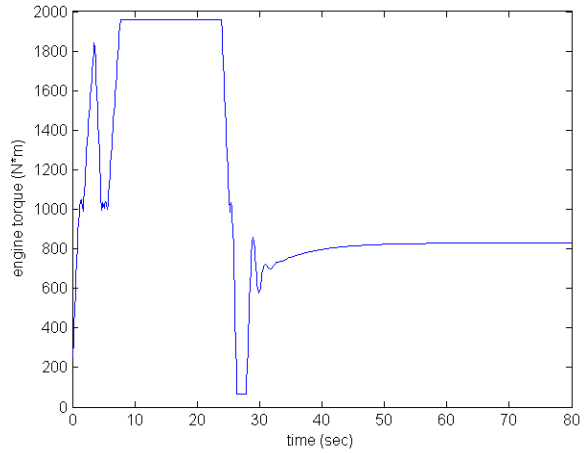
(a)



(b)

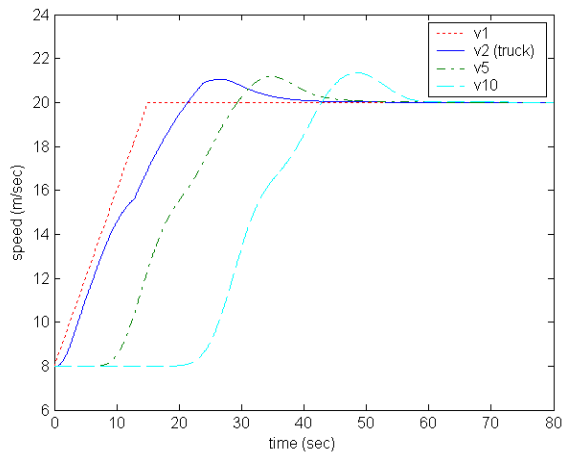


(c)

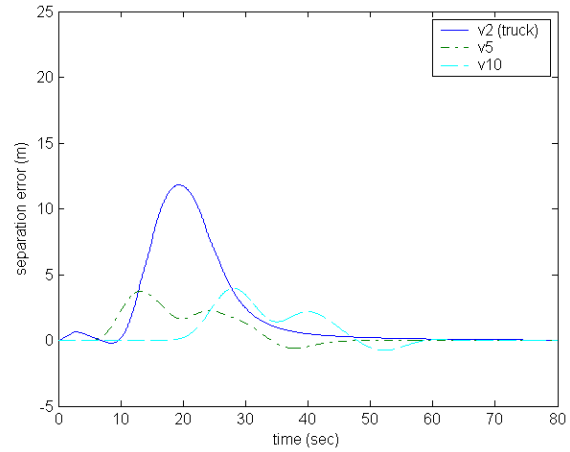


(d)

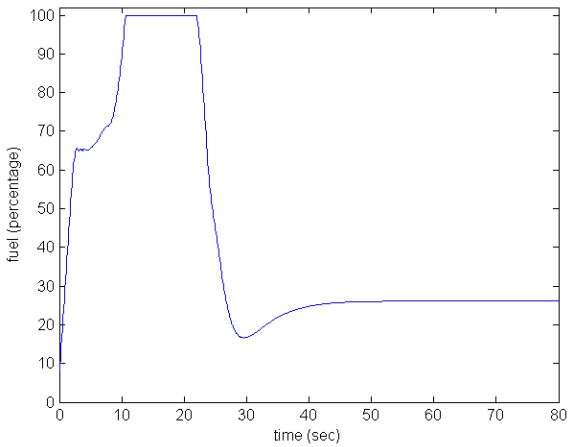
Figure 12. Low acceleration: (a) speed responses and (b) separation error responses of the vehicles in string 3 (the second vehicle is an ACC truck with the nonlinear spacing rule), (c) fuel response and (d) engine torque response of the ACC truck



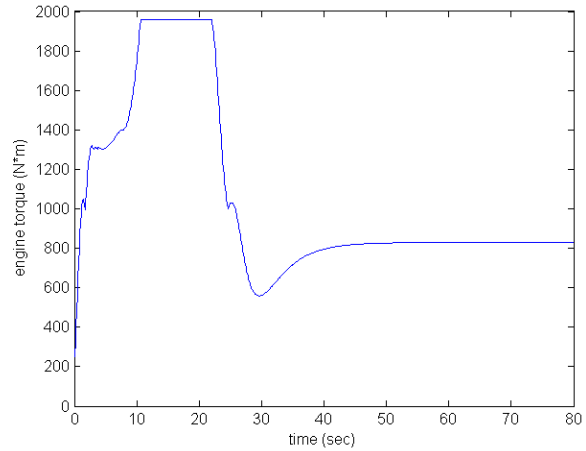
(a)



(b)

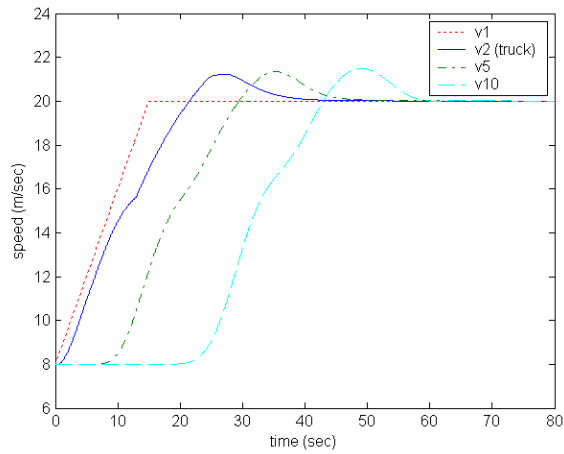


(c)

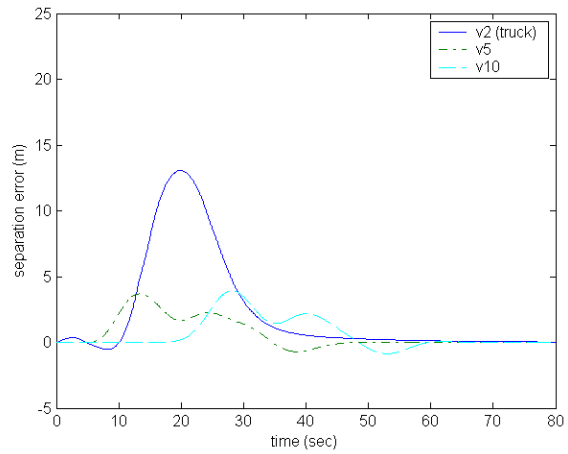


(d)

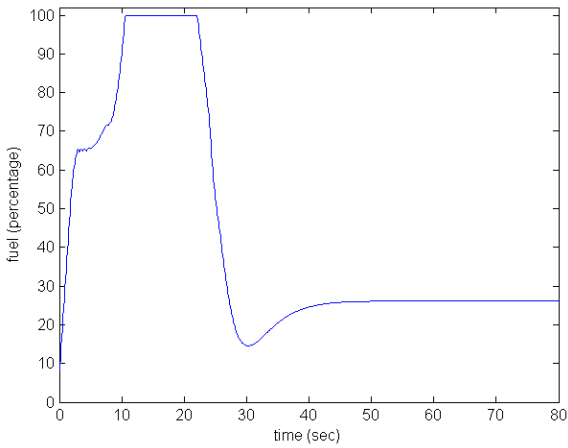
Figure 13. Low acceleration: (a) speed responses and (b) separation error responses of the vehicles in string 4 (the second vehicle is an ACC truck with the quadratic spacing rule), (c) fuel response and (d) engine torque response of the ACC truck



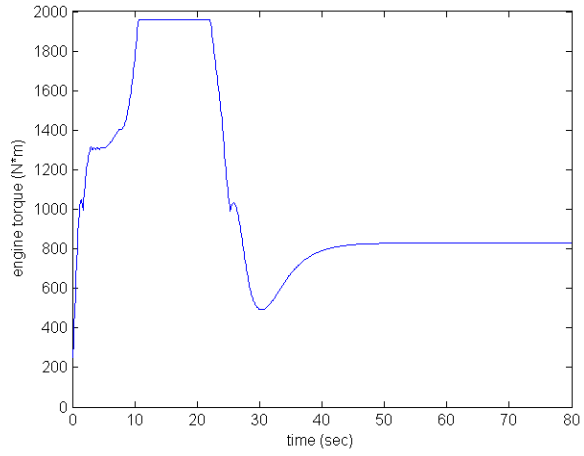
(a)



(b)

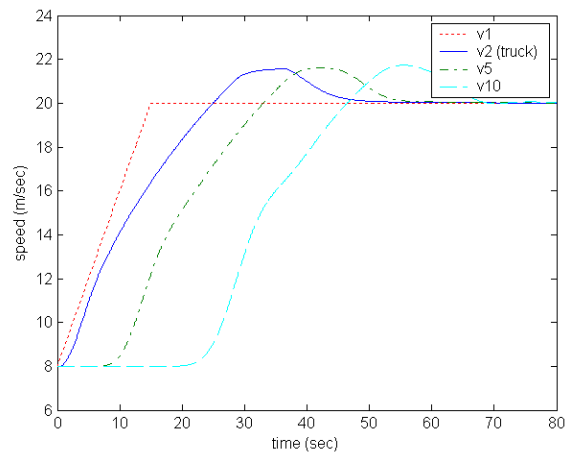


(c)

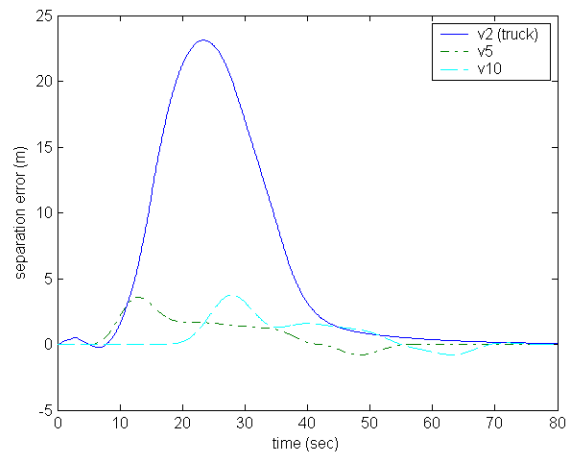


(d)

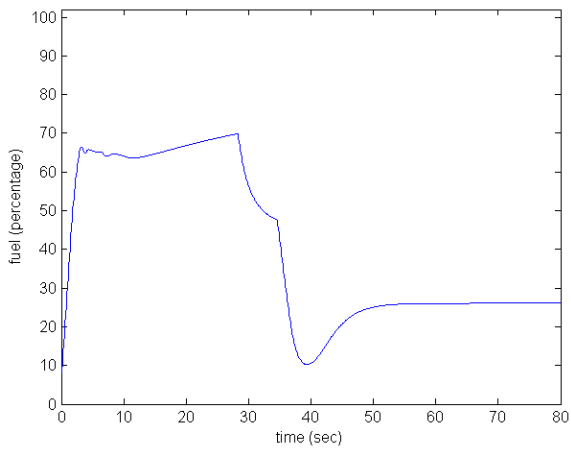
Figure 14. Low acceleration: (a) speed responses and (b) separation error responses of the vehicles in string 5 (the second vehicle is an ACC truck with the constant time headway spacing rule), (c) fuel response and (d) engine torque response of the ACC truck



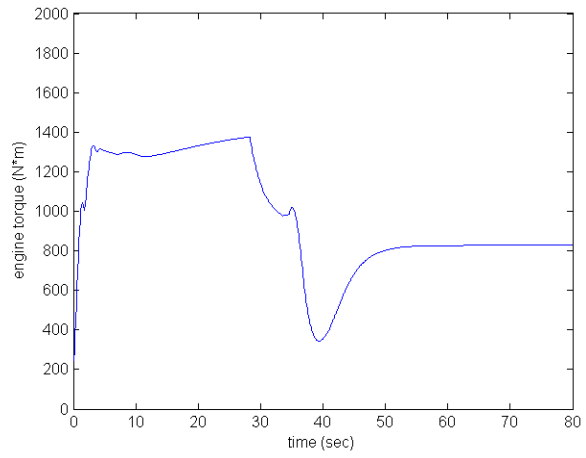
(a)



(b)



(c)



(d)

Figure 15. Low acceleration: (a) speed and separation error responses of the vehicles in string 6 (the second vehicle is an ACC truck with the new controller), (c) fuel response and (d) engine torque response of the ACC truck

3.4.2 High Acceleration Maneuvers

In this case, we want to investigate how heavy trucks would affect the responses of the following passenger vehicles when the lead vehicle accelerates rapidly. In the simulations, the lead passenger vehicle accelerates from 8m/s to 20m/s with a constant acceleration of 2m/s^2 , and then cruises at a constant speed.

Figures 16 and 17 show the speed and separation error responses in vehicle string 1 and 2, respectively. The separation error for the manual truck is temporarily large due to its inability to accelerate as fast as the lead passenger vehicle. The truck driver regulates the vehicle speed to be higher than that of the lead vehicle in order to close in and maintain the desired separation distance. This leads to a peak in the speed response as shown in Figure 17(a). It indicates the slinky effect of a manually driven heavy truck is more serious than that of a passenger vehicle. Figures 18, 19, 20 and 21 show the speed, separation error and truck fuel and engine torque responses in vehicle string 3, 4, 5 and 6, respectively. Figures 18(c), 19(c) and 20(c) indicate that the traditional ACC controllers lead to fuel system saturation very soon in order to track the speed of the lead vehicle and maintain the desired separation. The new ACC controller regulates the truck's speed in a smooth way without having to saturate the fuel system, and the control objective in (3-15) can be achieved eventually.

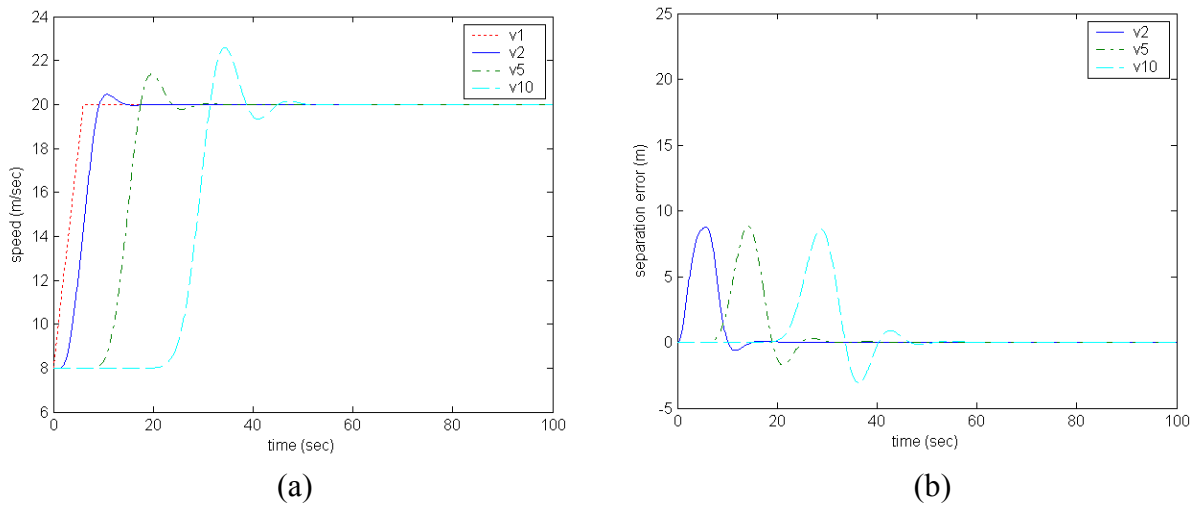


Figure 16. High acceleration: (a) speed responses and (b) separation error responses of the vehicles in string 1 (all the vehicles are manually driven passenger vehicles)

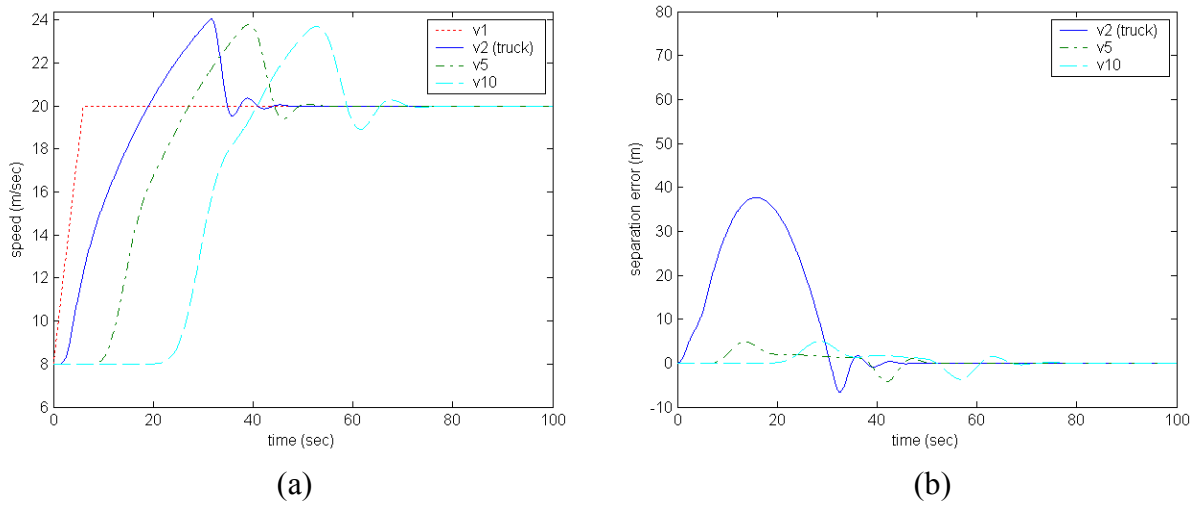


Figure 17. High acceleration: (a) speed responses and (b) separation error responses of the vehicles in string 2 (the second vehicle is a manually driven heavy truck)

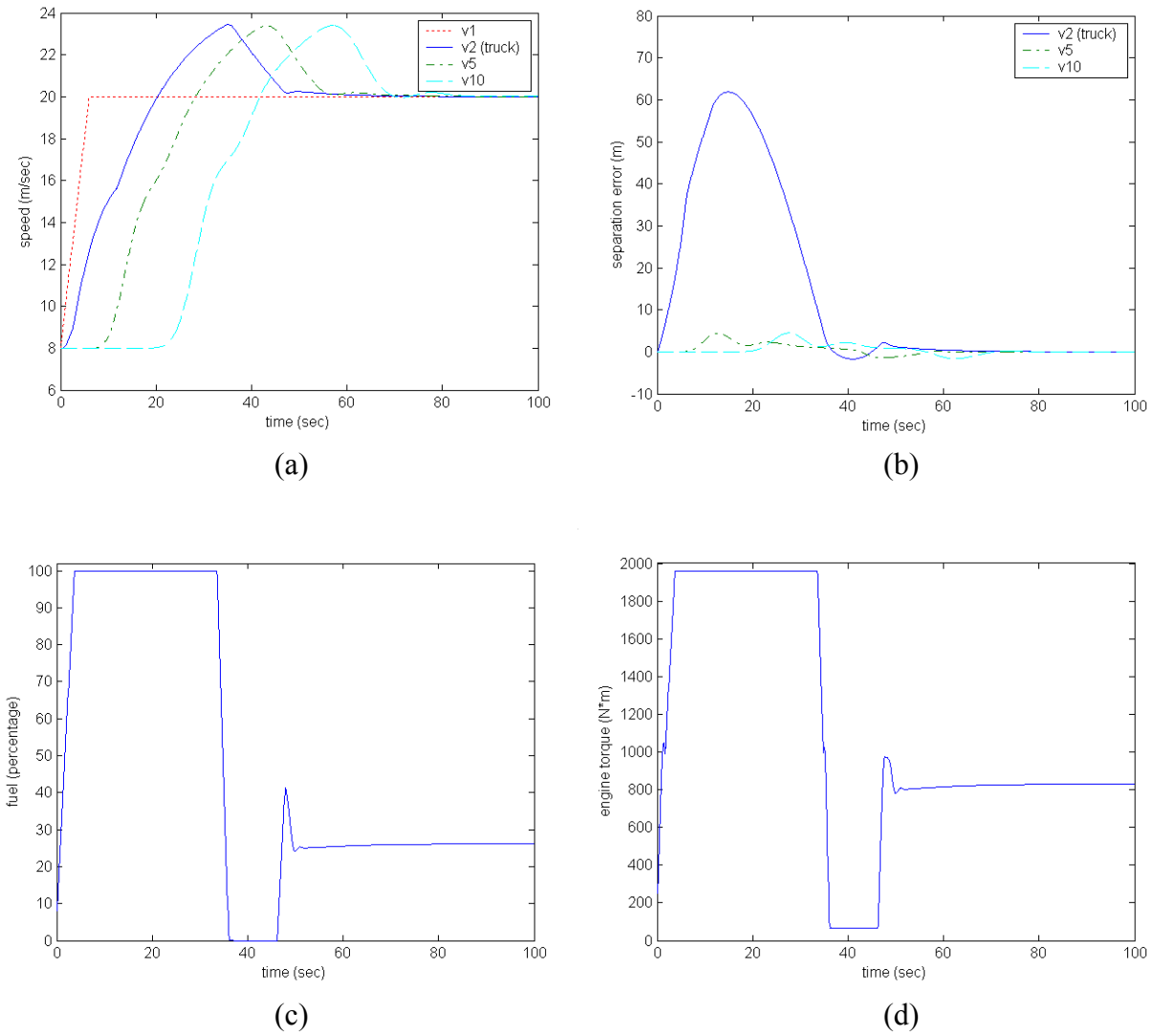
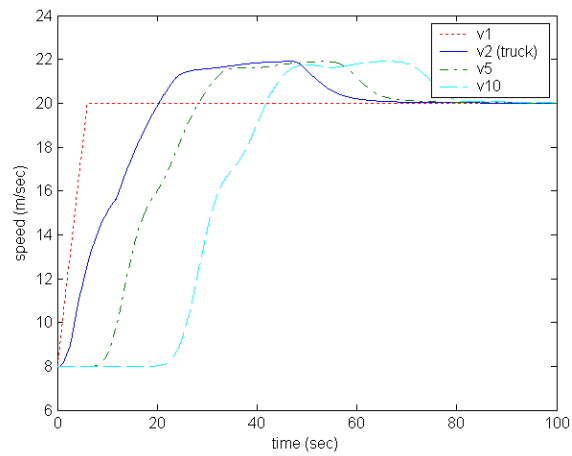
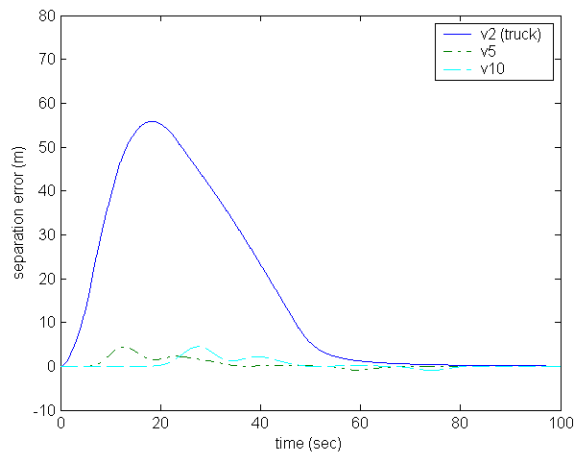


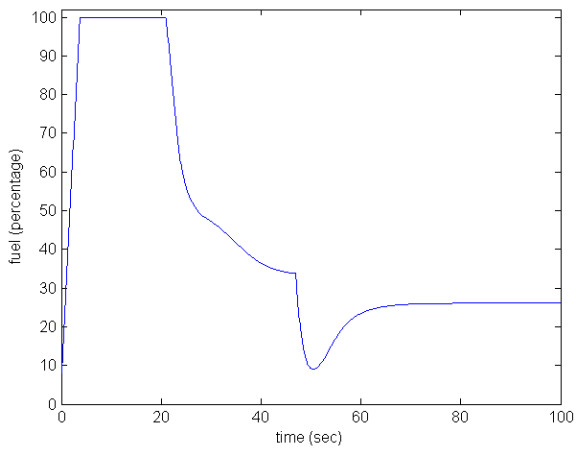
Figure 18. High acceleration: (a) speed responses and (b) separation error responses of the vehicles in string 3 (the second vehicle is an ACC truck with the nonlinear spacing rule), (c) fuel response and (d) engine torque response of the ACC truck



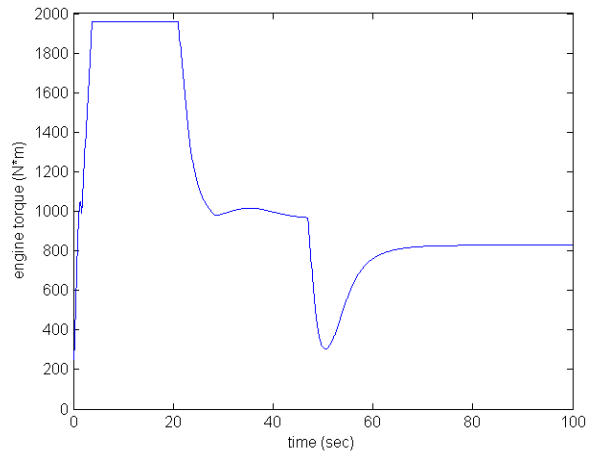
(a)



(b)



(c)



(d)

Figure 19. High acceleration: (a) speed responses and (b) separation error responses of the vehicles in string 4 (the second vehicle is an ACC truck with the quadratic spacing rule), (c) fuel response and (d) engine torque response of the ACC truck

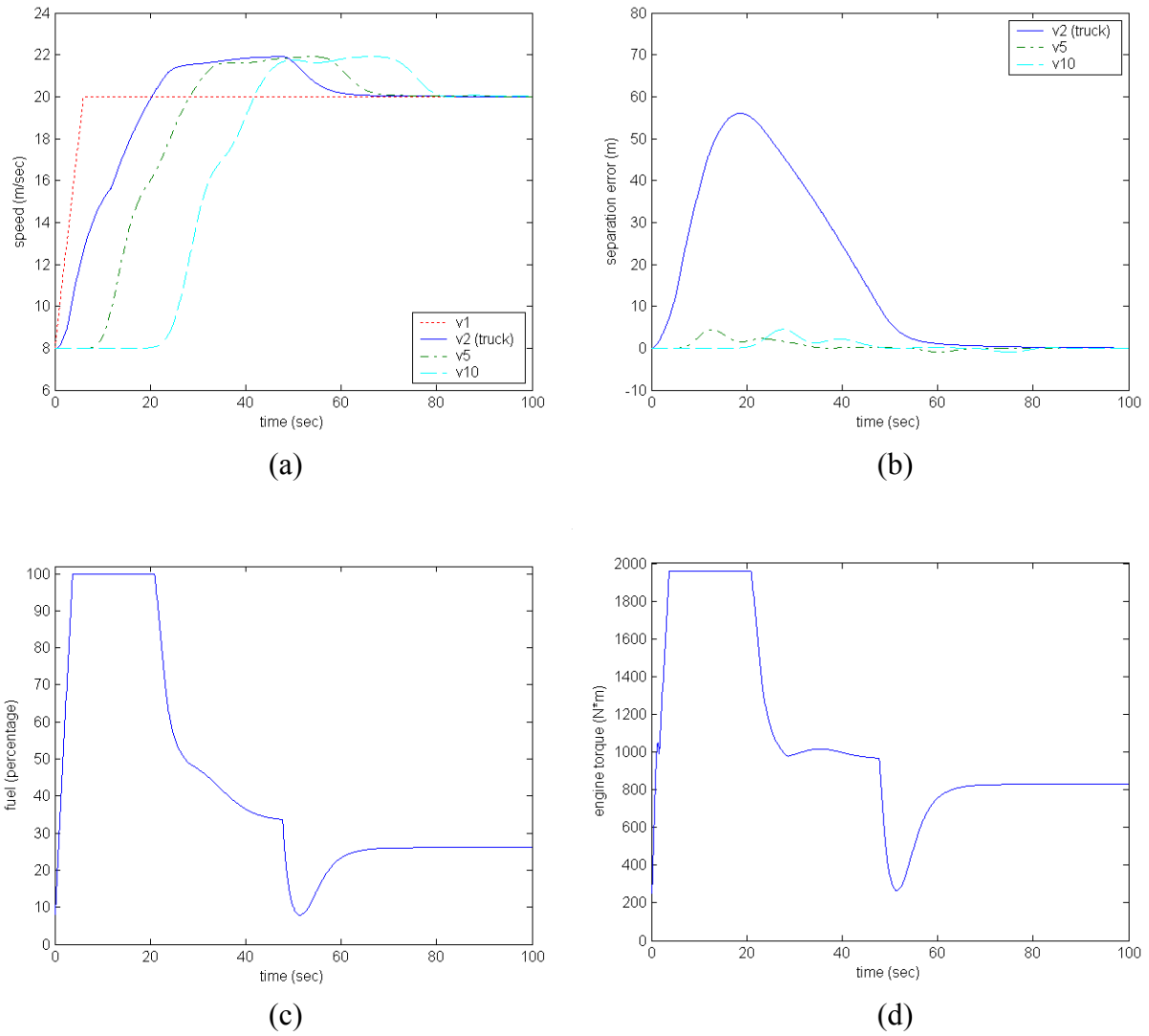
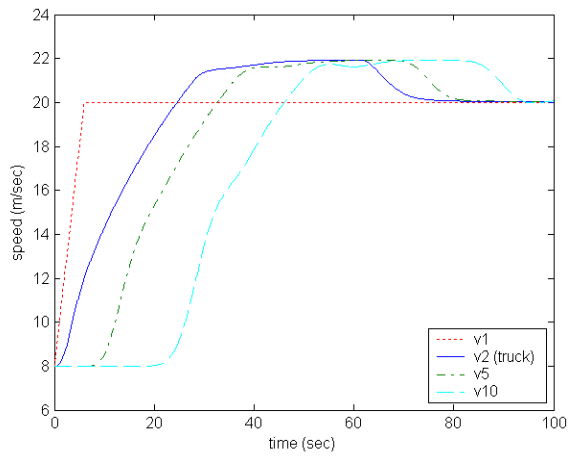
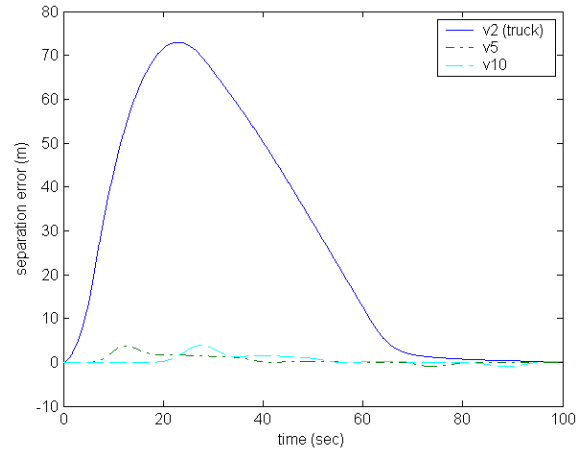


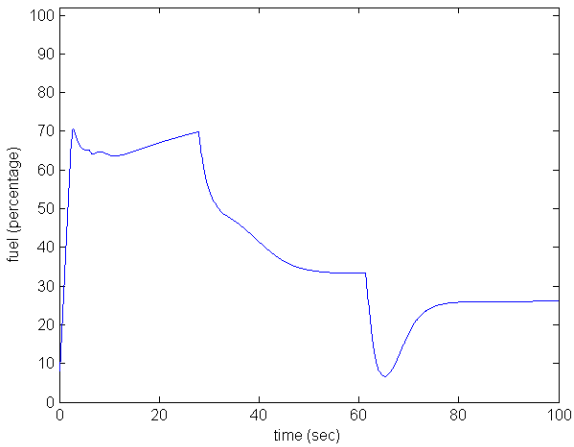
Figure 20. High acceleration: (a) speed responses and (b) separation error responses of the vehicles in string 5 (the second vehicle is an ACC truck with the constant time headway spacing rule), (c) fuel response and (d) engine torque response of the ACC truck



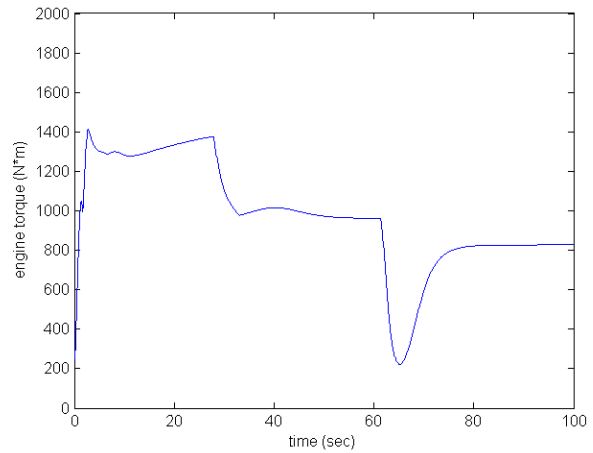
(a)



(b)



(c)



(d)

Figure 21. High acceleration: (a) speed responses and separation error responses of the vehicles in string 6 (the second vehicle is an ACC truck with the new controller), (c) fuel response and (d) engine torque response of the ACC truck

3.4.3 High Acceleration Maneuvers with Oscillations

In this subsection we simulated the situation where the lead passenger vehicle accelerates from 8m/s to 16m/s with a constant acceleration of 2.0m/s^2 , and its speed oscillates around 16m/s before settling to the constant speed of 16m/s. This situation may arise in today's traffic where traffic disturbances downstream create a situation where the driver speeds up and then slows down in an oscillatory fashion before reaching steady state. The speed oscillations may also arise due to lane change behaviors before the lead vehicle. In this situation, the temporary separation distance between the first and second vehicles will be very large, and we would like to investigate how the vehicles in the various strings of vehicles considered will behave with respect to the speed oscillations of the lead vehicle.

Figures 22, 23, 24, 25 and 26 show the speed and separation error responses in vehicle string 1, 2, 3, 4 and 5, respectively. In Figures 22 and 23, the speed disturbance introduced by the lead vehicle is transferred upstream unattenuated due to the aggressive behavior of human drivers. Figure 24 shows that the responses of ACC_N are similar to those of the manually driven truck. ACC_Q behaves better than ACC_N. However, when its speed is larger than that the lead vehicle, the speed disturbance is transferred upstream unattenuated. This is due to the use of $\text{sat}(\delta)$. The control effort generated by (3-17) will be directly affected by v_l , since $\text{sat}(\delta)$ is always a constant when δ is large. The same is true for ACC_C.

Figure 27 shows the speed and separation error responses in vehicle string 6. In this case due to the new ACC truck controller, the speed disturbance is attenuated. This attenuation is due to the use of (3-34). Note, the speed disturbance can only be attenuated when the separation error is positive. When the separation error is negative, the ACC truck's response will be to reduce the separation error for safety reasons rather than reduce the oscillations.

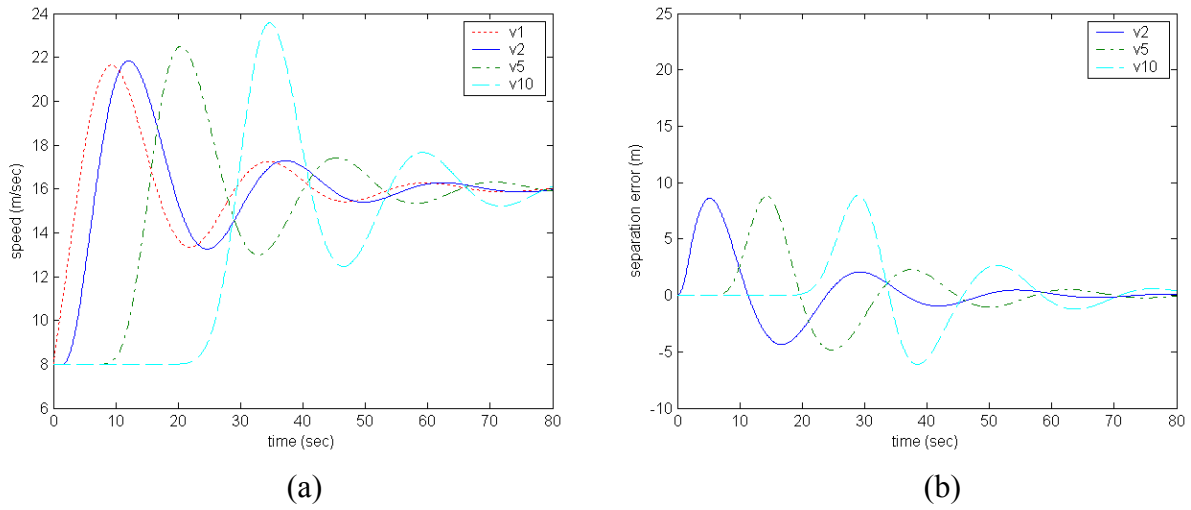


Figure 22. High acceleration with oscillations: (a) speed responses and (b) separation error responses of the vehicles in string 1 (all the vehicles are manually driven passenger vehicles)

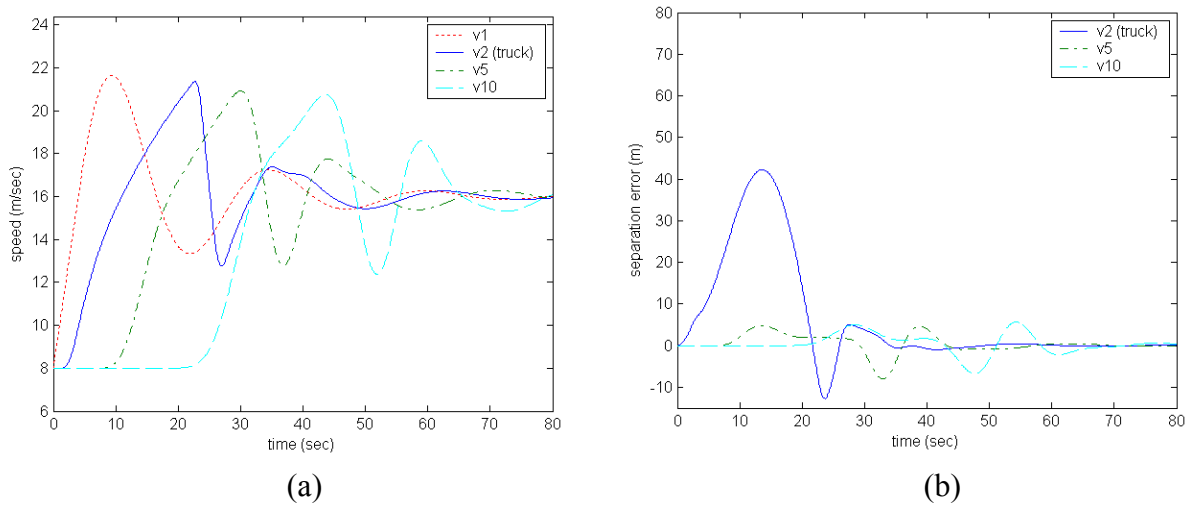
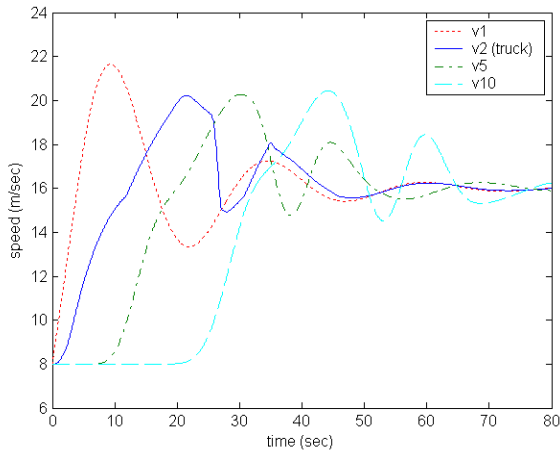
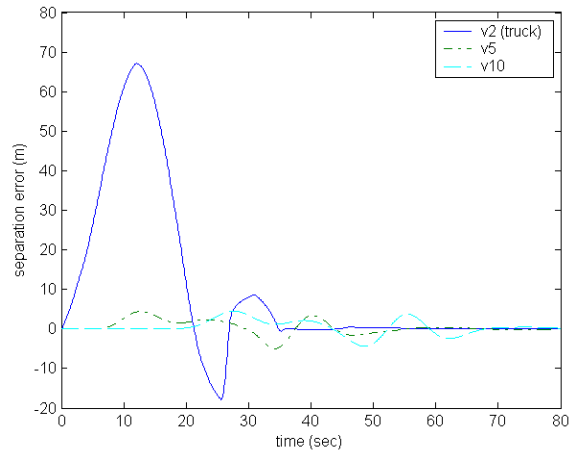


Figure 23. High acceleration with oscillations: (a) speed responses and (b) separation error responses of the vehicles in string 2 (the second vehicle is a manually driven heavy truck)

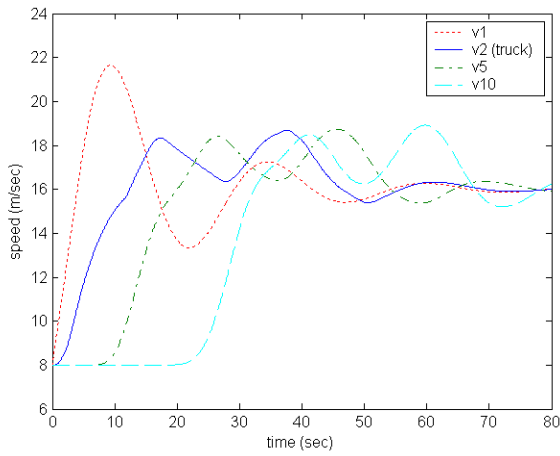


(a)

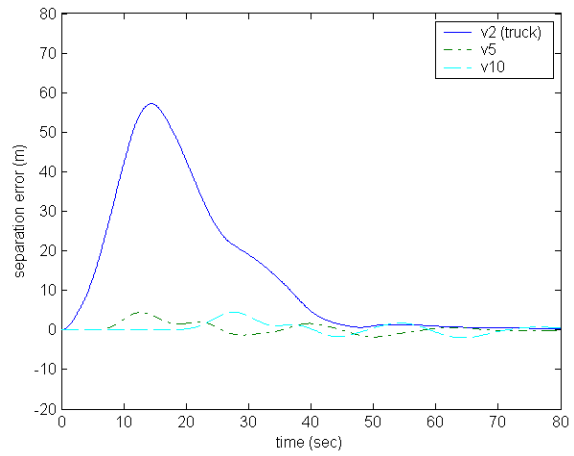


(b)

Figure 24. High acceleration with oscillations: (a) speed responses and (b) separation error responses of the vehicles in string 3 (the second vehicle is an ACC truck with the nonlinear spacing rule)

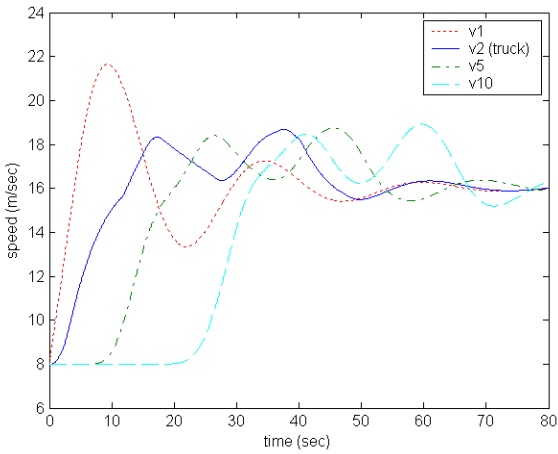


(a)

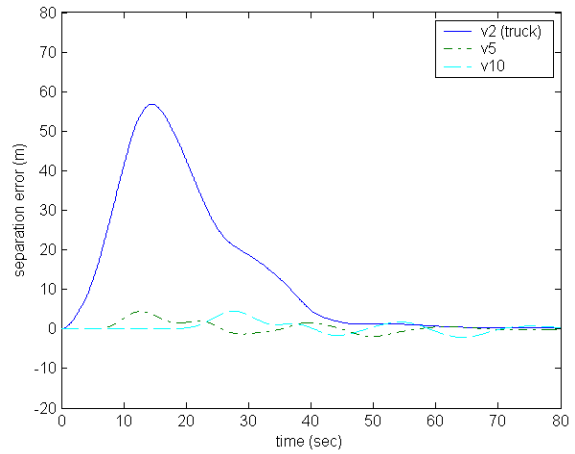


(b)

Figure 25. High acceleration with oscillations: (a) speed responses and (b) separation error responses of the vehicles in string 4 (the second vehicle is an ACC truck with the quadratic spacing rule)

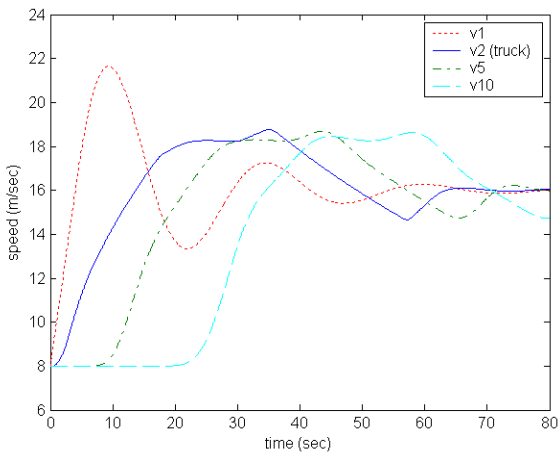


(a)

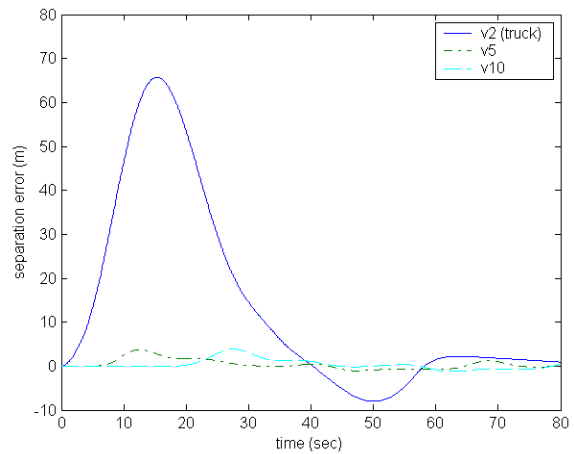


(b)

Figure 26. High acceleration with oscillations: (a) speed responses and (b) separation error responses of the vehicles in string 5 (the second vehicle is an ACC truck with the constant time headway spacing rule)



(a)



(b)

Figure 27. High acceleration with oscillations: (a) speed responses and separation error responses of the vehicles in string 6 (the second vehicle is an ACC truck with the new controller)

3.5 Experimental Testing

Experiments are conducted at Crows Landing test field on December 5th, 2003 to verify the theoretical and simulation results. Due to time limitation and limited number of passenger vehicles, we only tested how the four different ACC systems affect the response of a heavy truck in a string consisting of three vehicles. The lead vehicle was a Buick LeSabre with an automatic speed tracking system. The second vehicle was the heavy truck with different ACC systems. The tractor mass was about eight tons and the trailer mass was about seven tons. The third vehicle was a Buick LeSabre driven by a human driver, following the truck as in normal traffic. The lidar system installed on the truck was used as the ranging sensor providing separation distance and relative speed between the preceding vehicle and the truck. More detailed information about the hardware and software configurations can be found in [26]. Each vehicle was equipped with a Data Acquisition System recording useful experimental data. In the experiments, the parameters for ACC trucks were chosen as:

ACC_N: $h_0=1.6s$, $k_0=1s^{-1}$, $c_h=0.2s$, $c_k=0.5s^{-1}$, $\sigma=0.1m^{-2}$ and $s_0=6.0m$

ACC_Q: $h_1=0.8s$, $h_2=0.03s^2/m$, $k=0.2s^{-1}$ and $s_0=6.0m$

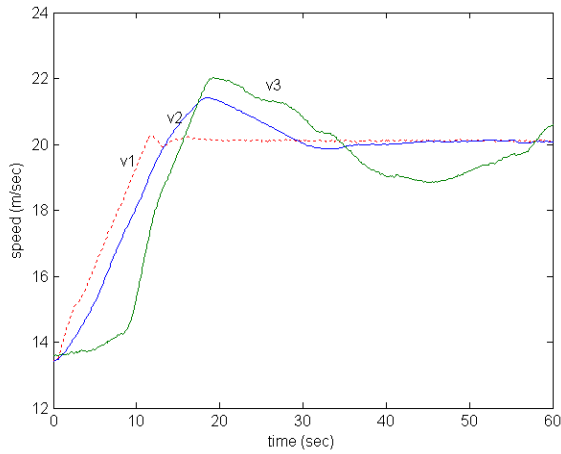
ACC_C: $h=1.6s$, $k=0.2s^{-1}$ and $s_0=6.0m$

ACC_NEW: $h=1.6s$, $k=0.2s^{-1}$, $s_0=6.0m$, $p=10s^{-1}$, $m_v=2.0m/s$, $M_v=8.0m/s$, and a_{max} and a_{min} are acceleration limits chosen based on the capabilities of the truck and desired driver comfort considerations.

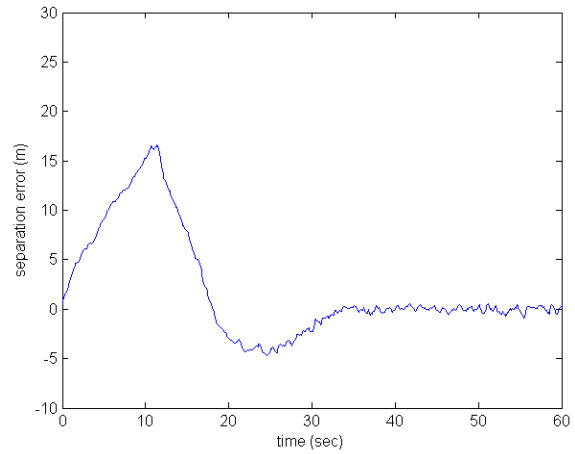
A low-pass filter is placed after each ACC controller to limit the rate of change of the control effort. In ACC_N, ACC_Q and ACC_C, the velocity of the preceding vehicle is passed through the nonlinear filter (the same way as in the simulations).

3.5.1 Low Acceleration Maneuvers

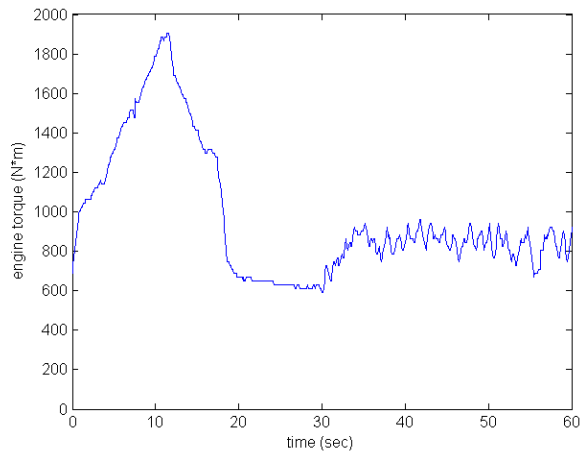
The lead passenger vehicle accelerates from 13.4m/s (about 30 miles per hour) to 20.1m/s (about 45 miles per hour) with a constant acceleration of $0.6m/s^2$, and then cruises at a constant speed. Figures 28, 29, 30 and 31 show the speed responses of the three vehicles (labeled as v1 v2 and v3), and the separation error and engine torque responses for the heavy truck with controllers ACC_N, ACC_Q, ACC_C and ACC_NEW respectively. The controllers ACC_N, ACC_Q and ACC_C behave aggressively in regulating the engine torque in order to follow the lead vehicle tightly. The engine torque is close to the maximum value (about 1966 N-m) for short periods of time. As shown in Figure 31, the new ACC system regulates the engine torque in a smooth way at the expense of a larger separation error.



(a)

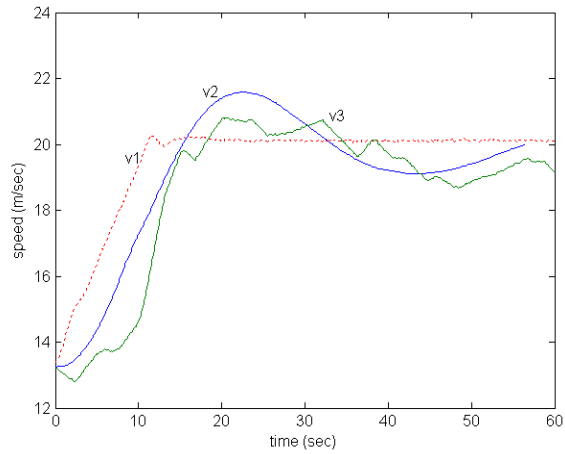


(b)

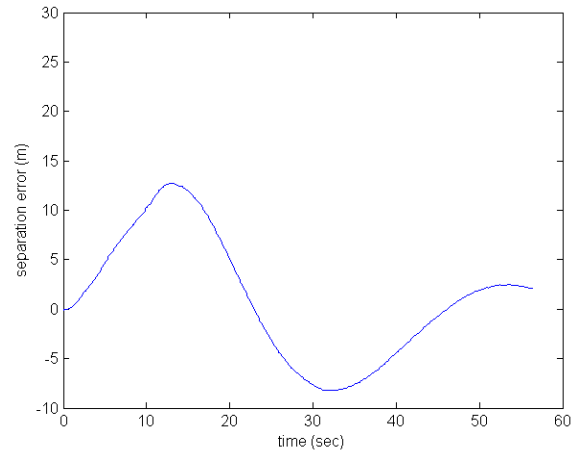


(c)

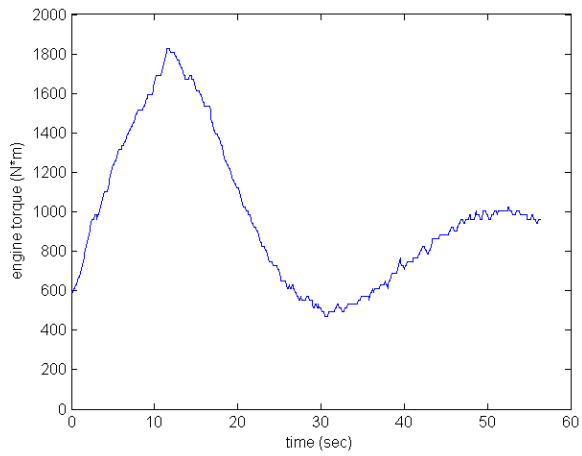
Figure 28. Low acceleration (experiment data): (a) speeds of the three vehicles, (b) separation error and (c) engine torque responses of the ACC truck with the nonlinear spacing rule



(a)

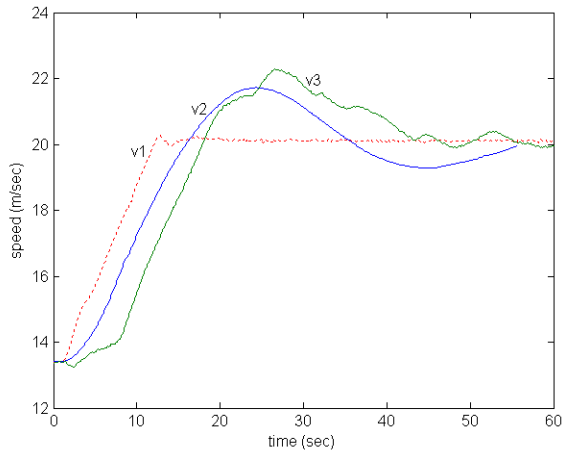


(b)

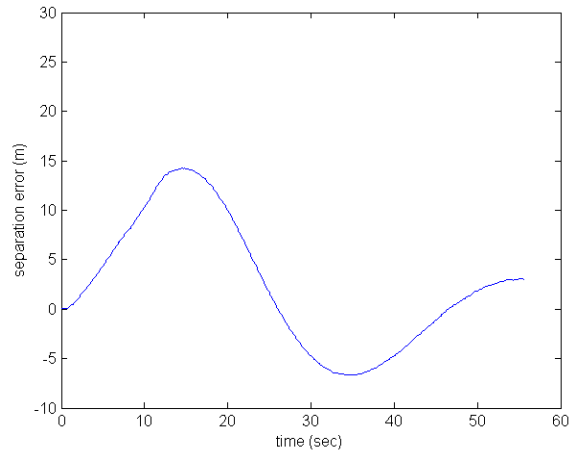


(c)

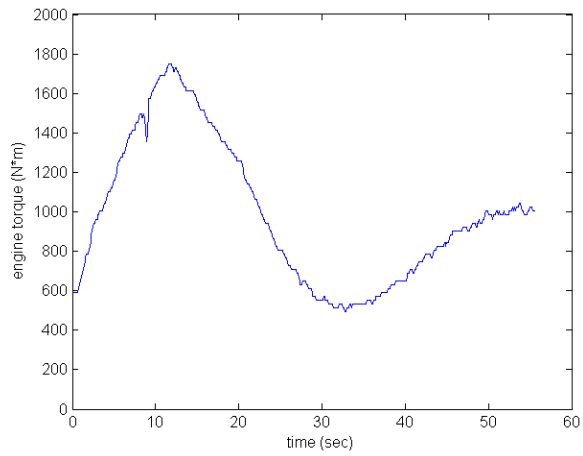
Figure 29. Low acceleration (experiment data): (a) speeds of the three vehicles, (b) separation error and (c) engine torque responses of the ACC truck with the quadratic spacing rule



(a)

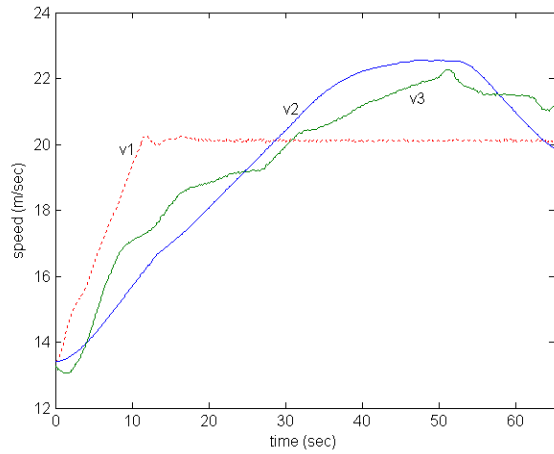


(b)

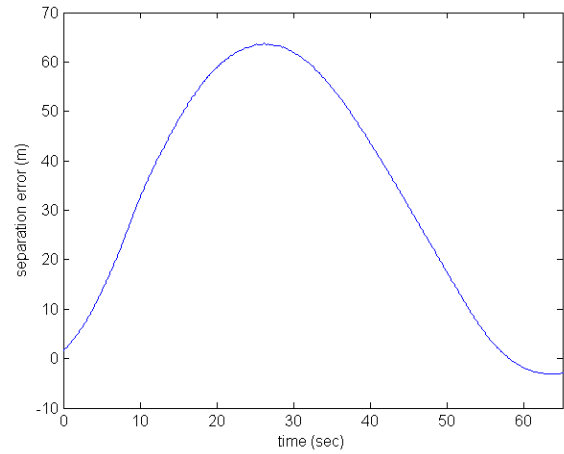


(c)

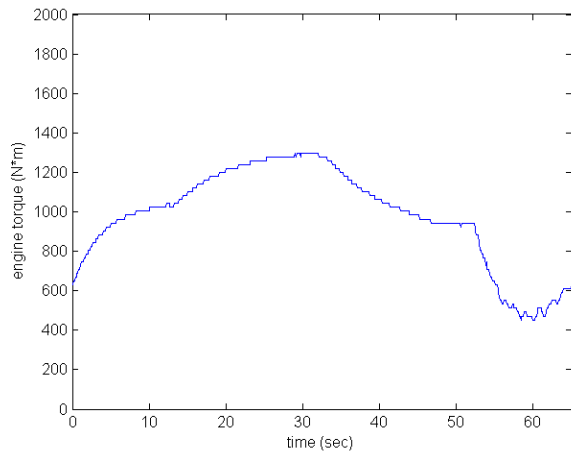
Figure 30. Low acceleration (experiment data): (a) speeds of the three vehicles, (b) separation error and (c) engine torque responses of the ACC truck with the constant time headway spacing rule



(a)



(b)

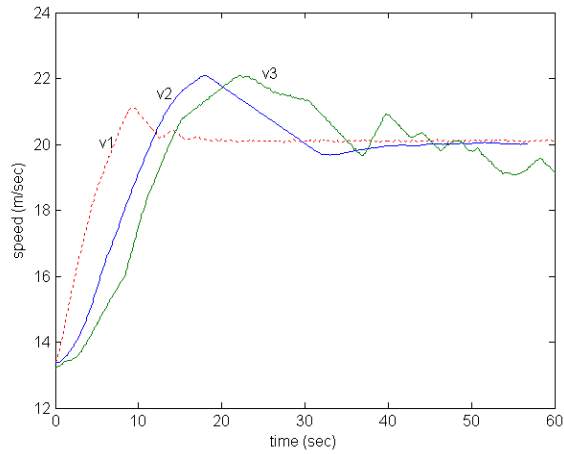


(c)

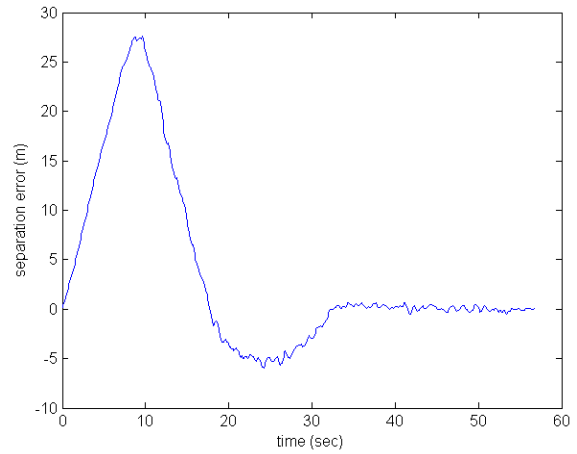
Figure 31. Low acceleration (experiment data): (a) speeds of the three vehicles, (b) separation error and (c) engine torque responses of the ACC truck with the new controller

3.5.2 High Acceleration Maneuvers

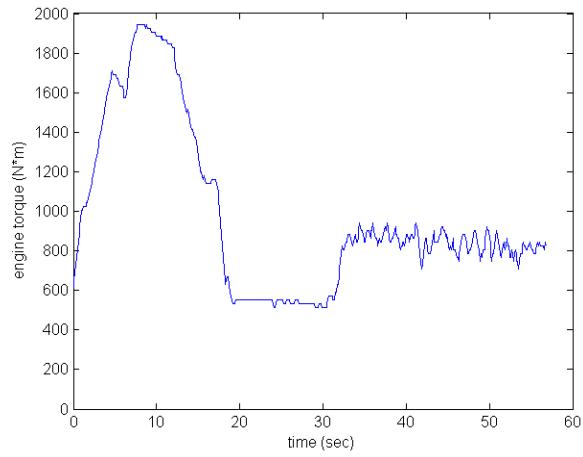
The lead passenger vehicle accelerates from 13.4m/s (about 30 miles per hour) to 20.1m/s (about 45 miles per hour) with acceleration around 1.2m/s^2 , and then cruises at a constant speed. Figures 32, 33, 34 and 35 show the speed responses of the three vehicles, and separation error and engine torque responses for the heavy truck with controllers ACC_N, ACC_Q, ACC_C and ACC_NEW respectively. As before, the controllers ACC_N, ACC_Q and ACC_C behave aggressively in regulating the engine torque, while the new ACC system regulates the engine torque in a smooth way at the expense of creating a larger separation error. It should be noted that in this experiment, the acceleration bounds, a_{\max} and a_{\min} , used for the nonlinear filter in the ACC_NEW controller are different from those used in the previous experiment, and the response of the ACC_NEW is not as sluggish as before.



(a)

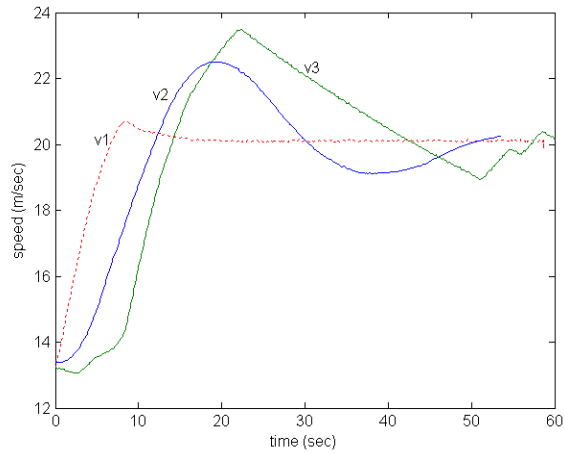


(b)

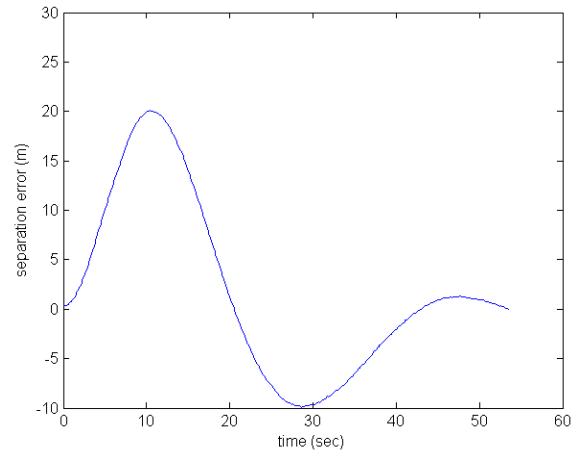


(c)

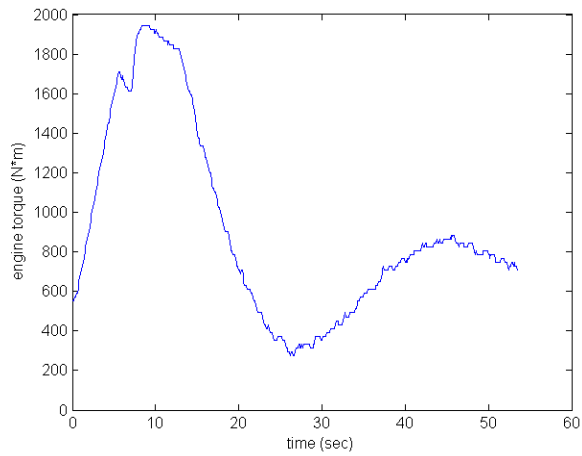
Figure 32. High acceleration (experiment data): (a) speeds of the three vehicles, (b) separation error and (c) engine torque responses of the ACC truck with the nonlinear spacing rule



(a)

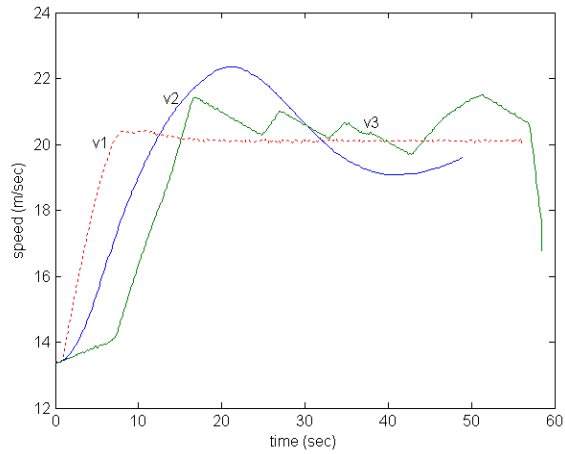


(b)

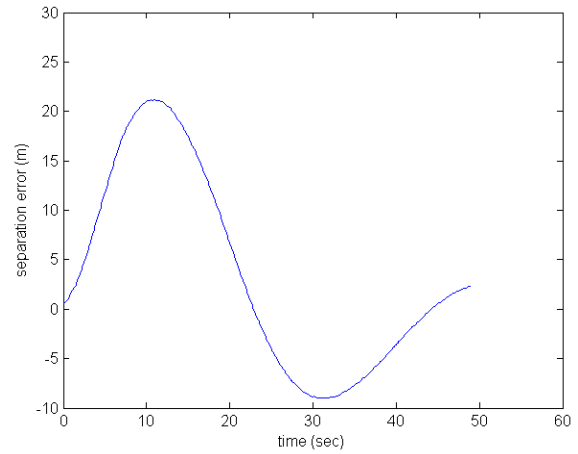


(c)

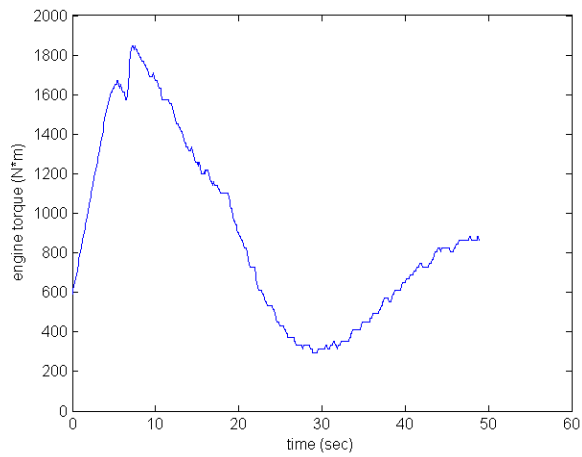
Figure 33. High acceleration (experiment data): (a) speeds of the three vehicles, (b) separation error and (c) engine torque responses of the ACC truck with the quadratic spacing rule



(a)

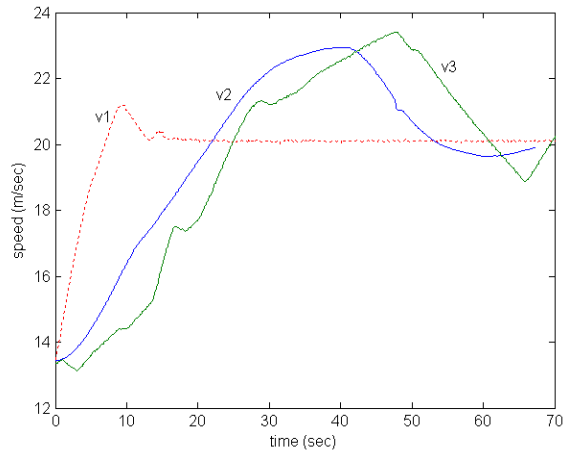


(b)

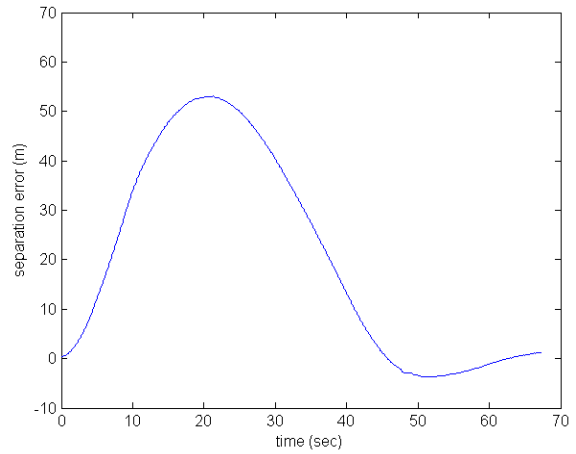


(c)

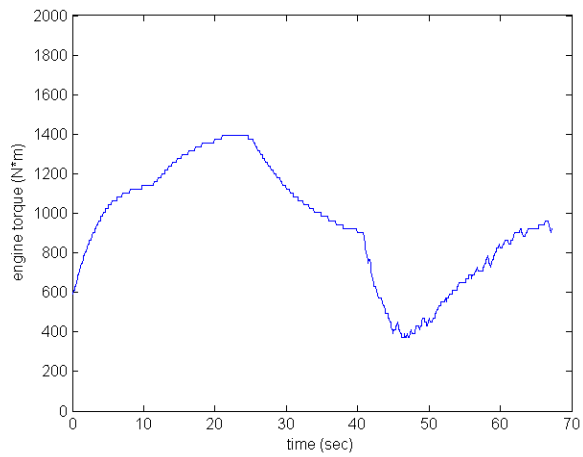
Figure 34. High acceleration (experiment data): (a) speeds of the three vehicles, (b) separation error and (c) engine torque responses of the ACC truck with the constant time headway spacing rule



(a)



(b)



(c)

Figure 35. High acceleration (experiment data): (a) speeds of the three vehicles, (b) separation error and (c) engine torque responses of the ACC truck with the new controller

3.5.3 Model Validation

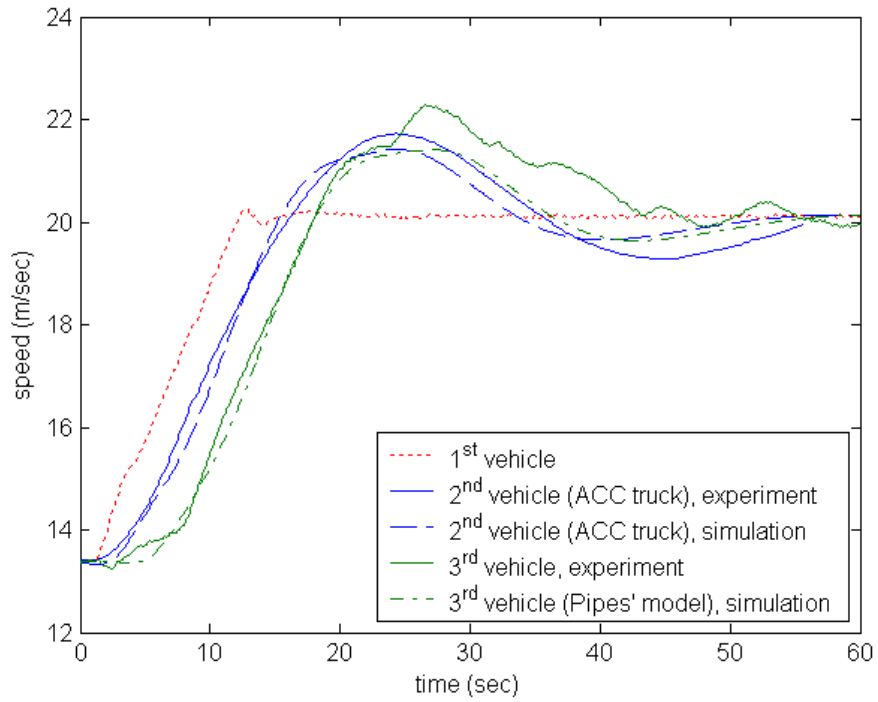
The experiments demonstrated that all the ACC controllers are working on an actual truck in a vehicle following and cruising driving environment. They all have similar responses except for the new ACC controller that is designed to give a smoother response. Even though the number of experiments was limited, the experimental results are valuable in validating our simulation models for the ACC truck and human driver. Our model validation approach is described below.

We simulated the same scenarios as in the experiments using our simulation models. In particular we consider a string of three vehicles where the first and third are manually driven vehicles and the second one is the ACC truck. The first vehicle is made to generate the same speed trajectories as in the experiments. The second vehicle is a heavy truck modeled in the Appendix with one of the ACC systems and the third vehicle is modeled using the Pipes' model.

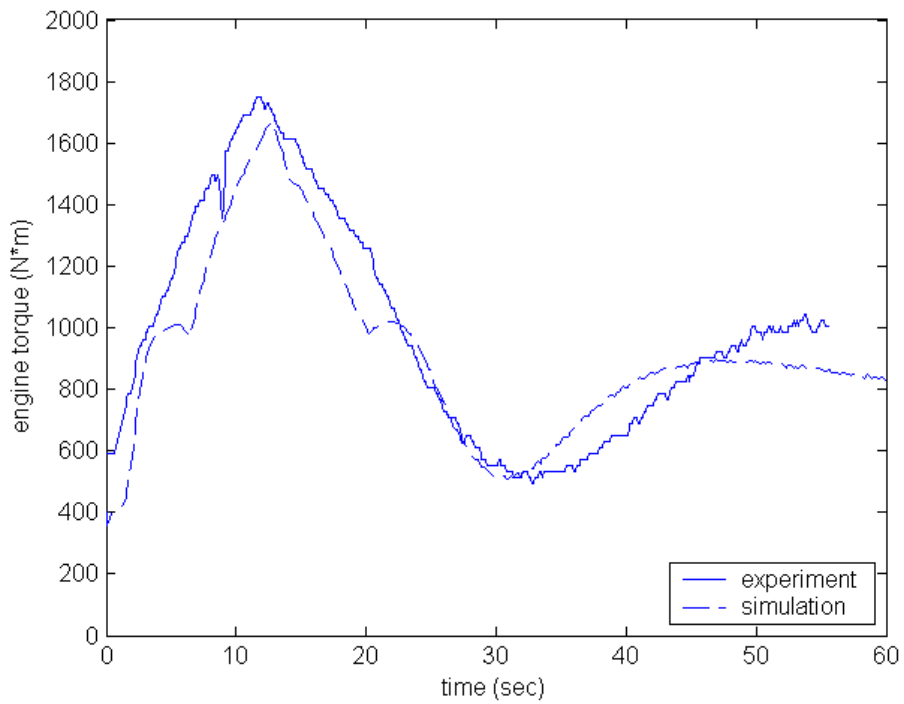
In the first validation test, the first vehicle generates the speed trajectory with low acceleration that was used in the experiments, which is plotted with the red dotted line in Figure 36(a), labeled as "1st vehicle". The speed responses of the ACC truck (with the constant time headway policy) and the passenger vehicle are plotted in Figure 36(a) with broken lines and labeled as "2nd vehicle (ACC truck), simulation" and "3rd vehicle (Pipes' model), simulation", respectively. The corresponding experimental data are also plotted in Figure 36(a) with solid lines and labeled as "2nd vehicle (ACC truck), experiment" and "3rd vehicle, experiment", respectively. It can be seen that the speed responses in the simulation are very close to those in the experiment, which indicates the validation of the used models. The engine torque responses in the simulation and experiment are plotted in Figure 36(b), and they are very similar to each other.

In the second validation test we use the speed trajectory with high acceleration for the first vehicle and the ACC control with the nonlinear spacing rule in (3-31) for the heavy truck. As shown in Figure 37, the similarity between the simulation and experimental results strongly supports that the nonlinear model used for trucks and the Pipes' model are valid.

Additional validation tests supported the same conclusion: the nonlinear model used for heavy trucks and the Pipes' model used to model human driver response in the longitudinal direction are valid models to be used for studying vehicle following in a mixed traffic situation. Consequently our simulation models and results can be used with confidence in studying vehicle following characteristics and effects involving more vehicles in a mixed traffic situation.

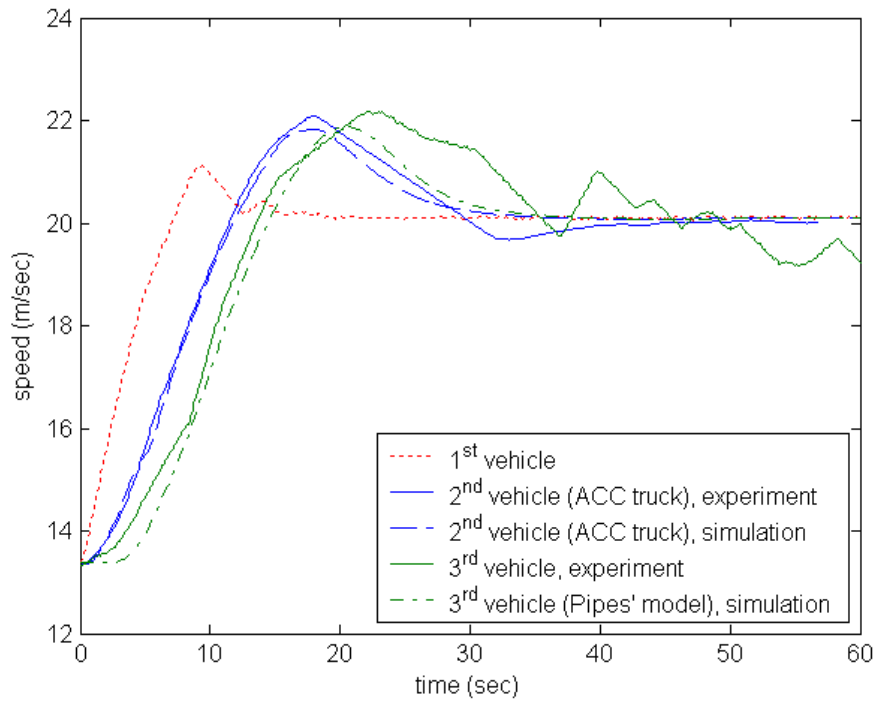


(a)

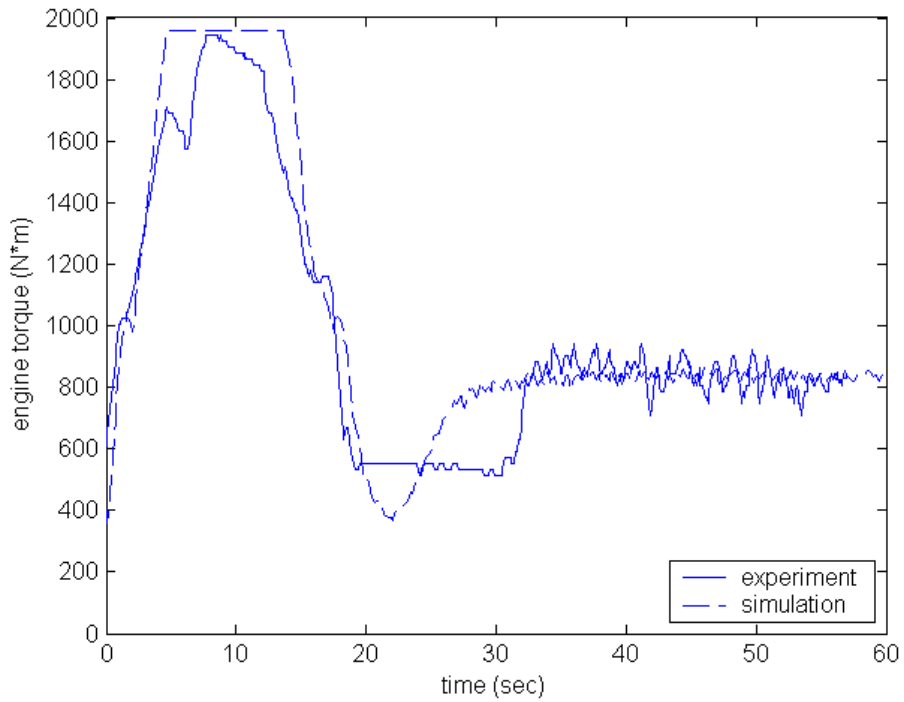


(b)

Figure 36. Model validation: (a) speed responses of the three vehicles (the second is ACC_C) and (b) engine torque responses of ACC_C in experiment and simulation



(a)



(b)

Figure 37. Model validation: (a) speed responses of the three vehicles (the second is ACC_N) and (b) engine torque responses of ACC_N in experiment and simulation

4 IMPACT OF HEAVY TRUCKS ON MIXED TRAFFIC

4.1 Emission and Fuel Consumption

In this section we investigate the impact of heavy trucks on mixed traffic in terms of emission and fuel consumption using the simulation results discussed in the previous section. The emission levels and fuel consumption of an individual vehicle are determined by vehicle parameters such as second-by-second speed, acceleration, road grade, wind gust, and variables associated with vehicle accessories. In the emission analysis, the quantities measured are the tailpipe emissions of unburned hydrocarbons (HC), oxides of carbon (CO, CO₂), oxides of nitrogen (NO, NO₂, denoted by NO_x) and fuel consumption.

4.1.1 Emission Models for Passenger Vehicles and Heavy Trucks

For passenger vehicles, the Comprehensive Modal Emissions Model (CMEM) developed at UC Riverside is used to analyze the vehicle data and calculate the air pollution and fuel consumption [3]. It calculates vehicle emissions and fuel consumption as a function of the vehicle operating mode, i.e. idle, steady state cruise, various levels of acceleration/deceleration, and other variables associated with road and vehicles characters. A simple diagram for the CMEM model is shown in Figure 38. In our simulations, we selected the vehicle category to be 5, which is the most common vehicle type in California: high-mileage, high power-to-weight. The inputs for the CMEM model are vehicle longitudinal speed and acceleration data, while road grade is taken to be zero and no wind gust is considered. Other variables associated with vehicle accessories like air-conditioning are also neglected. The outputs generated by the CMEM models include second-by-second tailpipe emissions of HC, CO, CO₂ and NO_x, and fuel consumption.

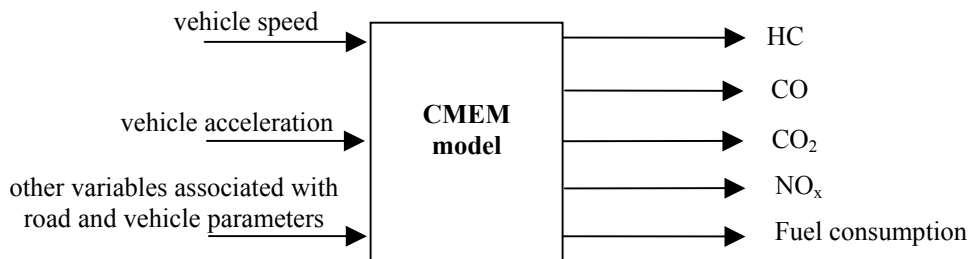


Figure 38. Diagram of the CMEM model

The emission prediction model used for heavy trucks is developed by the same research group at UC Riverside, under PATH TO 4215. Similarly to the CMEM model for passenger vehicles, this model takes as its input the operating parameters such as the vehicle's speed and acceleration data, wind speed, road grade and accessory power.

Vehicle parameters such as vehicle weight, maximum horsepower, gear ratios are pre-set for one specific truck. The output results are instantaneous values of tailpipe pollutant emissions of HC, CO, CO₂ and NO_x, and fuel consumption. More detailed information about the emission models can be found in [2, 3].

4.1.2 Vehicle Following Disturbances

We investigate how the heavy trucks affect the travel time, fuel efficiency and emissions of the passenger vehicles in traffic using the emission models presented in Section 4.1.1 and the simulation results presented in Section 3.4. At the same time, we investigate how different ACC systems affect the fuel efficiency and emissions of the heavy trucks in the presence of different vehicle following disturbances. In this subsection, we assume that no lane changes take place despite the creation of possible large intervehicle spacings during vehicle maneuvers. The effect of lane changes is considered in a separate subsection.

We investigate and compare the behavior of six vehicle strings, each containing ten vehicles using the simulation tests we completed in section 3.4. In vehicle string 1, all the ten vehicles are passenger vehicles (modeled using the Pipes' model (2-4)). Vehicle strings 2, 3, 4, 5 and 6 are almost the same as vehicle string 1, but their second vehicle is replaced by a manually driven truck (modeled using the modified Bando's model in (2-11), an ACC truck with the nonlinear spacing policy in (3-31), an ACC truck with the quadratic spacing policy, an ACC truck with the constant time headway policy and an ACC truck with the newly developed controller, respectively. The same as before, we use ACC_N, ACC_Q, ACC_C and ACC_NEW to represent ACC trucks with nonlinear spacing rule, quadratic spacing rule, constant time headway rule and the newly developed controller, respectively.

Test 1: Low Acceleration Maneuvers

The purpose of this test is to examine the effect of the truck (2nd in the string) on the behavior of the following 8 passenger vehicles when the lead vehicle performs a low acceleration maneuver creating a disturbance that propagates upstream.

The lead passenger vehicle accelerates from 8m/s to 20m/s with a constant acceleration of 0.8m/s², and then cruises at a constant speed. We calculate the fuel consumption and emissions of each vehicle from the time the lead vehicle begins to accelerate, until the string covers a distance of 1.2km. The travel time is recorded over a distance of 1.2km as this is the distance taken by the vehicles to reach a steady state speed after completing the acceleration maneuver.

Table 1 shows the travel time, fuel and emission benefits for the last eight passenger vehicles in each vehicle string in the presence of different truck in the 2nd position in the string of the 10 vehicles. The data in the second column are for vehicle

string 1 (all manually driven passenger vehicles), and the fuel and emission benefits are denoted by 0% and this case is used as the basis for comparison. The data in columns 3-7 are for vehicle strings 2-6, respectively. For the fuel and emission data, a positive number means improvement while a negative number means deterioration. The notation “ ≈ 0 ” in the table represents benefits between -4% and 4% , and is considered to be negligible due to inaccuracies in the emission model. As we can see, the presence of different trucks in the 2nd position in the string will not affect the travel time of the following passenger vehicles. Due to the aggressive response of the manual truck, the fuel and emission benefits are minor except for NO_x as shown in column 3 of Table 1. The smooth response of the ACC trucks filters the disturbance created by the lead vehicle presenting a smoother speed response to be tracked by the passenger vehicles following the truck. As a result some benefits with respect to fuel and emissions are shown in Table 1. These benefits are small due to the fact that the disturbance created was a rather smooth one (low acceleration).

We also evaluate the fuel consumption and emission results for heavy trucks in these simulations and the data are presented in Table 2. The ACC trucks lead to better fuel consumption and emission results compared to the manually driven truck. However, there is little difference among the four different ACC trucks. The benefits are small however due to low level of disturbance.

String of 10 vehicles	Manual Passenger Vehicle in the 2 nd position	Manual truck in the 2 nd position	ACC_N in the 2 nd position	ACC_Q in the 2 nd position	ACC_C in the 2 nd position	ACC_NEW in the 2 nd position
Travel Time (sec)	73.7	73.9	73.3	73.3	73.3	73.3
Fuel (g)	0% (617.8)	≈ 0	≈ 0	≈ 0	≈ 0	4.2%
CO ₂ (g)	0% (1924)	≈ 0	≈ 0	≈ 0	≈ 0	4.2%
CO (g)	0% (20.6)	≈ 0	7.3%	6.4%	6.0%	9.2%
HC (g)	0% (0.93)	≈ 0	7.1%	6.3%	5.9%	9.0%
NO _x (g)	0% (1.51)	9.1%	10.0%	12.1%	10.7%	24.0%

Table 1. Travel time, fuel and emission benefits of the 8 passenger vehicles following the truck in a string of 10 vehicles for low acceleration maneuvers of the lead vehicle (no cut-ins)

	Manual Truck	ACC_N	ACC_Q	ACC_C	ACC_NEW
Fuel (g)	0% (594.8)	5.8%	6.0%	5.4%	6.6%
CO ₂ (g)	0% (1901)	5.9%	6.0%	5.4%	6.5%
CO (g)	0% (5.27)	5.3%	5.3%	5.1%	6.0%
HC (g)	0% (0.26)	≈ 0	≈ 0	≈ 0	≈ 0
NO _x (g)	0% (12.42)	4.8%	4.8%	4.2%	5.4%

Table 2. Fuel and emission benefits of the heavy truck during low acceleration maneuvers of the lead vehicle (no cut-ins).

Test 2: High Acceleration Maneuvers

The purpose of this test is to examine the effect of the truck (2nd in the string) on the behavior of the following 8 passenger vehicles when the lead vehicle performs a high acceleration maneuver creating a disturbance that propagates upstream.

The lead passenger vehicle accelerates from 8m/s to 20m/s with a constant acceleration of 2.0m/s², and then cruises at a constant speed. As in test 1, we consider the same six strings of vehicles with 10 vehicles in each string. The travel time is recorded over a distance of 1.7km as this is the distance taken by the vehicles to reach a steady state speed after completing the acceleration maneuver.

Table 3 shows the travel time, fuel consumption and emission results for the last eight passenger vehicles in the simulations with high acceleration maneuvers. The presence of different trucks in the 2nd position in the string of 10 vehicles does not affect travel time as despite the sluggish response of the truck and the creation of a large intervehicle spacing, the truck eventually closes in by using a higher speed than the lead vehicle. The strings with heavy trucks significantly increase the fuel efficiency and decrease emissions of the following passenger vehicles. The trucks act as low-pass filters presenting a much smoother speed response to be tracked by the vehicles following the trucks in the string. Furthermore, it is observed that all the ACC trucks lead to better fuel consumption and emissions compared with the manual truck. The new ACC system has the best improvements.

String of 10 vehicles	Manual Passenger Vehicle in the 2 nd position	Manual truck in the 2 nd position	ACC_N in the 2 nd position	ACC_Q in the 2 nd position	ACC_C in the 2 nd position	ACC_NEW in the 2 nd position
Travel Time (sec)	96.0	96.2	95.4	95.4	95.4	95.4
Fuel (g)	0% (1020)	15.5%	21.5%	22.7%	22.4%	23.9%
CO ₂ (g)	0% (2828)	5.5%	12.1%	13.4%	13.1%	14.5%
CO (g)	0% (251.2)	87.9%	89.4%	89.9%	89.9%	90.4%
HC (g)	0% (4.02)	65.1%	68.4%	71.5%	71.4%	73.1%
NO _x (g)	0% (4.21)	52.1%	56.0%	60.6%	60.3%	67.7%

Table 3. Travel time, fuel and emission benefits of the 8 passenger vehicles following the truck in a string of 10 vehicles for high acceleration maneuvers of the lead vehicle (no cut-ins)

Table 4 shows the fuel consumption and emission results for different trucks. All the ACC trucks have better results in terms of fuel efficiency and emissions compared with the manually driven truck. This is due to the smoother response of the ACC trucks compared with the more aggressive manually driven truck. However, there is little difference among the four different ACC trucks.

	Manual Truck	ACC N	ACC Q	ACC C	ACC NEW
Fuel (g)	0% (802.0)	10.6%	12.7%	12.6%	12.6%
CO ₂ (g)	0% (2564)	10.4%	12.6%	12.5%	12.5%
CO (g)	0% (7.09)	9.2%	11.1%	11.0%	10.9%
HC (g)	0% (0.34)	4.4%	5.2%	5.1%	5.1%
NO _x (g)	0% (18.14)	7.6%	9.5%	9.5%	10.2%

Table 4. Fuel and emission benefits of the heavy trucks in high acceleration maneuvers (no cut-ins)

Test 3: High Acceleration Maneuvers with Oscillations

The purpose of this test is to examine the effect of the truck (2nd in the string) on the behavior of the following 8 passenger vehicles when the lead vehicle performs a high acceleration oscillatory maneuver creating a disturbance that propagates upstream.

The lead passenger vehicle accelerates from 8m/s to 16m/s with a constant acceleration of 2.0m/s², and its speed oscillates around 16m/s before settling to the constant speed of 16m/s. The travel time is recorded over a distance of 1.3km as this is the distance taken by the vehicles to reach a steady state speed after completing the acceleration maneuver.

Table 5 shows the travel time, fuel consumption and emission results for the last eight passenger vehicles in each vehicle string. The travel time of the following passenger vehicles is little affected by the trucks. It follows from Table 5, that the presence of heavy trucks can significantly improve the fuel efficiency and decrease most of the emissions. This is due to the fact that the inherent sluggish characteristics of the heavy trucks can attenuate the high frequency components in the speed of the lead vehicle. Among the ACC trucks, the ACC_NEW leads to the best results in all aspects, since it filters the oscillations in the lead vehicle's speed more effectively than the others.

String of 10 vehicles	Manual Passenger Vehicle in the 2 nd position	Manual truck in the 2 nd position	ACC_N in the 2 nd position	ACC_Q in the 2 nd position	ACC_C in the 2 nd position	ACC_NEW in the 2 nd position
Travel Time (sec)	88.0	88.1	87.5	87.5	87.6	87.6
Fuel (g)	0% (860.3)	23.9%	29.7%	34.2%	34.0%	36.3%
CO ₂ (g)	0% (2245)	9.8%	16.0%	21.3%	21.0%	23.6%
CO (g)	0% (298.3)	90.2%	93.5%	94.5%	94.5%	95.1%
HC (g)	0% (4.45)	73.7%	79.3%	82.4%	82.8%	84.2%
NO _x (g)	0% (4.87)	59.4%	65.0%	68.8	69.0%	78.7%

Table 5. Travel time, fuel and emission benefits of the 8 passenger vehicles following the truck in a string of 10 vehicles for high acceleration maneuvers with oscillations of the lead vehicle (no cut-ins)

Table 6 shows the fuel consumption and emissions results for different trucks. All the ACC trucks lead to better fuel consumption and emissions results compared with the manually driven truck, and the performance of the new ACC system is the best.

	Manual Truck	ACC_N	ACC_Q	ACC_C	ACC_NEW
Fuel (g)	0% (618.2)	12.0%	23.1%	22.9%	27.4%
CO ₂ (g)	0% (1976)	12.0%	23.0%	22.8%	27.4%
CO (g)	0% (5.55)	10.6%	20.0%	20.0%	23.6%
HC (g)	0% (0.28)	4.8%	8.5%	8.5%	12.4%
NO _x (g)	0% (13.2)	9.1%	17.0%	17.2%	21.5%

Table 6. Fuel and emission benefits of the trucks in high acceleration maneuvers with oscillations (no cut-ins)

From the data presented in Tables 1, 3 and 5, we can see that the presence of heavy trucks in the mixed traffic can improve fuel consumption and emissions of the passenger vehicles, especially in the presence of disturbances due to high acceleration maneuvers. The heavy trucks act as filters due to their sluggish response and present to the following vehicles upstream smoother speed responses to be tracked. Furthermore, the ACC trucks lead to better fuel and emissions results than the manually driven trucks due to their smoother response. In the case of high acceleration maneuvers with oscillations, the heavy truck with the newly developed ACC controller (ACC_NEW) filters the oscillations more effectively leading to better fuel and emission results than the other ACC trucks.

The results obtained raised several questions that require further investigation. First the validity of the emission models and their accuracy needs to be revisited in collaboration with the UC Riverside researchers that developed the emission models for passenger vehicles and trucks. While most of the benefits obtained make sense qualitatively a quantitative validation is necessary by using actual experiments and measuring fuel and pollutants in real time. In our approach we assume that the lead vehicle reaches a steady state giving time for the truck to close in by using a higher speed leading to a travel time that is not affected by the presence of the truck. We can also create scenarios where the travel time will be affected when the truck does not speed up to close in with the lead vehicle especially when the truck cannot achieve a higher speed due to load and speed limits. In such situations another effect takes place as the sluggish response of the truck creates large inter vehicle gaps inviting vehicles from neighboring lanes to cut in front of the truck. This effect is investigated in the next subsection.

4.1.3 Lane Change Effect

The motivation for studying lane change effects in mixed traffic with heavy trucks and passenger vehicles is based mostly on the fact that the sluggish response of the heavy truck results in a large temporary gap between the truck and the accelerating passenger

vehicle in front, giving rise to multiple cut-ins from the neighboring lanes. In this subsection, we consider various cut-in situations, and study the effects of lane changes using microscopic simulations. It is assumed that when the spacing between the truck and its preceding vehicle is large enough (larger than $s_0 + 2.8v_t$, where v_t is the truck speed), one or more passenger vehicles from the neighboring lane cut in between the two vehicles and position themselves with safe intervehicle spacings. In this simulation, the truck is considered to be equipped with the new ACC system, followed by eight passenger vehicles. We like to investigate how the disturbance created by the cut-ins will affect the response of the truck and that of the passenger vehicles following the truck.

We consider the situation where the passenger vehicle leading the ACC truck accelerates from 8m/s to 20m/s with a constant acceleration of 2m/s^2 , and then cruises with a constant speed creating a large inter vehicle spacing. We assume that three vehicles cut in at 5, 10.6 and 17.5 seconds, respectively, and with the speeds of 12.2, 18.0 and 21.0m/s, respectively. These cut-ins are shown in Figure 39. We consider the travel time, fuel consumption and emissions for the last eight passenger vehicles after they have traveled 1.7km, and present them in the right column of Table 7. For comparison purpose, the corresponding data for the situation without cut-in vehicles are also presented in Table 7. From Table 7, we can see that the disturbance created by the cut-ins has a small negative effect on fuel consumption and emissions. However, the travel time is increased by about 4 seconds due to the cut-ins.

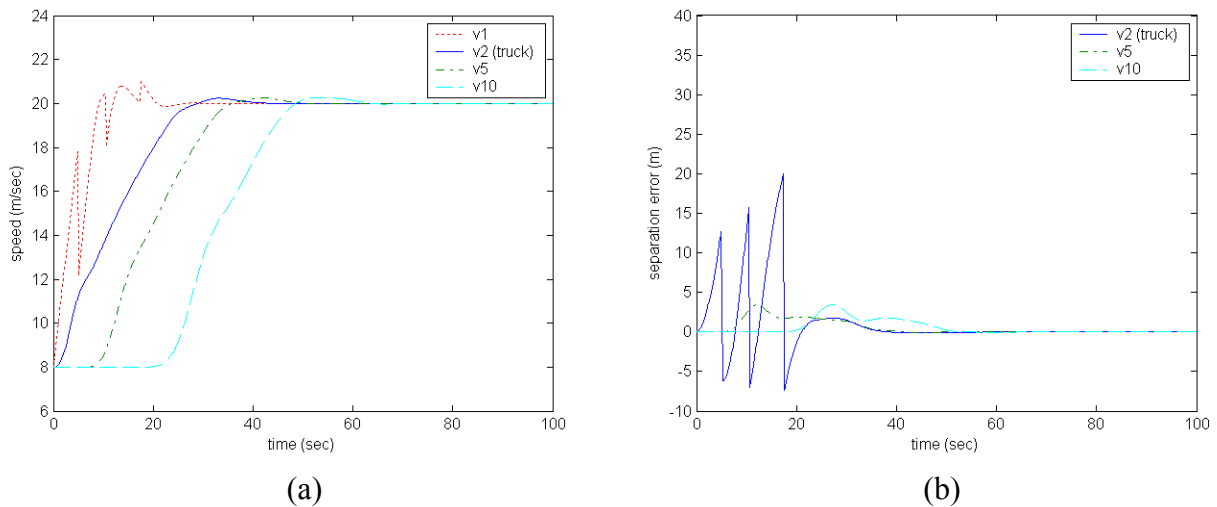


Figure 39. Responses of the vehicles in string 6 in high acceleration maneuvers with three cut-in vehicles: (a) speed responses and (b) separation error responses

	Without Cut-in(s)	With Cut-in(s)
Travel Time (sec)	95.4	99.5
Fuel (g)	776	811 (-4.5%)
CO₂ (g)	2418	2531 (-4.5%)
CO (g)	24.2	24.3 (-0.4%)
HC (g)	1.08	1.11 (-2.8%)
NO_x (g)	1.36	1.40 (-2.9%)

Table 7. Travel time, fuel and emission data of the 8 passenger vehicles following ACC_NEW in high acceleration maneuvers, without cut-in(s) and with three cut-ins

Note that the above simulation results are based on the cut-in situations considered. If we consider more aggressive cut-ins for example, a passenger vehicle at a low speed cuts in just a few meters ahead of the heavy truck forcing the truck to decelerate and then speed up, different results may be obtained as the disturbance created in such scenario may have a more adverse effect on fuel economy and pollution. Furthermore cut-ins will create disturbances in the neighboring lane too with adverse effects on fuel economy and pollution for the vehicles in those lanes. Our conclusion is that while the heavy trucks with ACC or not have smooth responses and filter traffic disturbances their sluggish behavior will create large gaps inviting cut-ins which may take away any benefits their filtering response will have for the vehicles in their lane. Furthermore, the cut-ins will create additional disturbances in the neighboring lanes that will also have a negative effect on fuel economy and pollution.

4.2 Macroscopic Traffic Flow Analysis

In this section we investigate the effect of heavy trucks manually driven and with ACC on traffic flow characteristics in mixed traffic on the macroscopic level using the fundamental flow-density diagram. A fundamental flow-density diagram defines the steady-state relation between the traffic flow rate and the traffic density [17]. We outline flow-density diagrams for 100% manual and 100% ACC vehicles traffic, and discuss the impact on the flow-density curves caused by heavy trucks. The manual traffic flow-density curve discussed in this report is constructed using the linear relationship between speed and density hypothesized by Greenshields [9]. The 100% ACC traffic flow-density curve is constructed using the ACC design with the constant time headway policy. The effect of heavy trucks mixed with passenger vehicles in the presence of traffic flow disturbances is also analyzed.

4.2.1 Fundamental Flow-Density Diagram

The fundamental flow-density diagram defines the steady-state relation between the traffic flow rate q and the traffic density ρ . The precise definitions of these two traffic

variables and the means of measuring them are explained in [17]. In this subsection we focus on the flow-density diagrams for 100% manual and 100% ACC traffic and the impact of heavy trucks on these flow-density diagrams.

4.2.1.1 Manual/ACC Traffic without Heavy Trucks

In this subsection, we assume all the vehicles in the traffic stream are passenger vehicles. The presence of heavy trucks will be considered in the next subsection. In constructing the fundamental flow-density diagram for the 100% manual vehicles traffic, we consider the hypothesis in [9] that

$$v = \left(1 - \frac{\rho}{\rho_{\max}}\right)v_f \quad (4-1)$$

where v is the vehicles' mean speed (or traffic flow speed), v_f is the free speed corresponding to negligible traffic density when there is no interaction among vehicles, and ρ_{\max} is the density corresponding to the jam condition when all the vehicles are in standstill due to congestion. The maximum value of ρ_{\max} is equal to $1/L$ where L is the average length of vehicles and corresponds to the case where vehicles are bumper to bumper. In practice, the bumper-to-bumper situation will never happen. Hence we add some intervehicle spacing to L . In the following analysis, L is larger than the average length of a vehicle.

The traffic flow rate q at steady state measures the number of vehicles moving in a specified direction on the road per unit time and is given by

$$q = \rho v \quad (4-2)$$

With (4-1), the manual traffic flow-density relationship at steady state is given by

$$q = \rho \left(1 - \frac{\rho}{\rho_{\max}}\right)v_f \quad (4-3)$$

The fundamental $q-\rho$ diagram labeled as "100% manual" in Figure 40 is generated using (4-3). It follows from (4.3) that the traffic flow rate achieves its maximum value

$$q_{mm} = \frac{\rho_{\max} v_f}{4} \text{ when the traffic density is } \rho_{cm} = \frac{\rho_{\max}}{2}.$$

While the behavior of human drivers is random and at best we can develop a manual traffic flow-density model that is qualitatively valid, the response of ACC vehicles is more deterministic due to the use of a specific spacing policy. In this report we consider the ACC designs that use a constant time headway policy. For simplicity we assume that all ACC vehicles have the same length L and use the same time headway h_a .

When the traffic density is low, we can assume no vehicle interaction and all the ACC vehicles operate close to the free speed v_f . As the traffic density increases, and reaches the value

$$\rho_{ca} = \frac{1}{h_a v_f + L} \quad (4-4)$$

the ACC vehicles begin to interact with each other. The total spacing, s , occupied by an ACC vehicle using a constant time headway h_a at a speed v is given by

$$s = h_a v + L \quad (4-5)$$

Note, the safe distance term s_0 in the spacing policy (3-14) has been incorporated into L . Since s is the reciprocal of ρ , from (4-5), we can get

$$v = \frac{1}{h_a} \left(\frac{1}{\rho} - L \right) \quad (4-6)$$

According to (4-6), the steady-state speed of the ACC vehicles decreases with increasing ρ until ρ reaches its maximum value $\rho_{\max} = 1/L$. The fundamental flow-density diagram for the traffic with 100% ACC vehicles is given by

$$q = \begin{cases} \rho v_f & 0 \leq \rho \leq \rho_{ca} \\ (1 - \rho L)/h_a & \rho_{ca} < \rho \leq \rho_{\max} \end{cases} \quad (4-7)$$

Equation (4-7) does not capture effects that are due to individual vehicle responses but describes the average steady state traffic flow characteristics. The relationship described by (4-7) can be graphically viewed as the curve labeled as “100% ACC” in Figure 40.

The maximum traffic flow rate for the 100% ACC traffic, q_{mc} , is equal to $\frac{v_f}{h_a v_f + L}$.

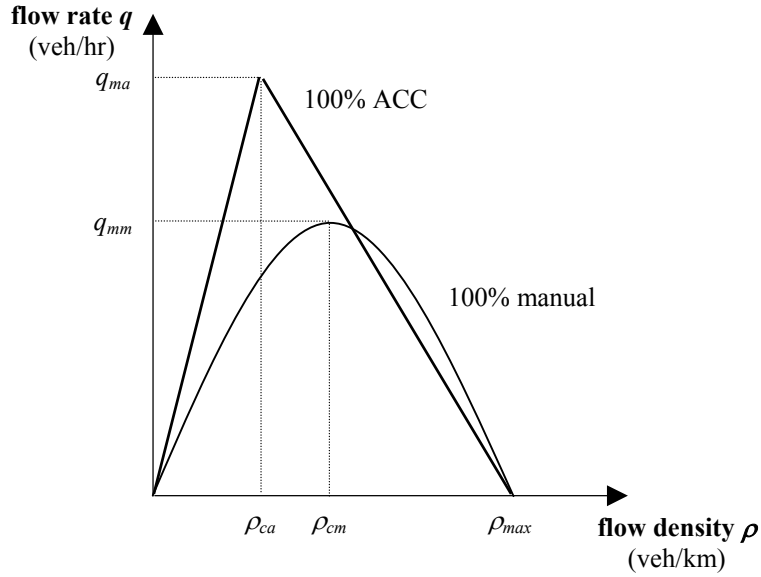


Figure 40. Fundamental flow-density diagrams of the manual traffic and the ACC traffic

If the traffic is dense enough to be viewed as a fluid, then from the conversation of mass equation, we have

$$\frac{\partial \rho}{\partial t} + \frac{\partial q}{\partial x} = 0 \quad (4-8)$$

Further assuming that the human driver or the ACC system can adjust the vehicle's speed instantaneously to the steady state value based on the current traffic density, we can treat q as a function that depends only on ρ , and (4-8) can be rewritten as

$$\frac{\partial \rho}{\partial t} + c \frac{\partial \rho}{\partial x} = 0 \quad (4-9)$$

where

$$c = \frac{dq}{d\rho} = v + \rho \frac{\partial v}{\partial \rho} \quad (4-10)$$

When the traffic density on any road section is close to a constant ρ_0 , c can be approximated as a constant equal to $v(\rho_0) + \rho_0 \left. \frac{\partial v}{\partial \rho} \right|_{\rho=\rho_0}$, which can be interpreted as the slope of the tangent to the $q - \rho$ curve at $\rho = \rho_0$. When c is a constant, the solution of (4-9) is a traveling wave

$$\rho(x,t) = F(x - ct) \quad (4-11)$$

where F is an arbitrary differentiable function. If v is a non-increasing function of ρ , which is true in practice, we can see that $c \leq v$ always holds. This means the traveling wave always propagates backwards relative to the traffic flow. If $c > 0$, then any density disturbance propagates as a forward traveling wave. If $c < 0$, then the density disturbance propagates as a backward traveling wave, which indicates that any density disturbance is traveling upstream in the space without any attenuation. Using the flow-density relationship of manual traffic described by (4-3), it can be shown that

$$c = v_f \left(1 - \frac{2\rho}{\rho_{\max}} \right) = 2v - v_f \quad (4-12)$$

It follows that c is a strictly decreasing function of ρ and

$$\begin{cases} c \geq 0, & \text{if } \rho \in [0, \rho_{cm}] \\ c < 0, & \text{if } \rho \in (\rho_{cm}, \rho_{\max}] \end{cases} \quad (4-13)$$

In the 100% manual traffic, the $q - \rho$ curve has a stationary point that corresponds to a critical density ρ_{cm} that gives the maximum traffic flow rate q_{mm} or the capacity on that section of the road. The point (q_{mm}, ρ_{cm}) has been empirically observed to be unstable, i.e. it leads to a breakdown in traffic flow [5]. When the traffic flow conditions exist at or near this point, the traffic flow rate and the average speed decrease as the traffic density increases, and the operating point moves towards the jam density ρ_{\max} on the $q - \rho$ curve. This observation is explained in [33]. As capacity is approached, the flow tends to become unstable as the number of available gaps reduces. Traffic flow at capacity means that there are no usable gaps left. A disturbance in such a condition due to lane changing or vehicle merging is not ‘effectively damped’ or ‘dissipated’. As indicated by (4-11) and (4-13), any disturbance propagates upstream without attenuation. This leads to a breakdown in traffic flow and ‘formation of upstream queues’. As pointed out in [33], this is the reason why all facilities are designed to operate at lower than the maximum traffic flow conditions.

For the ACC traffic described by (4-7), it follows that

$$c = \begin{cases} v_f, & \text{if } \rho \in [0, \rho_{ca}] \\ -\frac{L}{h_a}, & \text{if } \rho \in (\rho_{ca}, \rho_{\max}] \end{cases} \quad (4-14)$$

where ρ_{ca} is the critical density given in (4-4). From (4-13), it follows that the speed of the traveling wave is the same as the average speed of all the ACC vehicles when the

traffic density is lower than ρ_{ca} . When the traffic density is higher than ρ_{ca} , any disturbance in the traffic will propagate upstream with a constant speed L/h_a . As we can see, selecting large h_a can slow the speed of traveling waves, but decrease the maximum traffic flow rate.

Let us consider the stability of the point (q_{ma}, ρ_{ca}) , which corresponds to the point (q_{mm}, ρ_{cm}) in the manual traffic. It is not possible to empirically determine the stability of (q_{ma}, ρ_{ca}) . However, it is expected that the point (q_{ma}, ρ_{ca}) will also be unstable, i.e. at this operating point there will be a breakdown in traffic flow [5]. As in the manual traffic, flow will tend to become unstable as capacity is approached and the number of available gaps reduces. At critical density there will be no usable gaps left. Any disturbance generated at this condition is expected to lead to the formation of upstream queues and a breakdown in traffic flow, as observed in the manual traffic [5]. From (4-14), it can be shown that when $\rho \in (\rho_{ca}, \rho_{max}]$, the traffic is unstable in the sense that disturbances propagate upstream unattenuated [22].

4.2.1.2 Manual/ACC Traffic with Heavy Trucks

In the previous subsection, we have developed a flow-density model that qualitatively describes manual traffic flow characteristics, and a deterministic flow-density model for ACC traffic. We have assumed that all the vehicles in the traffic stream are passenger vehicles of the same size and use the same spacing rule. In this subsection, we consider how the heavy trucks affect the fundamental flow-density diagrams and the traveling waves, i.e. the traffic disturbances. To simplify the analysis, we consider the case where the vehicles are all manually driven or ACC operated. In either situation (manual or ACC), there are only two classes of vehicles, passenger vehicles and heavy trucks. The vehicles of the same class have the same size and use the same spacing rule. Hence, at steady state conditions, vehicles of the same class use identical intervehicle spacings. For the ACC case, the intervehicle spacing is equal to the designed value for the ACC controller considered. For the manual case, the inter vehicle spacing is taken to be equal to the average value observed in manual traffic.

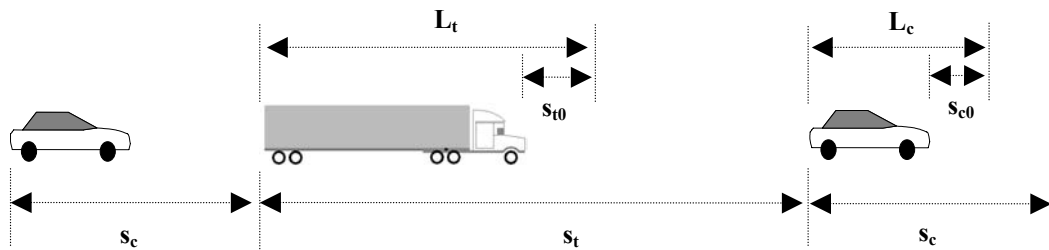


Figure 41. Mixed traffic with passenger vehicles and heavy trucks

Consider the mixed traffic flow shown in Figure 41, where L_t and L_c are the average lengths of heavy trucks and passenger vehicles, respectively, and s_t and s_c are the average intervehicle spacings used by trucks and passenger vehicles, respectively. Note, the safety distances at the congestion conditions (s_{t0} and s_{c0}) are incorporated in L_t and L_c , as done in the previous analysis. The average intervehicle spacing at steady state, \bar{s} , is given by

$$\bar{s} = ps_t + (1-p)s_c \quad (4-15)$$

where p is the penetration of heavy trucks in traffic. The average traffic density, ρ_{mix} , is given by

$$\rho_{mix} = \frac{1}{\bar{s}} = \frac{1}{ps_t + (1-p)s_c} \quad (4-16)$$

Due to the lack of studies for truck driver behavior, we have no data as to how truck drivers adjust the intervehicle spacing as a function of the traffic density or traffic speed. We assume that the average time headway kept by truck drivers is r_{hm} times of that kept by passenger vehicle drivers, and r_{hm} is a constant for all speeds. In our analysis, we assume $r_{hm} > 1$ since trucks have lower braking capabilities than passenger vehicles and tend to maintain larger intervehicle spacings for safety reasons. From (4-1), we can see that the average time headway used by passenger vehicles is given as:

$$h_{cm} = \frac{L_c}{v_f - v} \quad (4-17)$$

where L_c is the average length of a passenger vehicle. Equation (4-17) indicates that drivers decrease the time headway as the traffic density increases. Based on our assumption, the average time headway used by truck drivers, h_{tm} , is

$$h_{tm} = r_{hm} h_{cm} = \frac{r_{hm}}{r_L} \cdot \frac{L_t}{v_f - v} \quad (4-18)$$

where $r_L = L_t/L_c$, and $r_L > 1$. From (4-15) and (4-16), we get

$$\rho_{mix} = \frac{1}{\bar{p}_h h_{cm} v + \bar{p}_L L_c} \quad (4-19)$$

where $\bar{p}_h = pr_{hm} + (1-p)$, $\bar{p}_L = pr_L + (1-p)$ and v is the traffic speed. In (4-19), $\bar{p}_L L_c$ and $\bar{p}_h h_{cm}$ represent the average vehicle length and time headway, respectively. With (4-17), it follows that

$$v = \frac{1 - \bar{L}\rho}{1 - \bar{L}\rho + r_{\bar{p}}\bar{L}\rho} v_f = \left(1 - \frac{r_{\bar{p}}\bar{L}\rho}{1 - \bar{L}\rho + r_{\bar{p}}\bar{L}\rho} \right) v_f \quad (4-20)$$

where $\bar{L} = \bar{p}_L L_c$ and $r_{\bar{p}} = \bar{p}_h / \bar{p}_L$. Here, ρ is used to represent ρ_{mix} , and in the following analysis, we will always use ρ . When $p = 0$, (4-20) is the same as (4-1), and the corresponding fundamental flow-density diagram is labeled as the “0% trucks” in Figures 42, 43, 44, 45 and 46. With (4-2) and (4-20), the traffic flow rate q is given by

$$q = \left(1 - \frac{r_{\bar{p}}\bar{L}\rho}{1 - \bar{L}\rho + r_{\bar{p}}\bar{L}\rho} \right) \rho v_f \quad (4-21)$$

From (4-21), it follows that

$$\frac{dq}{d\rho} = \frac{(1 - \bar{L}\rho)^2 - r_{\bar{p}}\bar{L}^2\rho^2}{(1 - \bar{L}\rho + r_{\bar{p}}\bar{L}\rho)^2} v_f \quad (4-22)$$

and

$$\frac{d^2q}{d\rho^2} = -\frac{2r_{\bar{p}}\bar{L}}{(1 - \bar{L}\rho + r_{\bar{p}}\bar{L}\rho)^3} v_f \quad (4-23)$$

$\rho \in [0, 1/\bar{L}]$ indicates $(1 - \bar{L}\rho + r_{\bar{p}}\bar{L}\rho) > 0$, and then $\frac{d^2q}{d\rho^2} < 0$. Hence, q is a strictly concave function of ρ on $[0, 1/\bar{L}]$, and $c = \frac{dq}{d\rho}$ is a strictly decreasing function of ρ on $[0, 1/\bar{L}]$. The maximum traffic flow rate, \bar{q}_{mm} , is achieved at $\bar{\rho}_{cm}$, where \bar{q}_{mm} and $\bar{\rho}_{cm}$ are given as

$$\bar{\rho}_{cm} = \frac{1}{(1 + \sqrt{r_{\bar{p}}})\bar{L}} \quad (4-24a)$$

$$\bar{q}_{mm} = \frac{v_f}{(1 + \sqrt{r_{\bar{p}}})^2 \bar{L}} \quad (4-24b)$$

From (4-22), it follows that the speed of the traveling waves, c , is given by

$$c = \frac{dq}{d\rho} = \frac{(1 - \bar{L}\rho)^2 - r_{\bar{p}}\bar{L}^2\rho^2}{(1 - \bar{L}\rho + r_{\bar{p}}\bar{L}\rho)^2} v_f \quad (4-25)$$

At the same time, from (4-20), we get

$$\rho = \frac{v_f - v}{\bar{L}(v_f - v + r_{\bar{p}}v)} \quad (4-26)$$

Substituting (4-28) into (4-27), we get

$$c = \frac{v^2}{v_f} - \frac{(v_f - v)^2}{r_{\bar{p}}v_f} \quad (4-27)$$

Using the above equations we examine how the presence of trucks affect the traffic flow characteristics. If the truck is counted as a single vehicle it is trivial to see that the traffic flow rate will decrease because a heavy truck occupies more space than a single passenger vehicle due to its larger length and bigger spacing used ($r_{hm} > 1$ and $r_L > 1$). Furthermore, it is easy to verify that $\bar{\rho}_{cm} < \rho_{cm}$ and $\bar{q}_{mm} < q_{mm}$. However, if we treat one truck as r_L passenger vehicles, how does the appearance of trucks affect the traffic throughput? Another question is how it affects the speed with which a traveling wave generated by a density disturbance travels upstream. These answers depend on the value of $r_{\bar{p}}$. When p is nonzero, $r_{\bar{p}} > 1 \Leftrightarrow r_{hm} > r_L$, $r_{\bar{p}} = 1 \Leftrightarrow r_{hm} = r_L$ and $r_{\bar{p}} < 1 \Leftrightarrow r_{hm} < r_L$.

When we treat one heavy truck as equivalent to r_L passenger size vehicles, each of which has the length of L_c and uses a time headway $h'_{cm} = \frac{r_{hm}}{r_L} h_{cm}$, and the penetration of heavy trucks is p means the equivalent penetration in passenger size vehicles is $p' = \frac{r_L p}{1 + (r_L - 1)p}$. It can be seen that the previous analysis for the traffic including heavy trucks based on (4-21) can also be applied to the analysis for the traffic where trucks are treated as equivalent to r_L passenger size vehicles with proper replacement of variables. In the following analysis, we denote the traffic density and flow rate for the traffic including trucks as ρ' and q' , respectively, when one truck is treated as r_L passenger size vehicles. The maximum density, critical density and maximum traffic flow rate are denoted as ρ'_{max} , ρ'_{cm} and q'_{mm} , respectively.

We consider the following cases:

Case 1: $r_{hm} = r_L$

In this case, we consider $r_{hm} = r_L$, i.e. the time headway ratio of truck versus passenger vehicle is equal to the length ratio of truck versus passenger vehicle, or equivalently, $r_{\bar{p}} = 1$ for all p . The assumed average time headway used by truck drivers is

$$h_{tm} = \frac{L_t}{L_c} h_{cm} \quad (4-28)$$

Hence, (4-20) can be rewritten as

$$v = \left(1 - \frac{\rho}{\bar{\rho}_{\max}} \right) v_f \quad (4-29)$$

where $\bar{\rho}_{\max} = 1/\bar{L}$. Using the similarity of (4-29) with (4-1), we can conclude that the previous analysis based on (4-1) can be applied to (4-29) by simply taking $\rho_{\max} = \bar{\rho}_{\max}$ and $L = \bar{L}$. The fundamental flow-density diagram based on (4-29) is labeled as the “100p% trucks” in Figure 42. Due to the presence of heavy trucks, the maximum traffic flow rate \bar{q}_{mm} and the corresponding critical density $\bar{\rho}_{cm}$ are less than q_{mm} and ρ_{cm} , respectively. If the mixed traffic has the same speed as the “0% trucks” traffic, the traveling waves in the two traffic flows have the same speed, as indicated by (4-12). This point can be graphically viewed in Figure 42. Suppose A_0 is an arbitrary point on the curve labeled as “0% trucks”, and the line connecting O and A_0 intersects the curve “100p% trucks” at point A_p . At A_p and A_0 , the two traffic streams have the same speed, which is equal to the slope of the line passing through O and A_0 . The slopes of the two tangents at A_p and A_0 , which correspond to the speeds of the traveling waves in the two traffic flows, are the same for all $0 \leq p \leq 1$. This means the presence of heavy trucks does not affect the speed of the traveling waves, provided the speeds of the two different traffic flows are the same.

In this case, when one heavy truck is treated as r_L passenger size vehicles, each of these vehicles uses the same average time headway as the passenger vehicles in the manual traffic. Hence the $q' - \rho'$ curve is the same as the curve labeled as “0% trucks” in Figure 42, for $0 \leq p \leq 1$. This means the presence of heavy trucks doesn't affect the traffic flow-density diagram. In practice this case is possible to occur but it is not a frequent one as trucks tend to use much higher headways on the average than passenger vehicles for safety reasons and also due to their limited acceleration capabilities.

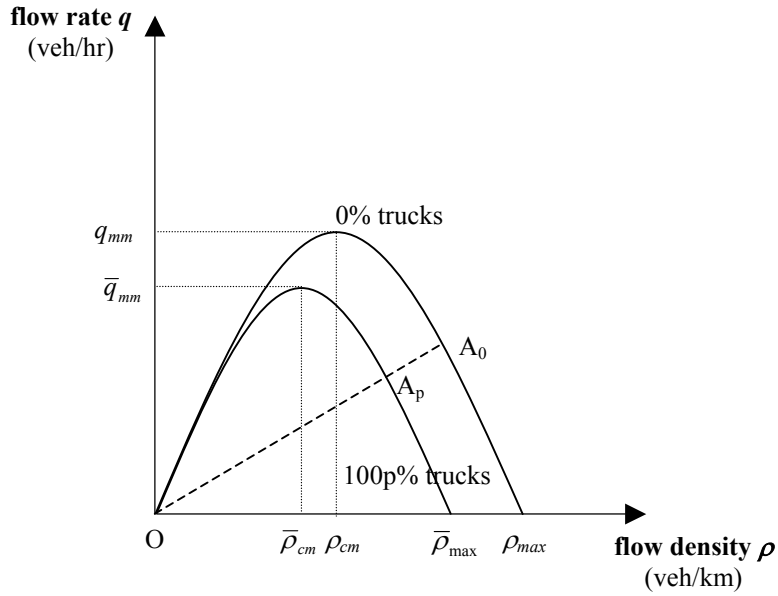


Figure 42. Fundamental flow-density diagrams of the manual traffic with/without heavy trucks
 $(r_{hm} = r_L)$

Case 2: $r_{hm} < r_L$

In this case, $r_{hm} < r_L$, i.e. the time headway ratio of truck versus passenger vehicle is smaller than the length ratio of truck versus passenger vehicle. Equivalently, $r_p = 1$ if $p = 0$, and $0 < r_p < 1$ otherwise. The fundamental flow-density diagram is labeled as “100p% trucks” shown in Figure 43. From (4-24a) and (4-24b), we know that $\bar{\rho}_{cm} > \frac{1}{2L}$ and $\bar{q}_{mm} > \frac{v_f}{4L}$. It is obvious that for two traffic flows at the same speed, the one with 100p% of trucks will have traveling waves propagating upstream faster, based on (4-27). This point can be graphically viewed as in Figure 43: the slope of the tangent at point A_p is smaller (more negative) than that at point A_0 . Following the same analysis, we conclude that for two traffic flows at the same speed, the one with more percentages of trucks will have traveling waves transferring upstream faster.

In this case, when one heavy truck is treated as r_L passenger size vehicles, each of these vehicles uses the time headway $\frac{r_{hm}}{r_L} h_{cm}$, which is smaller than h_{cm} . The fundamental flow-density diagram is labeled as “100p% trucks” shown in Figure 44. It is easy to verify that this curve can be achieved by scaling the curved labeled as “100p% trucks” in Figure 43 with \bar{p}_L in both q and ρ axes. Now we can see that

$\rho'_{\max} = \rho_{\max} = \frac{1}{L_c}$, $\rho'_{cm} > \frac{1}{2L_c}$ and $q'_{mm} > \frac{v_f}{4L_c}$. This indicates the presence of heavy trucks increases the critical density and traffic throughput if we treat each of them as r_L passenger size vehicles. This is due to the fact that in this case the drivers of heavy trucks use relatively small time headway. As case 1, this case is unlikely to take place frequently in practice as trucks will employ high headways on the average for safety reasons but also due to their inability to accelerate as fast and maintain as high speeds as passenger vehicles.

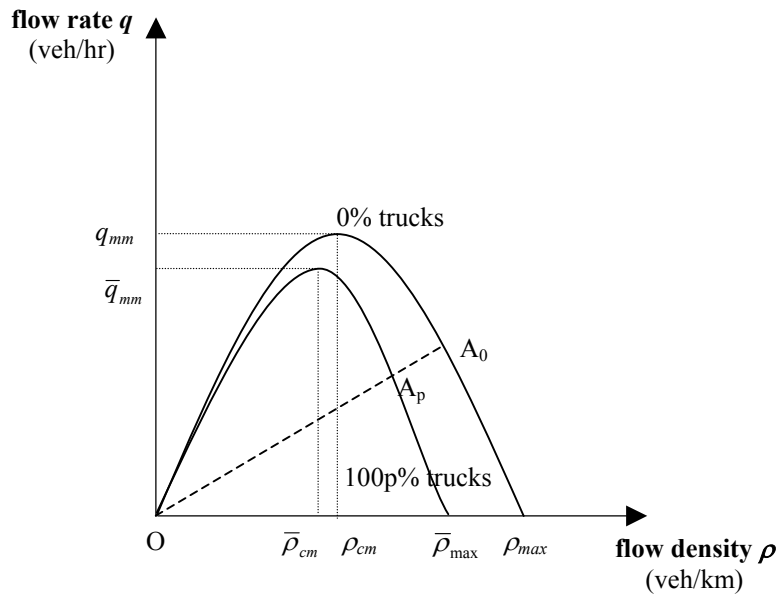


Figure 43. Fundamental flow-density diagrams of the manual traffics with/without heavy trucks
 $(r_{hm} < r_L)$

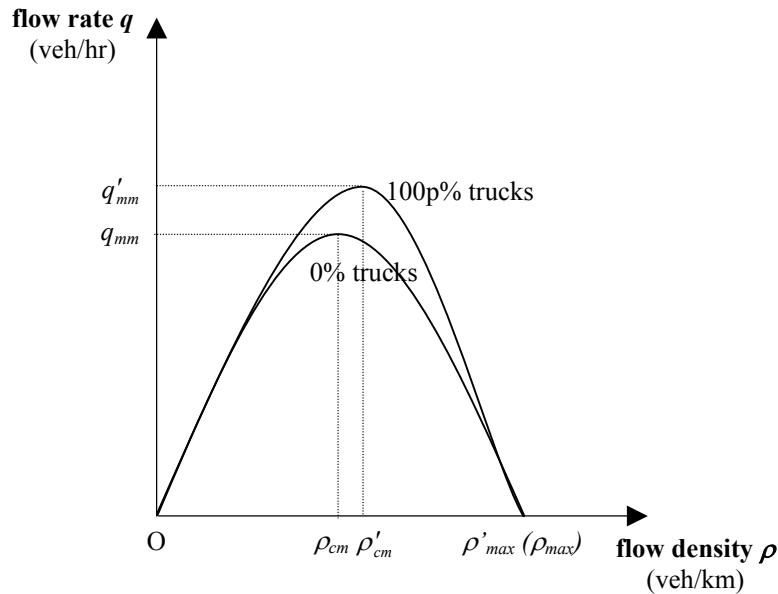


Figure 44. Fundamental flow-density diagrams of the manual traffics with/without heavy trucks (one truck is treated as r_L passenger vehicles, $r_{hm} < r_L$)

Case 3: $r_{hm} > r_L$

In this case, $r_{hm} > r_L$, i.e. the time headway ratio of truck versus passenger vehicle is larger than the length ratio of truck versus passenger vehicle. Equivalently, $r_{\bar{p}} = 1$ if $p = 0$, and $r_{\bar{p}} > 1$ otherwise. In practice it is more likely that $r_{hm} > r_L$. This is due to the fact that trucks are more likely to maintain higher headways due to safety reasons as well as due to their sluggish response. The fundamental flow-density diagram is labeled as “100p% trucks” shown in Figure 45. From (4-24a) and (4-24b), we know that $\bar{\rho}_{cm} < \frac{1}{2\bar{L}}$

and $\bar{q}_{mm} < \frac{v_f}{4\bar{L}}$. For two traffic flows at the same speed, the one with trucks will have traveling waves propagating upstream slower, based on (4-27). This point can be graphically viewed as in Figure 44: the slope of the tangent at point A_p is larger (less negative) than that at point A_0 . Following the same analysis, we conclude that for two traffic flows at the same speed, the one with more percentages of trucks will have traveling waves transferring upstream slower.

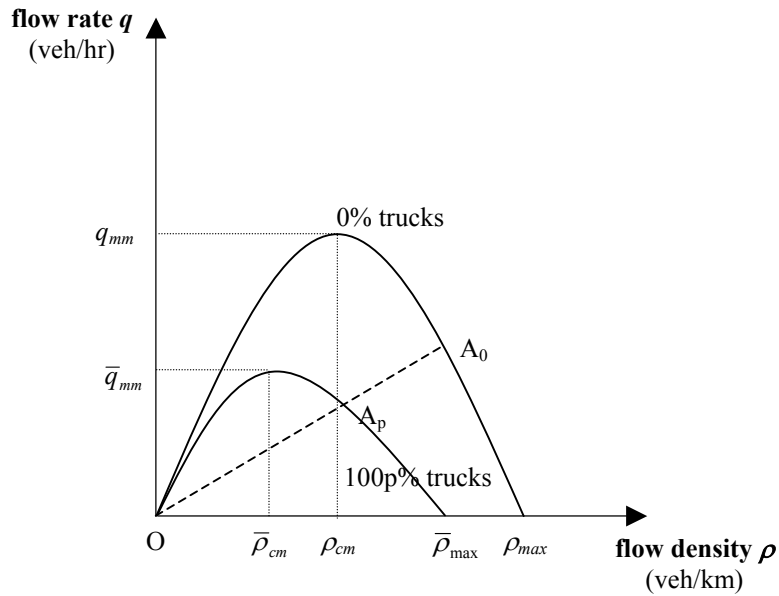


Figure 45. Fundamental flow-density diagrams of the manual traffics with/without heavy trucks
 $(r_{hm} > r_L)$

In this case, when one heavy truck is treated as r_L passenger size vehicles, each of these vehicles uses the time headway $\frac{r_{hm}}{r_L} h_{cm}$, which is larger than h_{cm} . The fundamental flow-density diagram is labeled as “100p% trucks” shown in Figure 46. It is developed by scaling the curved labeled as “100p% trucks” in Figure 45 with \bar{p}_L in both q and ρ axes. Now we can see that $\rho'_{max} = \rho_{max} = \frac{1}{L_c}$, $\rho'_{cm} < \frac{1}{2L_c}$ and $q'_{mm} < \frac{v_f}{4L_c}$. This indicates that the presence of heavy trucks decreases the critical density and traffic throughput if we treat each of them as r_L passenger size vehicles. This is due to the drivers of heavy trucks using larger time headways relative to that of passenger vehicles. Furthermore a density disturbance will travel upstream slower in the case of mixed traffic with trucks taking longer time to dissipate. We believe that this case is the most dominant one in practice as trucks due to their limited acceleration and speed capabilities will average high time headways with negative effects on traffic flow characteristics predicted in this case.

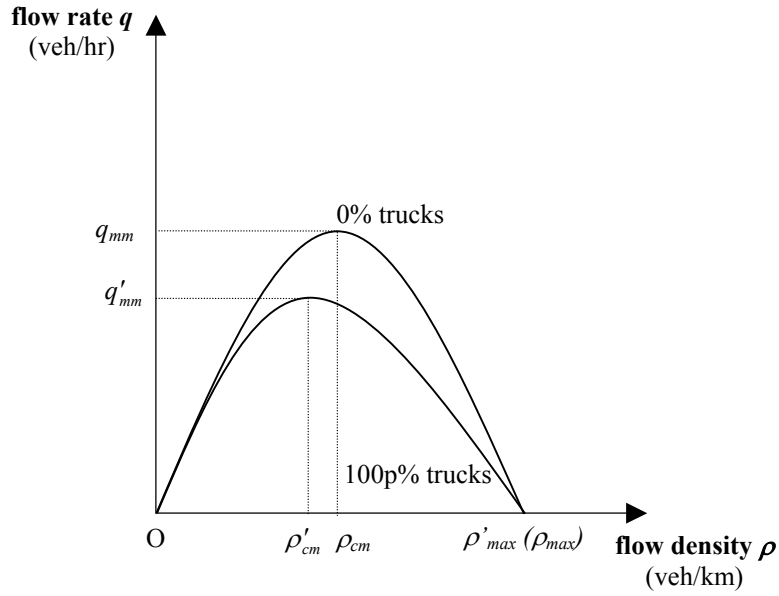


Figure 46. Fundamental flow-density diagrams of the manual traffics with/without heavy trucks (one truck is treated as r_L passenger vehicles, $r_{hm} > r_L$)

In the ACC traffic, the fundamental flow density diagram is easy to construct since all the vehicles in the traffic stream are guided by the designed ACC systems. Let us assume that the trucks use the spacing rule

$$s_{ta} = h_{ta}v + L_t \quad (4-30)$$

where s_{ta} is the spacing occupied by one ACC truck and h_{ta} is the time headway. We also assume that the passenger vehicles use the spacing rule

$$s_{ca} = h_{ca}v + L_c \quad (4-31)$$

where s_{ca} is the spacing occupied by one ACC passenger vehicle and h_{ca} is the time headway. From (4-15), it is derived that at speed v , the average intervehicle spacing is given as

$$\bar{s}_a = \bar{h}_a v + \bar{L} \quad (4-32)$$

where $\bar{s}_a = ps_{ta} + (1-p)s_{ca}$, $\bar{h}_a = ph_{ta} + (1-p)h_{ca}$ and $\bar{L} = pL_t + (1-p)L_c$. If the traffic density is lower than $\bar{\rho}_{ca} = \frac{1}{\bar{h}_a v_f + \bar{L}}$, then there is no vehicle interaction and all vehicles

travel at the free speed v_f . When the traffic density reaches or exceeds $\bar{\rho}_{ca}$, (4-32) leads to

$$\rho = \frac{1}{\bar{h}_a v + \bar{L}} \quad (4-33)$$

or equivalently

$$v = \frac{1}{\bar{h}_a} \left(\frac{1}{\rho} - \bar{L} \right) \quad (4-34)$$

The steady-state speed of the ACC vehicles decreases with increasing ρ until ρ reaches its maximum value $\bar{\rho}_{\max} = 1/\bar{L}$. The steady-state flow-density relationship is given by

$$q = \begin{cases} \rho v_f & \rho \leq \bar{\rho}_{ca} \\ (1 - \rho \bar{L})/\bar{h}_a & \rho > \bar{\rho}_{ca} \end{cases} \quad (4-35)$$

The flow-density relationship in (4-35) is similar to that in (4-7), and the previous analysis for the ACC traffic with passenger vehicles can be applied to the mixed ACC traffic with proper replacement of variables.

If the truck is counted as a single vehicle it is trivial to see that the traffic throughput will decrease because a heavy truck occupies more space than a single passenger vehicle. However, if we treat one truck as r_L passenger size vehicles, how does the appearance of trucks affect the traffic throughput? How do heavy trucks affect the speed of traveling waves? When the traffic density is extremely low, the appearance of heavy trucks will not affect throughput since there is no interaction among vehicles and all vehicles move at the free speed. If we assume the traffic density is relatively high, then all the traffic disturbances will be propagated upstream at the speed $-\bar{L}/\bar{h}_a$. Let's define $r_{ha} = h_{ta}/h_{ca}$, $\bar{p}_h = p r_{ha} + (1 - p)$, and keep the definitions for \bar{p}_L , r_L and $r_{\bar{p}}$ as used for the manual traffic. It can be verified that $\bar{L}/\bar{h}_a = 1/r_{\bar{p}}$. Again, we can see how heavy trucks affect the traveling waves depends on the value of $r_{\bar{p}}$, and the conclusions to be presented are the same as those for the manual traffic.

Case 1: $r_{ha} = r_L$

In this case, the time headway ratio of truck versus passenger vehicle is equal to the length ratio of truck versus passenger vehicle, i.e. $r_{\bar{p}} = 1$ for all possible values of p . This means the presence of heavy trucks does not affect the speed of the traveling waves. If

we treat one heavy truck as r_L passenger size vehicles, the flow density curve for the mixed traffic is the same as that of the traffic without trucks.

Case 2: $r_{ha} < r_L$

In this case, the time headway ratio of truck versus passenger vehicle is smaller than the length ratio of truck versus passenger vehicle. Equivalently, $r_{\bar{p}} = 1$ if $p = 0$, and $0 < r_{\bar{p}} < 1$ otherwise. The fundamental flow-density diagram is given in Figure 47, labeled as “100p% trucks”. For comparison purposes, the fundamental flow-density diagram for the ACC traffic without trucks is also given in Figure 47, labeled as “0% trucks”. It is easy to see that for high traffic densities, the appearance of heavy trucks will make traveling waves propagate upstream faster. It can also be shown that for two traffic flows with the same speed, the one with higher percentage of trucks will have traveling waves propagating upstream faster.

If one heavy truck is treated as r_L passenger size vehicles, the flow density curve can be developed by scaling the curve labeled as “100p% trucks” in Figure 47 with \bar{p}_L in both q and ρ axes. In this case, this appearance of heavy trucks increases the critical density and traffic throughput.

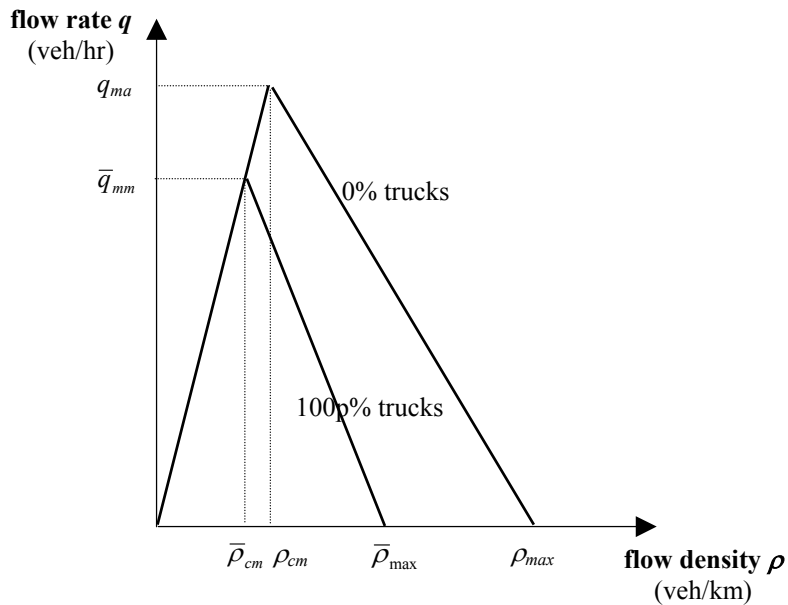


Figure 47. Fundamental flow-density diagrams of the ACC traffic with/without heavy trucks
 $(r_{ha} < r_L)$

Case 3: $r_{ha} > r_L$

In this case, the time headway ratio of truck versus passenger vehicle is smaller than the length ratio of truck versus passenger vehicle. Equivalently, $r_{\bar{p}} = 1$ if $p = 0$, and $r_{\bar{p}} > 1$ otherwise. Following (3-35), we know that the appearance of heavy trucks will make traveling waves propagate upstream slower. It can also be shown that for two traffic flows with the same speed, the one with higher percentage of trucks will have traveling waves propagating upstream slower.

If one heavy truck is treated as r_L passenger size vehicles, the appearance of heavy trucks decreases the critical density and traffic throughput. The conclusion is the same as that in Case 3 of the manual traffic: the traffic is more susceptible to instability due to the presence of heavy trucks.

The three cases above related to ACC vehicles indicate very similar conclusions as in the corresponding cases of manually driven vehicles. In the manually driven vehicles we argue that the limited acceleration and speed capabilities of trucks will create large intervehicle gaps frequently raising the average headway used to be much greater than that of passenger vehicles therefore in manual traffic case 3 will dominate. For the ACC traffic however it is more likely that cases 1, 2 will be dominant as ACC trucks will use lower average headways than in case 3 leading to a more stable traffic characteristics than those in manual traffic.

4.2.2 Shock Waves Analysis

Shock waves are discontinuous waves that occur when traffic on a section of a road is denser downstream than upstream. The waves on the less dense section travel faster than those in the dense section ahead and catch up with them. Then the continuous waves coalesce into a discontinuous wave or a “shock wave” [17]. It can be shown that shock waves travel at a speed given by [17]

$$u = \frac{q_2 - q_1}{\rho_2 - \rho_1} \quad (4-36)$$

where (q_1, ρ_1) and (q_2, ρ_2) are the traffic flow rates and traffic densities on the two sections, respectively. In the fundamental diagram, this is given by the slope of the chord connecting the two points that represent conditions ahead and behind the shock wave at a and b , respectively (see Figure 48). In this report, we use (4-21) and (4-36) to analyze shock waves. Suppose the traffic speeds ahead and after the shock wave are v_1 and v_2 , respectively. The speed of shock waves given by (4-36) is

$$u = v_f + \frac{(v_f - v_2)^2 v_1 - (v_f - v_1)^2 v_2}{(v_1 - v_2)v_f} - \frac{(v_f - v_2)(v_f - v_1)}{v_f} \cdot \frac{1}{r_{\bar{p}}} \quad (4-37)$$

Given $r_{\bar{p}}$, we can estimate how heavy trucks affect the shock waves.

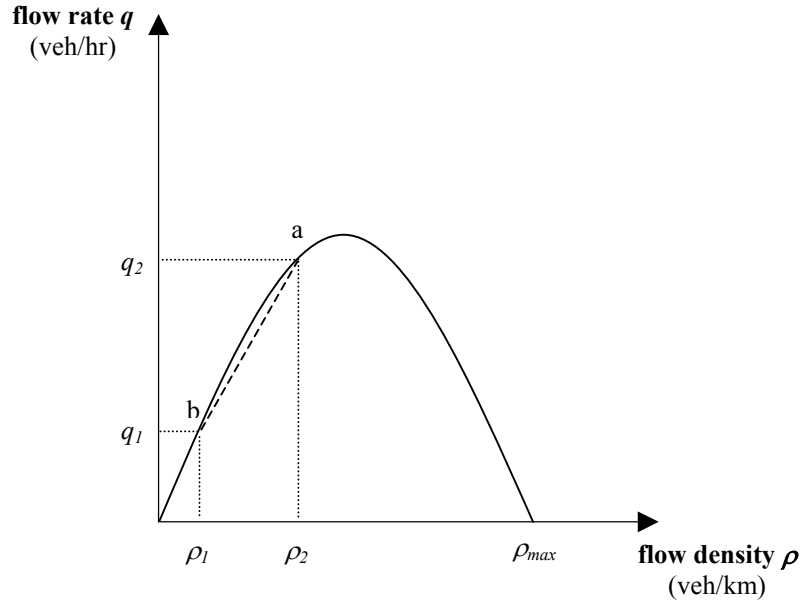


Figure 48. Illustration of shock wave in transportation traffic

Case 1: $r_{hm} = r_L$

$r_{\bar{p}} = 1$ for all possible values of p means the presence of heavy trucks does not affect the speed of shock waves.

Case 2: $r_{hm} < r_L$

$r_{\bar{p}} = 1$ if $p = 0$, and $0 < r_{\bar{p}} < 1$ otherwise. This indicates the shock waves are propagated upstream faster in the case of mixed traffic with heavy trucks.

Case 3: $r_{hm} > r_L$

$r_{\bar{p}} = 1$ if $p = 0$, and $r_{\bar{p}} > 1$ otherwise. This indicates the shock waves are propagated upstream slower in mixed traffic with heavy trucks.

The question that should be raised is that which one of these cases corresponds to real traffic. Based on our microscopic studies and simulations we claim that for manual traffic case 3 will be more dominant case while for ACC mixed traffic cases 1, 2 will be more dominant. Therefore the presence of ACC vehicles both passenger and trucks will improve the traffic characteristics on the macroscopic level as due to ACC, smaller headways could be used and the frequency of traffic disturbances would be reduced due to the smooth response of ACC vehicles.

5 CONCLUSIONS

The sluggish dynamics of trucks whether manual or ACC due to limited acceleration and speed capabilities make their response to disturbances caused by lead passenger vehicles smooth. The vehicles following the truck are therefore presented with a smoother speed trajectory to track. This filtering effect of trucks is shown to have beneficial effects on fuel economy and pollution. The quantity of these benefits depends very much on the level of the disturbance and scenario of maneuvers. For example if the response of the truck is too sluggish relative to the speed of the lead vehicle then a large intervehicle spacing may be created inviting cut-ins from neighboring lanes. These cut-ins create additional disturbances with negative effects on fuel economy and pollution. Situations can be easily constructed where the benefits obtained due to the filtering effect of trucks are eliminated due to disturbances caused by possible cut-ins. Furthermore cut-ins are shown to increase travel time for the vehicles in the original traffic stream.

The ACC trucks improve performance as they are designed to respond smoothly during vehicle following while maintaining safe intervehicle spacings. The spacing rule adopted influences the performance and response of the ACC truck. For the same spacing rule however different ACC designs behave in a very similar manner. The new ACC design developed, analyzed and tested under this project is shown to have better filtering properties than existing ones leading to improved benefits for fuel economy and pollution during traffic disturbances. Furthermore the new ACC design provides a smooth response and filters oscillations that may appear in the speed response of the lead vehicle.

The behavior of trucks in mixed traffic on the macroscopic level is analyzed and found to depend on a particular number that characterizes the ratio of the time headway used by trucks versus that of the passenger vehicles. For relatively low ratios the presence of trucks appears to improve the traffic flow characteristics whereas for high ratios the traffic flow of mixed traffic becomes unstable at lower traffic densities and at lower traffic flows compared with traffic with no trucks. In practice for safety reasons and due to limited acceleration and speed capabilities of trucks this ratio is large most of the time leading to the conclusion that trucks will tend to make traffic flow more unstable at lower traffic densities and at lower traffic flows. The use of ACC however will reduce this ratio and improve the traffic flow characteristics.

The limited experiments performed validated our simulation models at least on the microscopic level. In addition they demonstrated that our new ACC design works in real time and under actual driving conditions in a satisfactory manner. Additional experiments of larger scale are essential in order to validate the results of the emission models as well as some of the macroscopic phenomena predicted by simulations and the fundamental diagram.

ACKNOWLEDGMENT

The authors would like to thank Ms. Margareta Stefanovic for numerous discussions on truck dynamics and vehicle control.

Appendix : TRUCK LONGITUDINAL MODEL

The nonlinear longitudinal truck model involving the diesel engine, automatic transmission and drivetrain developed in [29, 30] is highly detailed and complicated. The input to this model is fuel/brake command, and the output is the longitudinal acceleration and speed. In the following, we present the basic equations and dynamics of the truck model used in this report for control design and simulation purposes.

The following notation is used:

m – vehicle mass
 v - longitudinal speed
 u - control input (fuel or brake)
 τ - variable indicating dynamics
 $F_a = c_a v^2$ - aerodynamic drag force
 F_r - rolling resistance force
 F_t - tractive force (force that accelerates or decelerates the vehicle)
 i_a, i_b – tire slips
 h_w - the driving wheels radius
 ω_w - angular speed of the wheels
 J_w - total inertia of the wheels
 R_{total} - total reduction gear ratio
 M_b - applied brake torque
 M_{bc} - commanded brake torque
 M_T - driving torque (from torque converter turbine part)
 α_i - constants fitted from experimental data
 ω_p - angular speed of the pump of torque converter
 ω_t - angular speed of the turbine of torque converter
 J_e - effective inertia of the engine
 M_f - friction torque of the engine
 M_{load} - load torque produced in the transmission subsystem.
 M_{ind} - indicated torque (developed in the cylinders)
 η_{ind} - indicated efficiency
 m_{fi} - quantity of the fuel injected into cylinders
 Q_{lhv} - lower heating value of the fuel
 k_f - constant of proportionality
 Y - fuel index, scaled value of the actual fuel command u
 u_f – output signal of the fuel (or brake) actuator

The dominant state of the longitudinal model is the one associated with the truck longitudinal speed. The longitudinal dynamics associated with the *longitudinal speed* v are described by the equation:

$$\dot{v} = \frac{F_t - F_a - F_r}{m}$$

where

$$\begin{cases} F_a = c_a v^2 \\ F_r = \frac{c_r mg}{h_w} \end{cases}$$

The reactive aerodynamic drag and rolling resistance forces are counteracted by the tractive tire force F_t to produce the force that accelerates or decelerates the vehicle. The tractive force depends linearly on the tire slip (up to $\sim 15\%$ slip) as

$$F_t = k_i i_d \quad \text{or} \quad F_t = -k_i i_b$$

The plus or minus sign depends on whether the tire is under the driving or braking torque. The tire longitudinal slip is determined by the non-negative one of

$$i_d = 1 - \frac{v}{h_w \omega_w} \quad \text{and} \quad i_b = 1 - \frac{h_w \omega_w}{v}$$

The dynamics of the angular speed of the wheels ω_w are determined by

$$J_w \dot{\omega}_w = \frac{M_T}{R_{total}} - F_t h_w - M_b$$

The variable in the above equation that depends on the *control input* (which is the *applied throttle angle* - translated into the *amount of fuel injected* into the cylinders) is the converter turbine torque M_T . This torque is modeled, under the assumption of instantaneous gear shift and no torsion in the driveline, as a static relation

$$M_T = \alpha_0 \omega_p^2 + \alpha_1 \omega_p \omega_T + \alpha_2 \omega_T^2$$

The angular speed of the pump ω_p is in fact the angular speed of the engine crankshaft ω_e , and its dynamics are

$$J_e \dot{\omega}_e = M_{ind}(t - \tau_i) - M_f(t) - M_{load}(t)$$

Here, M_{ind} (indicated torque, generated in the cylinders) is calculated as

$$M_{ind} = \eta_{ind} m_{fi} Q_{LHV}$$

where m_{fi} , the quantity of the fuel injected into cylinders, is determined as

$$m_{fi} = k_f Y$$

where Y is the fuel index (defined as the position of the fuel pump rack, which determines the amount of fuel provided for combustion). It is a scaled version of the actual fuel command, u . The dynamics of the fuel pump and the actuators that issue the fuel command to the injectors are modeled as a 1st order system

$$\dot{u}_f = \frac{1}{\tau_f}(-u_f + u)$$

The above equations also include dependence on the brake torque M_b , which plays a role if a brake command is issued. The following first order system models the dynamics of the brake actuator

$$\dot{M}_b = \frac{M_{bc} - M_b}{\tau_b}$$

The equations stated above concisely describe the vehicle dynamics. The complete model of the diesel engine, transmission and drive-train consists of a series of differential equations, algebraic relations and look-up maps, compiled from experimental data and can be found in [29, 30].

REFERENCES

- [1] Bando M., Hasebe K., Nakayama A., Shibata A. and Sugiyama Y., “*Dynamical Model of Traffic Congestion and Numerical Simulation*”, Phys. Rev., E 51, pp. 1035-1042, 1995.
- [2] Barth M.J., et al, “*Development of a heavy-duty diesel modal emissions and fuel consumption module for SmartAHS*”, California PATH Project, TO 4215.
- [3] Barth M.J., et al, “*User’s Guide: Comprehensive Modal Emissions Model, Version 2.0*”, University of California, Riverside, 2001.
- [4] Bose A., Ioannou P., “*Analysis of Traffic Flow With Mixed Manual and Intelligent Cruise Control Vehicles: Theory and Experiments*”, California PATH Research Report, UCB-ITS-PRR-2001-13, 2001.
- [5] Bose A., Ioannou P., “*Mixed Manual/Semi-Automated Traffic: A Macroscopic Analysis*”, California PATH Research Report, UCB-ITS-PRR-2001-14, 2001.
- [6] Broqua F., Lerner G., Mauro V., and Morello E., “*Cooperative driving: Basic concepts and a first assessment of “intelligent cruise control” strategies*” in Advanced Telematics in Road Guidance. Proceedings of the DRIVE Conference, pp. 908-929, Elsevier, February 4-9 1991.
- [7] Chandler P.E., Herman R. and Montroll E., “*Traffic Dynamics: Studies in Car Following*”, Operations Research, vol. 6, pp. 165-184, 1958.
- [8] Desoer C.A. and Vidyasagar M., “*Feedback Systems: Input-Output Properties*”, Academic Press Inc., New York, 1975.
- [9] Greenshilds B.D., “*A study in Highway Capacity*”, Highway Res. Board Proc, vol. 14, p. 468, 1934.
- [10] Hingwe P., Wang J., Tai M. and Tomizuka M., “*Lateral Control of Heavy Duty Vehicles for Automated Highway System: Experimental Study on a Tractor Semi-trailer*”, California PATH Program, UCB-ITS-PWP-2000-01, 2000.
- [11] Hopper S., “*Modifications of Bando’s car following model with explicit delay*”, M.Sc. Thesis, University of Bristol, 2000.
- [12] Horan T.A., Hempel L.C., Jordan D.R. and Alm E. A., “*ITS and the Environment: Issues and Recommendations for ITS Deployment in California*”, California PATH Research Report, UCB-ITS-PRR-96-18.
- [13] Ioannou P. and Sun J., “*Robust Adaptive Control*”, Prentice Hall, 1996.

- [14] Ioannou P. and Xu T., “*Throttle and Brake Control*”, IVHS Journal, vol. 1(4), pp. 345-377, 1994.
- [15] Jolibois S.C. and Kanafani A., “*An Assessment of IVHS-APTS Technology Impacts on Energy Consumption and Vehicle Emissions of Transit Bus Fleets*”, California PATH Research Report, UCB-ITS-PRR-94-19, 1994.
- [16] Kelly T., “*Keeping Trucks on Track*”, ITS World, pp. 20-21, July/August 1999.
- [17] Lighthill M.J. and Whitham G.B., “*On Kinematic Waves II. A Theory of Traffic Flow on Long Crowded Roads*”, Proceedings of the Royal Society of London, Series A 229, pp. 317-345, 1955.
- [18] Mason A. and Woods A., “*Car-following model of multi-species systems of road traffic*”, Phys. Rev., E 55, pp. 2203-2214, 1997.
- [19] Parker J.G., “*Trucks in a Row*”, Traffic World, pp. 23, July 12, 1999.
- [20] Pipes L.A., “*An Operational Analysis of Traffic Dynamics*”, Journal of Applied Physics, vol. 24, pp. 271-281, 1953.
- [21] Sheikholeslam S. and Desoer C.A., “*Longitudinal Control of a Platoon of Vehicles with no Communication of Lead Vehicle Information*”, Proceedings of the American Control Conference, Boston, MA, pp. 3102-3106, 1991.
- [22] Swaroop D. and Rajagopal K.R., “*Intelligent Cruise Control Systems and Traffic Flow Stability*”, Transportation Research, Part C: Emerging Technologies, 7(6), pp. 329-352, 1999.
- [23] Swaroop D. and Huandra R., “*Intelligent Cruise Control System Design Based on a Traffic Flow Specification*”, California PATH Research Report UCB-ITS-PRR-99-5, 1999.
- [24] Swaroop D. and Hedrick J.K., “*String Stability of Interconnected Systems*”, IEEE Trans. on Automatic Control, vol. 41, No. 3, pp. 349-357, 1996.
- [25] Swaroop D., Hedrick J.K., Chien C.C. and Ioannou P., “*A Comparison of Spacing and Headway Control Laws for Automatically Controlled Vehicles*”, Vehicle System Dynamics, vol.23, No.8, pp.597-625, 1994.
- [26] Tan Y. and Kanellakopoulos I., “*longitudinal Control of Commercial Heavy Vehicles: Experimental Implementation*”, California PATH Research Report, UCB-ITS-PRR-2002-25, 2002.

[27] Palmquist, U, “*Intelligent Cruise Control and Roadside Information*”, IEEE Micro, pp.20-28, 1993.

[28] Yanakiev D., Eyre J. and Kanellakopoulos I., “*Analysis, Design and Evaluation of AVCS for Heavy-Duty Vehicles with Actuator Delay: Final report for MOU 240*”, California PATH Research Report, UCB-ITS-PRR-98-18, 1998.

[29] Yanakiev D., Eyre J. and Kanellakopoulos I., “*Analysis, Design, and Evaluation of AVCS for Heavy-Duty Vehicles: Phase 1 Report*”, California PATH Research Report, UCB-ITS-PWP-95-12, 1995.

[30] Yanakiev D. and Kanellakopoulos I., “*Engine and Transmission Modeling for Heavy-Duty Vehicles*”, California PATH Research Report, Tech Note 95-06, 1995.

[31] Zhang J., Ioannou P. and Chassiakos A., “*Automated Container Transport System between Inland Port and Terminals*”, Final Report for METRANS, Dec. 2002.

[32] ERTICO-ITS Europe, 1999.

[33] 1985 Highway Capacity Manual.